DESIGN OF A PHOTO-RESPONSIVE POLYMERIC INJECTABLE NANOSYSTEM FOR THE SUSTAINED DELIVERY OF MACROMOLECULES

PAKAMA MAHLUMBA

UNIVERSITY OF THE
WITWATERSRAND,
JOHANNESBURG

A dissertation submitted to the Faculty of Health Science, University of the Witwatersrand, in fulfilment of the requirements for the degree of Master of Pharmacy

Supervisor:

Professor Viness Pillay

University of the Witwatersrand, Department of Pharmacy and Pharmacology, Johannesburg, South Africa

Co-Supervisors:

Professor Yahya Essop Choonara

Associate Professor Lisa Claire du Toit

Associate Professor Pradeep Kumar

University of the Witwatersrand, Department of Pharmacy and Pharmacology, Johannesburg, South Africa

2020

DECLARATION

I, Pakama Mahlumba, declare that this dissertation is my own work. It is being submitted for the Degree of Master of Pharmacy at the University of the Witwatersrand, Johannesburg. It has not been submitted before for any degree or examination at this or any other University.

_____

Signed at Wits University day of 26 March 2021

RESEARCH OUTPUTS

1. Research Publications

Stimuli Responsive Polymeric Systems for controlled Protein and Peptide Delivery: Future implications for ocular delivery. Pakama Mahlumba, Yahya E. Choonara, Pradeep Kumar, Lisa C. du Toit and Viness Pillay*. Molecules. 2016 Aug; 21(8): 1002. Published online 2016 Jul 30. doi: 10.3390/molecules21081002 (Abstract in Appendix A).

Fabrication and characterisation of a Photo-Responsive , Injectable Nanosystem for Sustained Delivery of Macromolecules. Pakama Mahlumba, Pradeep Kumar, Lisa C. du Toit, Madan S. Poka, Philemon Ubanako and Yahya E. Choonara*. International Journal of Molecular Sciences. 2021; 22: 3359. Published online 2021 March 25. doi: 10.3390/ijms22073359 (Abstract in Appendix B)

2. Poster Presentations

Preparation and Characterisation of Photo-responsive Nanospheres for Intraocular Delivery. Pakama Mahlumba, Yahya E. Choonara, Pradeep Kumar, Lisa C. du Toit and Viness Pillay*. Presented at APSSA/SAAPI Conference 2015, (Abstract in Appendix C).

ANIMAL ETHICS DECLARATION

I, Pakama Mahlumba, hereby confirm the study entitled "*In vivo* assessment of anti-VEGF delivery from a Geocolloid system in a rabbit eye model" was approved by the Animal Ethics Screening Committee (AESC) of the University of the Witwatersrand with Ethics Clearance Number 2017/11/74/D (Appendix C).

ABSTRACT

Delivery of macromolecules has proven to be challenging due to molecular weight, instability and triggering of immune response. The demand for biodegradable sustained release carriers with minimally invasive and less frequent administration properties for such therapeutics has increased over the years. Stimuli responsive polymers have gained significant interest in drug discovery for their flexibility, site specificity and potential for remotely controlled drug release, especially for irregular targets such as intraocular sites which possess a complex anatomy. The purpose of achieving sustained minimally invasive and site-specific delivery of macromolecules led to the investigation of stimuli responsive materials for this study.

This research explored a biodegradable prolamin, zein, modified with 4,4'-dihydroxyazobenzene (DHAB) to synthesize photo-responsive azoprolamin (AZP) nanospheres incorporated in a hyaluronic acid (HA) hydrogel to formulate a novel injectable photo-responsive nanosystem (HA-NSP) for prolonged release of a model monoclonal antibody, Immunoglobulin G (IgG), as a potential approach for the treatment of chorioretinal diseases such as age related macular degeneration (AMD) and diabetic retinopathy. Photo-responsive AZP nanospheres incorporating IgG were prepared via coacervation technique, characterised for physicochemical properties via infrared spectroscopy (FTIR), X-ray diffraction (XRD) and thermogravimetric analysis (TGA). Size and morphology were studied via scanning electron microscopy (SEM) and dynamic light scattering (DLS). Further characterisation for photo-responsiveness of AZP nanospheres was studied using UV spectroscopy. Optimised nanospheres were dispersed in HA gel to form HA-NSP which was characterised for rheological properties and injectability through texture analyser and rheometer as well as cytotoxicity effect on HRPE cell lines.

Spherical nanoparticles were obtained with particle size <200nm and demonstrating photo-responsiveness to UV=365nm by decreasing particle diameter to 94nm which was confirmed by DLS. Encapsulation efficiency of the optimised nanospheres was 85% and IgG was released over 32 days up to 60%. Injectability of HA-NSP was confirmed with maximum force 10N required and shear-thinning behaviour observed in rheology studies. *In vitro* cell cytotoxicity effect of both NSPs and HA-NSP showed non-cytotoxicity where the relative cell viability was ≥80%. Cell death was further explored through apoptotic and necrotic pathways and necrosis from HA-NSP treatment was <1% after 48 hours of incubation. A biocompatible, biodegradable injectable photo-responsive nanosystem for sustained release of macromolecular IgG was successfully prepared.

ACKNOWLEDGEMENTS

I would like to express my sincere appreciation to my supervisor, Professor Viness Pillay for his mentorship, guidance and for believing in my research abilities. Without him, the goal of this project would not have been realised. I would also like to thank my co-supervisors, Prof. Yahya Choonara, Prof. Lisa du Toit and Prof Pradeep Kumar. I am grateful to have had the privilege to work under your mentorship, your excellent expertise, guidance, and support has made this possible.

A special thanks to Prof. Pierre Kondiah Dr Thashree Marimuthu and Dr Philemon Ubanako for their support, assistance, and expertise.

My sincere appreciation to the National Research Foundation (NRF) of South Africa and Hetero drugs for their financial assistance.

I wish to extend my heartfelt appreciation to my parents, Billy and Ziqelekazi Mahlumba, thank you for your patience, encouragement, and financial support. I am grateful to God for amazing parents like you and I pray that I continue making you proud.

A special thanks to my siblings for their support and love throughout my academic journey. To my sisters, Zukiswa Mahlumba who has been my anchor, thank you for your unwavering support emotionally and financially; Andiswa Mahlumba, you have always encouraged me to become the best of myself. To Mr Mzwekhaya Dindili, Mrs Nomvula Dindili and their family, thank you for opening your hearts and home to me. And my late brother Vries Mahlumba, whose investment in my education made all of this possible.

Thank you to Mr Sello Ramarumo, Mr Bafana Temba, Mrs Phumzile Moerane, Ms Nompumelelo Damane, Mr Kleinbooi Mohlabi, Dr Mduduzi Sithole, Zikhona Hayiyana, Kgaugelo Moshapo, and fellow colleagues at WADDP for the assistance and support provided to ensure the completion of this project.

DEDICATION

This dissertation is dedicated to my wonderful parents and the youth of my hometown, Bizana.

TABLE OF CONTENTS

CHAPTER ONE
INTRODUCTION AND BACKGROUND

1.1. BACKGROUND OF THIS STUDY **1**
1.2. RATIONALE AND MOTIVATION FOR THIS STUDY **3**
1.3. AIM AND OBJECTIVES OF THIS STUDY **4**
1.4. NOVELTY OF THIS STUDY **5**
1.5. OVERVIEW OF DISSERTATION **5**
1.6. REFERENCES **6**

CHAPTER TWO
STIMULI RESPONSIVE POLYMERIC SYSTEMS FOR CONTROLLED PROTEIN AND PEPTIDE DELIVERY: FUTURE IMPLICATIONS FOR OCULAR DELIVERY

2.1. INTRODUCTION **8**
2.2. RESPONSIVE PROTEIN AND PEPTIDE DELIVERY **11**
2.2.1. pH Responsive Systems **13**
2.2.2. Thermo-Responsive Systems **13**
2.2.3. Enzyme-Responsive Systems **14**
2.2.4. Light-Responsive Systems **15**
2.2.5. Ultrasound-Responsive Systems **16**
2.2.6. Multi-Responsive Systems **17**
2.3. THERAPEUTIC PROTEINS AND PEPTIDES FOR OCULAR DELIVERY **20**
2.4. CURRENT PROGRESS IN RESPONSIVE OCULAR DELIVERY **22**
2.4.1. *In Situ* Forming Ophthalmic/Ocular Delivery System **22**
2.4.2. Implantable Stimuli Responsive Ocular Delivery Systems **24**
2.5. FUTURE PROSPECTS **25**
2.6. CONCLUDING REMARKS **27**
2.7. RECENT ADVANCES **28**
2.8. REFERENCES **28**

CHAPTER THREE

PREPARATION AND CHARACTERIZATION OF PHOTO-RESPONSIVE NANOSPHERES FOR CONTROLLED DELIVERY OF MACROMOLECULES

3.1. INTRODUCTION **37**
3.2. MATERIALS AND METHODS **38**
3.2.1. Materials **38**
3.2.2. Preparation of AZP Nanospheres **39**
3.2.3. Determination of Particle Size and Surface Morphology of the Nanospheres **39**
3.2.4. Determination of Chemical interactions of the Nanospheres **39**
3.2.5. Evaluation of the Light Response Properties of the Nanospheres **40**
3.2.6. Determination of solid-state Structural Properties of the Nanospheres **40**
3.2.7. Determination of Thermal decomposition of the Nanospheres **40**
3.2.8. Ultra-Performance Liquid Chromatographic quantification of Immunoglobulin G **40**
3.3. RESULTS AND DISCUSSION **41**
3.3.1. Particle Size and Morphological Examination **42**
3.3.2. Chemical Transitions and Intermolecular Interactions of the Individual Components and the Nanospheres **43**
3.3.3. Photo-response Assessment of the AZP nanospheres using UV-Vis Analysis and Dynamic Light Scattering **44**
3.3.4. Powder X-Ray Diffraction pattern analysis of the Nanospheres and components **46**
3.3.5. Determination of Thermal Degradation of the Nanospheres **47**
3.3.6. *In Vitro* Drug Release and Encapsulation efficiency of the Nanospheres **48**
3.4. CONCLUDING REMARKS **51**
3.5. REFERENCES **52**

CHAPTER FOUR

DEVELOPMENT AND CHARACTERISATION OF INJECTABLE NANOSPHERES LADEN IN HYALURONIC ACID GEL NANOSYSTEM

4.1. INTRODUCTION **55**
4.2. MATERIALS AND METHODS **56**
4.2.1. Materials **56**
4.2.2. Preparation of Hyaluronic acid gel and Incorporation of AZP nanospheres **56**
4.2.3. Determination of Chemical Interactions of the Photo-responsive Nanosystem **56**
4.2.4. Determination of the Thermal Transitions of the Photo-responsive Nanosystem **57**

4.2.5. Determination of Thermal Decomposition of the Nanosystem **57**
4.2.6. Determination of Injectability of the Photo-responsive Nanosystem **57**
4.2.7. Determination of Rheological Properties of the Photo-responsive Nanosystem **57**
4.2.8. *In Vitro* Cytotoxicity Testing of the Photo-responsive Nanosystem using H-RPE Cell Lines..... **58**
4.2.8.1. Cell culturing using H-RPE Cell Lines..... **58**
4.2.8.2. Cell counting utilizing Trypan blue solution Assay and a Haemocytometer..... **59**
4.2.8.3. *In vitro* cytotoxicity evaluation of the Photo-responsive Nanosystem utilizing Annexin V and Dead cell assay..... **59**
4.3. RESULTS AND DISCUSSION..... **59**
4.3.1. Evaluation of Chemical Transitions and Intermolecular Interactions of the components and Photo-responsive Nanosystem **60**
4.3.2. Thermal and Thermodynamic Analysis of the Photo-responsive Nanosystem **61**
4.3.3. Thermogravimetric Analysis of the Photo-responsive Nanosystem **62**
4.3.4. Determination of Injectability of the Photo-responsive Nanosystem **63**
4.3.5. Rheological behaviour of the Photo-responsive Nanosystem..... **65**
4.3.6. Cell cytotoxicity studies..... **67**
4.4. CONCLUDING REMARKS **70**
4.5. REFERENCES **70**

CHAPTER FIVE

CONCLUSIONS AND FUTURE RECOMMENDATIONS

5.1. CONCLUSIONS..... **75**
5.2. FUTURE RECOMMENDATIONS..... **76**
5.3. REFERENCES **77**

LIST OF FIGURES

Figure 1.1: Schematic representation of the proposed mechanism of drug release by the Geocolloid insert a) The Geocolloid in the SCS b) drug loaded polymer matrix c) Polymeric coating for mechanical strength d) nanosphere before exposure to UV light e) bioactive released through the nanosphere wall after exposure to UV light. **4**

Figure 2.1: (a) Preparation of azobenzene modified dextran (AB–Dex) and cyclodextrin modified dextran (CD-Dex) through the thiol–maleimide reaction. (b) Schematic representation of photo-responsive protein release from the gel composed of trans AB–Dex and CD–Dex. Upon the UV light irradiation azobenzene moieties isomerise from trans to cis configurations, resulting in the dissociation of crosslinking points, and allow the entrapped protein to migrate into the media (Peng et al., 2010). (Reproduced from Peng et al., 2010 with permission of The Royal Society of Chemistry.) **15**

Figure 2.2: Illustration of the mechanism of drug release from a multi-stimuli responsive doxorubicin loaded hydrogel. (a) Physiological temperature (37˚C) causes the hydrogel to collapse and release doxorubicin, with time it regains its original state and (b) shows the application of external magnetic field causing the polymer network to vibrate and release doxorubicin via increased diffusion rate. **18**

Figure 2.3: Schematic representation of the mechanism of encapsulation and release of microparticles by the bilayer self-folding microtubes. The microtubes are formed from a film of poly(N-isopropylacrylamide-co-4-acryloylbenzophenone) (poly (NIPAM-ABP) and polycaprolactone (PCL) mixed with magnetic nanoparticles. The microparticle (a) adsorbs into the bilayer film; at low temperature (less than LCST), the film (b) folds forming a microtube that encapsulates the microparticle; and upon high temperature (above LCST) (c) it unfolds releasing the microparticle. (Reproduced from Zakharchenko et al. (Zakharchenko et al., 2010) with permission of The Royal Society of Chemistry.) **19**

Figure 2.4: Structures of therapeutic proteins and peptides used in the treatment of ocular/ophthalmic disorders as discussed in table 2.3 above. (a) Substance P; (b) Fibronectin; (c)Interferon α2a; (d) Interferon α2b; (e) Cyclosporine A; (f) Bevacizumab; (g) Pegaptinib **22**

Figure 2.5: Schematic presentation of possible ocular routes for administration of stimuli responsive drug delivery systems. (a) Suprachoroidal implantation, injected as liquid and solidifying in contact with stimuli (e.g. temperature, pH), (b) Intravitreal

implant which is also injectable and (c) Topical eye drops that gel when in contact with the eye due to pH and/or temperature. **27**
Figure 3.1: Particle size distribution for (a) blank and (b) IgG loaded AZP nanospheres. **42**
Figure 3.2: Micrographs of freeze-dried IgG loaded AZP nanospheres. **43**
Figure 3.3:FTIR spectra of (a) zein, (b) DHAB and (c) AZP in the range 650cm^{-1}– 4000cm^{-1}. **44**
Figure 3.4:FTIR spectra of (d) gelatin, (e) IgG and (f) IgG loaded AZP nanospheres in the range 650cm^{-1}– 4000cm^{-1}. **44**
Figure 3.5:UV-vis spectra of IgG loaded AZP nanosphere dispersion post-irradiation at different time points..... **45**
Figure 3.6: Diameter of IgG loaded AZP nanospheres upon irradiation with UV light (365nm) as a function of time..... **46**
Figure 3.7:X-ray diffractograms of (a) zein, (b) AZP, (c) DHAB, (d) gelatin, (e) IgG and (f) IgG loaded AZP nanospheres..... **47**
Figure 3.8:TGA thermograms of zein, AZP and DHAB. **48**
Figure 3.9:TGA thermograms of gelatin, IgG and IgG loaded AZP nanospheres. **48**
Figure 3.10: Chromatogram showing the separation peaks for IgG and Cysteine. **49**
Figure 3.11: Calibration curve for quantification of IgG in PBS (pH=7.4) **49**
Figure 3.12: Cumulative IgG release from pure zein nanospheres (red line) and AZP nanospheres post irradiation (black line) over 32 days..... **50**
Figure 3.13: Schematic representation of the transformation from *trans*-to-*cis*-to-*trans* and change in the size of AZP nanospheres upon UV irradiation and white light. .. **51**
Figure 4.1: Images of the formulations (a) pure HA gel, (b) HA-GP gel, (c) pure HA gel, and (d) HA-NSP nanosystem..... **60**
Figure 4.2:FTIR spectra of (a) genipin, (b) pristine HA and (c) HA-GP gel. **61**
Figure 4.3:FTIR spectra of (a) IgG loaded AZP nanospheres and (b) HA-NSP. **61**
Figure 4.4:DSC thermograms of (a) Pristine HA, (b) HA gel, (c) NSP and (d) HA-NSP, measured from 25ºC to 300ºC. **62**
Figure 4.5:TGA thermograms of HA, AZP nanospheres and HA-NSP. **63**
Figure 4.6: Maximum injection force for 1% HA gel and HA-NSP using two needle sizes, 27G and 31G..... **64**
Figure 4.7: Injectability test for (a) 1%w/v HA gel through 27G, (b) HA-NSP through 27G, (c) 1%w/v HA gel through 31G, (d) HA-NSP through 31G needles.. ..... **64**
Figure 4.8: Shear viscosity measurements of pure HA gel and HA-GP gel. **65**
Figure 4.9: Rheology of HA-NSP (a) frequency sweep, (b)stress sweep, and (c) yield stress. **66**

Figure 4.10: Cytotoxicity testing of native components, IgG and HA-NSP on HRPE cells cultured for up to 48 hours. **67**
Figure 4.11: Images showing the various treatments after 48 hours of incubation, (a) untreated cells, (b) IgG, (c) zein, (d) NSP, (e) HA gel and (d) HA-NSP. **68**
Figure 4.12: Apoptosis profiles for (a) untreated cells, (b) IgG, (c) zein, (d) NSP, (e) HA gel and (f) HA-NSP. **69**
Figure 4.13: HRPE cell death presented as percentage apoptosis and necrosis. **69**

LIST OF TABLES

Table 2.1: A summary of stimuli responsive polymers introduced to achieve various objectives for the delivery of active agents. **10**
Table 2.2: Stimuli responsive delivery systems for proteins and peptides. **12**
Table 2.3: A summary of the mechanism of action and delivery of ophthalmic proteins and peptides. **21**
Table 2.4: Examples of the *in situ* forming ocular drug delivery systems illustrated above.. **23**

LIST OF EQUATIONS

Equation 3.1: Determination of Particle yield..... **32**
Equation 3.2: Determination of Drug loading **40**
Equation 3.3: Determination Encapsulation efficiency..... **40**
Equation 4.1: Determination of Relative cell viability **59**

APPENDICES

APPENDIX A **78**
APPENDIX B **79**
APPENDIX C..... **80**
APPENDIX D..... **81**

CHAPTER ONE
INTRODUCTION AND BACKGROUND

1.1. BACKGROUND OF THIS STUDY

Age-related Macular Degeneration (AMD) is an ocular disorder dependent on a number of factors (both genetic and environmental) and results in central visual defect (Prasad et al., 2010). AMD has a harmful effect on the anatomy and function of the macula, involving inflammation, neovascularization and vascular leakage which leads to loss of vision (Ehmann and García, 2010). AMD is one of the main ocular diseases causing progressive bilateral complete vision loss in the elderly (Filloy and Arias, 2013). It is characterized by the presence of extracellular debris, known as the drusen, over the retinal pigmented epithelium (RPE). It is classified as exudative (wet, choroidal neovascularization (CNV), in which new choroidal vessels are formed) and non-exudative (dry, progressive degeneration of the RPE and geographic atrophy) (Ardeljan and Chan, 2013). If left untreated, the lesions of AMD progress to form a fibrous scar, called a disciform scar, which causes irreversible central vision loss. This disease has an enormous impact on the individual's ability to carry out daily activities (Wang et al., 2012). It is estimated that the number of people who suffer from blindness due to AMD exceeds 14 million worldwide. Furthermore, research estimates a 50% increase in the prevalence of the disease by the year 2020 as this continues to rise every year (Prasad et al., 2010).

Angiogenesis is a distinctive characteristic of exudative AMD as it is through this process that the formation of new blood vessels occurs (Miller, 2013). Enhanced release of Vascular Endothelial Growth factor (VEGF) is a significant factor in the process of angiogenesis. VEGF is a glycoprotein responsible for the activation of endothelial cells leading to endothelial cell proliferation. This results in CNV which causes accumulation of fluid between the RPE and photoreceptors, exudation, bleeding, RPE detachment, and vision loss consequential to scarring (Velez-montoya et al., 2013). Various treatments are being explored to target different factors associated with AMD, such as inflammation and neovascularization. After the use of intravitreal injections, prognosis of the disease significantly improved and there is a 90% possibility of a stable and increased vision. However, there are side-effects (cataracts, retinal detachment, retinal tear, uveitis, vitreous haemorrhage, traumatic lens damage and endophthalmitis) associated with intravitreal injections and the frequency of dosing (1.25mg monthly intravitreal dose) which becomes a challenge when it comes to patient compliance (Velez-montoya et al.,2013).

Anti-VEGF agents have been found to increase the visual prognosis more than other treatment options. Photodynamic therapy (PDT) reduces vision loss but does not improve visual acuity and photocoagulation therapy (PCT) shows high recurrence of neovascularisation and development of atrophic scars. For this reason, anti-VEGF agents are used as first line treatment for AMD, and they are able to reverse the pathological effects of AMD. Monoclonal antibodies are currently available as anti-VEGF treatment; examples include, pegaptanib sodium (Macugen®) injected into the vitreous cavity at 6 week intervals, ranibizumab (Lucentis®) a recombinant, humanized antibody that has a small molecular mass, administered monthly (half-life of 2-4 days) and bevacizumab (Avastin®) a full length recombinant, humanized monoclonal antibody with a half-life of approximately 20 days and molecular mass three times that of ranibizumab (Ehmann and García, 2010).

Currently, drugs are injected into the vitreous humour though the therapeutic site of action for AMD is the choroid and retina. Other potential routes of delivery to the back of the include the Peri-Ocular Space (POS) and the Suprachoroidal Space (SCS). The POS has the disadvantage of haemorrhage risk at the site of injection. The SCS route protects the retina from injection related damage. The SCS is located between the choroid layer and the sclera and is capable of expanding to accommodate an intraocular insert (Patel et al., 2012). Smart materials (Stimuli responsive polymers (SRPs) are capable of sensing the environment and changing their function to suit a pre-programmed purpose. SRPs have advantages of diverse stimuli response, they have a wide range of structural designs and different polymers can be used to achieve different various effects. These provide site-specific drug release which minimizes systemic side-effects and increase bioavailability (Hu et al., 2012). Application of stimulus from an external source has an advantage of controlling the rate of response and the specific location of release. To achieve photo-responsiveness, a chromophore such as azobenzene derivatives, spiropyran and pyrenylmethyl is added into the polymers. The chromophore is the photo-responsive moiety responsible for the change in structural conformation, solubility, degradability, and self-assembly behaviour leading to the release of the loaded drug (Roy et al., 2010).

Therefore, this study investigates a potential intraocular insert with minimal frequency of administration of at least 2 month intervals compared to the highly invasive monthly intravitreal injections. The insert will utilize an alternate route of administration to avoid damage to the retina and complications (cataracts, retinal detachment, retinal tear, uveitis, vitreous haemorrhage, traumatic lens damage and endophthalmitis) experienced with intravitreal injections while sustaining a curative amount of the bioactive at the target tissue.

1.2. RATIONALE AND MOTIVATION FOR THIS STUDY

Site-specificity of the Geocolloid insert may give a therapeutic advantage by minimizing systemic side-effects and localizing treatment at the site of disease, compared to the commonly used topical route for ocular drug delivery which is convenient but not ideal for the posterior segment of the eye due to tissue barriers that lead to low therapeutic concentration of the drug at the target site (choroid and retina).

Compared to the frequently administered, highly invasive intravitreal injections, the Geocolloid insert may provide a prolonged release and localized therapy via bypassing the vitreous humour. Photo-responsive properties of the Geocolloid (due to the incorporation of a photo-responsive moiety) allow for enhanced release, which is also reversible, therefore, can provide lower doses for maintenance therapy with less repeats of invasive procedures. Patient adherence is increased with the use of inserts due to the frequency of administration that is decreased. The insert may also be used in the treatment of other chorio-retinal diseases other than AMD.

The schematic in **Figure 1.1** explains the proposed mechanism of drug release from the nanosphere component. The bioactive and the photo-responsive moiety will be incorporated into the nanospheres which have a high loading capacity. The Geocolloid can be inserted by injection either into the SCS via peritomy and sclerotomy or via sub-Tenon route where it will release the bioactive. When exposed to light of wavelength ranging from 320nm to 380nm, the nanospheres undergo photo-isomerisation due to the presence of a chromophore (i.e. *trans* to *cis* conformation) and release the bioactive. The reaction is reversed thermally by exposing nanospheres to white light.

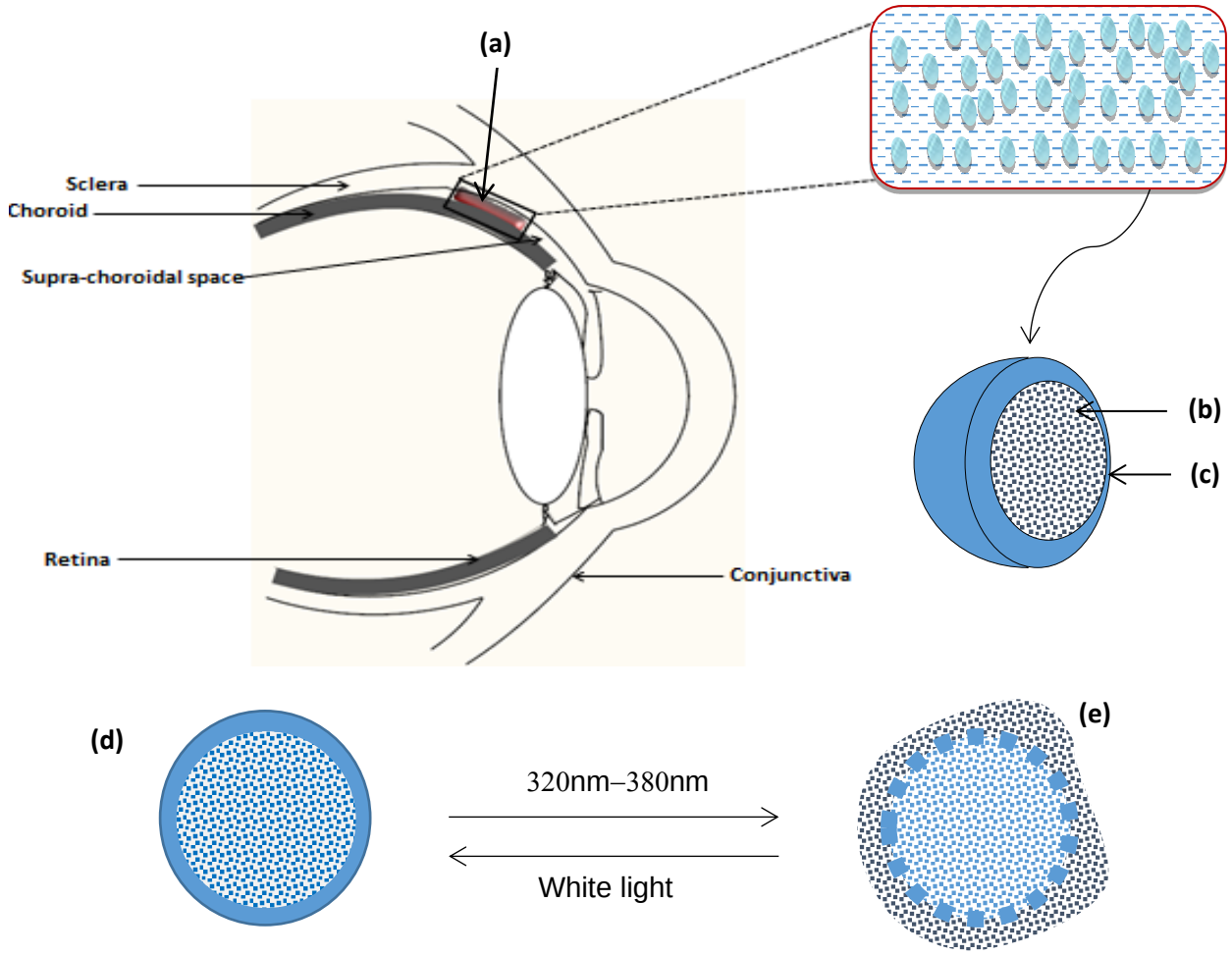

Figure 1.1: Schematic representation of the proposed mechanism of drug release by the Geocolloid insert a) The Geocolloid in the SCS b) drug loaded polymer matrix c) Polymeric coating for mechanical strength d) nanosphere before exposure to UV light e) bioactive released through the nanosphere wall after exposure to UV light.

1.3. AIM AND OBJECTIVES OF THIS STUDY

The aim of this study is to design a minimally invasive insertable Geocolloid system that when exposed to light of certain wavelength will geometrically reorganize at molecular level in a reversible manner, in order to achieve site-specific drug delivery. This can be achieved through the following objectives:

1. Selection of biocompatible, biodegradable, bio-adhesive polymers with drug entrapment and stimuli responsive properties for the preparation of a prolonged release, stimuli responsive intra-ocular insert.
2. To develop a drug-loaded Geocolloid insert with site-specificity and prolonged release of approximately 2 months. Determination of photo-responsiveness via analysis of the nanospheres before and after exposure to UV light to determine transitions and erosion.
3. To evaluate the physicochemical and physico-mechanical properties of the injectable nanosystem via determination of mechanical strength, particle size and morphology, drug

loading capacity, drug-polymer interactions, melting point of the polymers. drug release behaviour of the injectable insert using *in vitro* drug release studies.

4. To evaluate photo-responsive and drug release behaviour of the injectable nanosystem using *in vitro* drug release studies.
5. To evaluate cytocompatibility of the injectable insert via *in vitro* cell cytotoxicity studies.

1.4. NOVELTY OF THIS STUDY

The Geocolloid is a nanosystem that is stimuli responsive and the release of the bioactive can be controlled externally through manipulation of the photo-responsive groups (chromophore) using UV light (365nm). It is an injectable delivery system which can be administered with minimal invasion to tissue and able to reach irregular target sites such as the posterior segment of the eye via SCS/sub-Tenon routes, where treatment is localized to the diseased tissue, thus optimising therapeutic levels. Photo-responsiveness of the nanosystem further allows a less invasive approach of controlling release of the bioactive. This enhances therapeutic response and patient adherence, therefore improving disease prognosis.

1.5. OVERVIEW OF DISSERTATION

CHAPTER 1: This chapter presents the background of the current research in the field and provides shortcomings experienced in posterior ocular drug delivery, principally for the macromolecular monoclonal antibodies. Rationale for the research, the aim and objectives carried out are detailed.

CHAPTER 2: In this chapter, a literature review emphasizing the research investigating stimuli responsive materials for drug delivery. This chapter reviews stimuli responsive systems in the delivery of macromolecular therapeutics and their potential for the treatment of ocular abnormalities. A detailed discussion of stimuli responsive systems over conventional delivery systems is outline.

CHAPTER 3: This chapter outlines the synthesis and formulation of the injectable photo-responsive nanosystem (HA-NSP), physico-mechanical and physicochemical characterization of the delivery system, investigation of stimuli response of the nanospheres and *in vitro* release studies. Characterization methods discussed in this chapter include, attenuated total reflectance infrared spectroscopy (ATR-FTIR), thermogravimetric analysis (TGA), X-ray diffraction (XRD) and UV-visible spectroscopy.

CHAPTER 4: The main focus of this chapter is the development of the injectable photo-responsive nanosystem which comprises of the nanospheres dispersed in gel. In addition, characterisations of the photo-responsive nanosystem through rheology, thermal analysis and texture analysis, and *in vitro* cytotoxicity study of the photo-responsive injectable nanosystem (HA-NSP) on H-RPE cell lines are discussed.

CHAPTER 5: This chapter concludes the dissertation and provides recommendations for further improvements to the photo-responsive nanosystem for optimisation of its functionality in the controlled delivery of macromolecules.

1.6. REFERENCES

Ardeljan, D., Chan, C.-C., 2013. Aging is not a disease: distinguishing age-related macular degeneration from aging. Prog. Retin. Eye Res. 37, 68–89. https://doi.org/10.1016/j.preteyeres.2013.07.003

Ehmann, D., García, R., 2010. Triple therapy for neovascular age-related macular degeneration (verteporfin photodynamic therapy, intravitreal dexamethasone, and intravitreal bevacizumab). Can. J. Ophthalmol. 45, 36–40. https://doi.org/10.3129/i09-243

Filloy, a., Arias, L., 2013. Responses to ranibizumab in wet age-related macular degeneration patients with vitreomacular traction. Arch. la Soc. Española Oftalmol. (English Ed. 88, 380–386. https://doi.org/10.1016/j.oftale.2013.01.005

Hu, J., Zhu, Y., Huang, H., Lu, J., 2012. Recent advances in shape–memory polymers: Structure, mechanism, functionality, modeling and applications. Prog. Polym. Sci. 37, 1720–1763. https://doi.org/10.1016/j.progpolymsci.2012.06.001

Patel, S.R., Berezovsky, D.E., McCarey, B.E., Zarnitsyn, V., Edelhauser, H.F., Prausnitz, M.R., 2012. Targeted administration into the suprachoroidal space using a microneedle for drug delivery to the posterior segment of the eye. Invest. Ophthalmol. Vis. Sci. 53, 4433–41. https://doi.org/10.1167/iovs.12-9872

Prasad, P.S., Schwartz, S.D., Hubschman, J.-P., 2010. Age-related macular degeneration: current and novel therapies. Maturitas 66, 46–50. https://doi.org/10.1016/j.maturitas.2010.02.006

Roy, D., Cambre, J.N., Sumerlin, B.S., 2010. Future perspectives and recent advances in stimuli-responsive materials. Prog. Polym. Sci. 35, 278–301.

https://doi.org/10.1016/j.progpolymsci.2009.10.008

Velez-montoya, R., Oliver, S.C.N., Olson, J.L., Fine, S.L., Mandava, N., Quiroz-mercado, H., 1985. Age-related macular degeneration: Today's and Future Treatments. Retina 33, 1487–1502.

Wang, M.Y., Rousseau, J., Boisjoly, H., Schmaltz, H., Kergoat, M.-J., Moghadaszadeh, S., Djafari, F., Freeman, E.E., 2012. Activity limitation due to a fear of falling in older adults with eye disease. Invest. Ophthalmol. Vis. Sci. 53, 7967–72. https://doi.org/10.1167/iovs.12-10701

CHAPTER TWO

STIMULI RESPONSIVE POLYMERIC SYSTEMS FOR CONTROLLED PROTEIN AND PEPTIDE DELIVERY: FUTURE IMPLICATIONS FOR OCULAR DELIVERY

Published in Molecules as: *Stimuli-Responsive Polymeric Systems for Controlled Protein and Peptide Delivery: Future Implications for Ocular Delivery*

Pakama Mahlumba, Yahya E. Choonara, Pradeep Kumar, Lisa C. du Toit, Viness Pillay*

Molecules. 2016 Aug; 21(8): 1002. Published online 2016 Jul 30.

doi: 10.3390/molecules21081002

2.1. INTRODUCTION

Therapeutic proteins and peptides are advantageous over small molecule drugs in that they mimic similar molecules found in the human body; they are biocompatible and highly potent. However, limitations (drug related and patient related) do exist caused by high molecular weight, poor transfer across biological membranes, provocation of immune response, short half-lives and instabilities of the molecules (Pisal et al., 2010; Ratnaparkhi et al., 2011). The controlled release of therapeutic proteins is regarded as a way to increase the efficacy while reducing side effects, and therefore improving the patient's quality of life (Koyamatsu et al., 2014).

The most commonly used route of administration for proteins and peptides is the parenteral route i.e., injection/intravenous infusion providing direct administration into the bloodstream. Though this route can overcome some of the limitations, it is costly, painful and results in low patient acceptance (Antosova et al., 2009). Alternative routes comprise of the nasal route which provides rapid absorption of the active agent, increased bioavailability and ease of administration, and bypasses gastrointestinal tract related degradation. The use of nanoparticles as a carrier allows delivery directly into the brain via the nasal route but the dose range is restricted by the surface area of the nasal epithelium. The oral route which has come across a number of challenges involving probable degradation ascribed to the acidic environment in the stomach, first pass metabolism in the liver and the proteolytic enzymes in the intestinal tract. The pulmonary route with its large surface area and the thin alveolar epithelium permits rapid protein/peptide absorption and also avoids first pass metabolism. Vaginal route is used for systemic delivery of proteins and peptides through the rich blood supply in the vagina. Numerous limitations exist in this route as it is specific for females, sensitive, associated with irritation and patients are reluctant to use this route. Transdermal route favours the delivery of proteins and peptides with short half-lives and provides sustained

delivery. The limitation with this route is the stratum corneum which has a low permeability, and this becomes a major challenge in the delivery of proteins and peptides due to their size, therefore modifications of the drug delivery systems is required. The ocular route is potentially useful for systemic delivery of therapeutic proteins and peptides; however, it is often used for localized delivery of ophthalmic agents. This route attracts attention as the most interesting and challenging in drug delivery due to the sensitive and complex environment of the eye (Sharma et al., 2011). Challenges involve ocular barriers that interfere with absorption of proteins and peptides resulting in insufficient levels at the target site, reduced bioavailability caused by decreased residence time, invasive and frequent administration leading to poor patient compliance, and instability of these molecules (Kompella et al., 2013; Yasin et al., 2014). A group of polymers referred to as stimuli responsive materials is under investigation for use in the delivery of therapeutic proteins and peptides.

Stimuli responsive polymers (**Table 2.1**) are defined as materials that display rapid physicochemical transition in response to small changes in the surrounding environment. Such polymers in biomedical applications and drug delivery platform have become part of the main focus due to their distinct features and ability to control drug release (Roy et al., 2010). Classification of these polymers is based on two controls, the proximal (disease specific) and the remote (non-disease specific) control of stimuli response further classified as physical or biochemical stimuli. Desirable characteristics include biodegradability, biocompatibility, contaminant/pyrogen-free, non-toxic, low cost, high loading capacity and an excellent stability profile. The use of these polymers provides a less invasive delivery approach via externally controlled stimuli and extended stability in the body owing to their stimuli specific and therefore site-specific release (Oak et al., 2012). Their reversible mechanism upon removal of the trigger is likely to minimize the possibility of drug related toxicity. Stimuli responsive polymeric delivery systems have a potential to at most overcome the challenges faced with ocular protein and peptide delivery. A group of stimuli responsive drug delivery systems known as *in situ* forming systems has increasingly gained interest over the years. These systems consist of phase transition polymers which enable them to be injectable solidifying at the site of delivery via response to various stimuli such as ions, pH, and temperature. *In situ* formation can occur as a result of physical or chemical alteration in the delivery system. The rationale for these systems arises from a number of formulation shortcomings which will be discussed in detail below (Cohen et al., 1997; Ruel-Gariépy and Leroux, 2004).

This review explores possible alternatives for responsive ocular protein/peptide delivery by evaluating various stimuli employed, responsive systems that have been designed to deliver

these molecules as well as therapeutic proteins and peptides used in the treatment of ocular disorders. Examples of stimuli included are pH, temperature, glucose, enzymes, light, ultrasound, and magnetic field. This work also considers advances in stimuli responsive ocular delivery systems that have been designed over the years. This work evaluates the future of stimuli responsive delivery systems in ocular delivery of therapeutic proteins and peptides.

Table 2.1: A summary of stimuli responsive polymers introduced to achieve various objectives for the delivery of active agents.

Model drug	Polymer	Stimuli	Objective	Reference
Timolol Maleate	Poloxamer and Chitosan	Temperature	Improve mechanical and mucoadhesive properties and improve retention time for the treatment of ocular diseases.	(Gratieri et al., 2010)
Puerarin	Poloxamer and Carbopol	Temperature	Maintain sufficient drug concentration at precorneal area.	(Qi et al., 2007)
Timolol Maleate	Poly(N-isopropylacrylamide) and Chitosan	Temperature	Improve bioavailability and efficacy.	(Almeida et al., 2014)
Cyclosporine A	Gellan gum	Electrolytes	Increase drug loading capacity.	(Gan et al., 2009)
Ofloxacin	Polyacrylic acid and HPMC	pH	To provide sustained release of the drug during treatment.	(Srividya et al., 2001)
Gatifloxacin	Alginate and HPMC	Ions	Enhance ocular bioavailability and patient compliance.	(Kushwaha et al., 2012)
Pilocarpine hydrochloride	Xyloglucan	Temperature	To achieve sustained ocular delivery.	(Brown et al., 1976; Miyazaki et al., 2001)
Peurarin	Carbopol and Methylcellulose	Temperature and pH	Improve gel strength, increase precorneal residence time and bioavailability.	(Wu et al., 2007)
Diclofenac sodium	Thiolated poly(aspartic acid)	Oxidation	Prolong the residence time and reduce the administration frequency.	(Horvát et al., 2015)

2.2. RESPONSIVE PROTEIN AND PEPTIDE DELIVERY

Proteins and peptides are widely used in the field of therapeutics mainly because of their ability to mimic those that are produced by the human body which renders compatibility with the body and a relatively high potency. Biodegradable polymers have been used to achieve a delivery strategy that protects proteins and peptides from the human body and vice versa. These polymers are able to encapsulate proteins and peptides and release following degradation kinetics; however, when other formulation factors dominate they interfere with degradation kinetics (Ye et al., 2010). Using degradable responsive polymers and attaching responsive moieties to the polymers in use gives rise to stimuli responsive polymeric systems which are capable of sensing surrounding environmental changes and in response release the encapsulated therapeutic protein or peptide (Oak et al., 2012; Qi et al., 2007). Stimuli responsive polymers have the ability to respond to stimuli present in the human body enabling site specific delivery of therapeutic proteins and peptides. Response to stimulus can occur via formation or destruction of secondary forces such as hydrogen bonding and simple reactions like acid-base reaction from the responsive moieties in the polymer (Roy et al., 2010). These are advantageous in that they are capable of on and off release, that is, only the amount of drug required for a therapeutic effect at the time is released. **Table 2.2** summarizes various delivery systems employed responsive delivery of proteins and peptides.

Table 2.2: Stimuli responsive delivery systems for proteins and peptides.

Stimuli	Model Protein/Peptide	Responsive moiety	Mechanism	Delivery system	Reference
pH	Print 3G	Cholesterylhemisuccinate (CHEMS)	CHEMS possesses an inverted cone shape at physiological pH. Under acidic conditions, the carboxylic acid group becomes protonated and CHEMS loses the shape releasing the protein. This transition occurs within endosome where pH is decreased during endocytosis.	Liposomes	(Almeida et al., 2014; Huth et al., 2006; Schmucker et al., 2011)
pH	BSA	PLGA-carboxyl group	Undergoes deprotonation at neutral or basic pH which leads to release of the protein.	Micelles	(Garbern et al., 2010; Kang Derwent and Mieler, 2008)
Enzyme (Human Neutrophil elastase)	Anti-inflammatory proteins/peptides	HNE-sensitive peptides (Aminobutyric acid, Novarline, Norleucine)	HNE diffuses into the hydrogel and splits the substrate releasing the therapeutic agent into the site of action.	Hydrogel	(Cohen et al., 1997)
Enzyme (Chitosanase)	Fluorescein isothiocyanate-labelled albumin (FITC-albumin)	Chitosan	Enzymatic degradation weakens the capsule wall releasing the protein and the capsule is destroyed over time. Degradation is specific to chitosanase.	Hollow capsules	(Kumar et al., 1994)
Multi-stimuli (Magnetic field, temperature, pH)	Doxorubicin	α-amino acid residues, vinyl based polymers, Iron oxide nanoparticles	At pH 7.4 chain complexation occurs enhancing the stability of the polymer chains. At 37˚C, the hydrogel collapses and the release increased until the collapse is terminated after a few days and the release is decreased. After this, the magnetic field is applied which causes vibration of the hydrogel network accelerating diffusion rate.	Polyeletrolyte hydrogel	(Schoenwald, 1997)
Dual stimuli (pH,glucose)	Insulin	Concanavalin A, N-(2-(dimethylamino) ethyl)-methacrylamide	Decrease in pH causes ionization of the amino groups causing swelling. Concanavalin A binds glucose, reducing crosslinking density in mycrohydrogels and increasing hydrophilicity leading to swelling then release of Insulin.	Microhydrogel	(Cao et al., 2007)

2.2.1. pH Responsive Systems

The mostly used stimulus in oral drug delivery of proteins and peptides is the pH. This is to avoid the degradation of these agents; however, the stimulus can be employed ocularly especially for topical delivery to increase residence time via targeting the pH of the tear fluid. Ducat and co-workers (Ducat et al., 2011) proved the benefit of using pH sensitive liposomes in preference to conventional liposomes as a vector for the delivery of a peptide that antagonizes an oncoprotein in breast cancer, Print3G. The rationale being that the pH responsive liposomes improve efficacy and site specificity as they release the peptide inside the cell. The mechanism of these liposomes lies in the presence of the compound, Cholesterylhemisuccinate (CHEMS), which possesses an inverted cone shape at physiological pH. Under acidic conditions, the carboxylic acid group becomes protonated and CHEMS loses the shape releasing the protein. This transition occurs within endosome where pH is decreased during endocytosis (Kim and Lee, 2010).

In another study, Koyamatsu and colleagues (Koyamatsu et al., 2014) designed reverse polymer micelles using biodegradable, biocompatible poly (ethylene glycol) (PEG) and poly (D, L-lactic-co-glycolide) (PLGA) with the terminal carboxyl group in PLGA conferring the pH responsiveness of the micelles. Bovine serum albumin and streptavidin were used as model proteins to prove the encapsulation and controlled release of large molecules from the micelles. The micelles release the loaded protein at the targeted site and this is due to their pH-responsive property (Chiu et al., 2008). The swelling behaviour of hydrogels in combination with pH sensitivity is observed in microspheres and beads designed by El-Sherbiny and Gong et, al. respectively. These systems are designed to swell at a certain pH and release the loaded protein bypassing degradants and localizing therapy improving therapeutic outcomes and bioavailability (Kushwaha et al., 2012; Miyazaki et al., 2001).

2.2.2. Thermo-Responsive Systems

Temperature as a stimulus can either be external, that is change in temperature due to an external trigger e.g. radiation, or internal which is change in temperature caused by the disease state such as inflammation. These changes in temperature can be used to trigger drug delivery at higher or lower temperatures depending on the nature of the polymer employed. Thermo-responsive polymers have a lower critical solution temperature (LCST) which is the highest temperature at which the polymer is soluble and above that temperature they become insoluble or upper critical solution temperature (UCST), the lowest temperature of miscibility (Brown et al., 1976; Wu et al., 2007). Hydrogels are mostly preferred because of their macro-porous structure and swelling properties. In the delivery of proteins and peptides,

their macro-porous structure makes them good and efficient carriers for such macromolecular drugs. Responsive hydrogels are especially good for sustained delivery of proteins and peptides as their aqueous environment is able to protect these fragile drugs (Hoffman, 2002). An example of investigated responsive delivery of proteins is a poly (N-isopolyacrylamide) (NIPAM) based implantable hydrogel designed by Ninawe and colleagues (Ninawe et al., 2010). In this study NIPAM with LCST of 32˚C was used as the temperature responsive gelling polymer and a model protein immunoglobulin G (IgG) was loaded into the gel for delivery to the posterior segment of the eye via implantation in the sclera as the treatment of age-related macular degeneration (AMD). After implantation, the gel uses the mechanism of deswelling when it reaches body temperature releasing the drug to diffuse across the sclera reaching the target site which is the choroid and retinal pigment epithelium (RPE). The remaining protein is released via diffusion when deswelling is terminated. Thermo-responsive systems can also be used to enhance selectivity for targeted tissue to protect normal tissue from damage by the therapeutic peptides. The system is designed to release at local temperature of diseased tissue and release is terminated at body temperature therefore normal tissue is not affected.

2.2.3. Enzyme-Responsive Systems

Enzymes are biocompatible, function under mild conditions, and hold a high degree of selectivity and these are advantages that make them good candidates as triggers for stimuli responsive release. These can be enzymes responsible for degradation or enzymes over-expressed in disease states (disease specific). Upon exposure to the target enzyme (thermolysin), selective enzymatic hydrolysis of the enzyme-cleavable peptide resulted in the release of anionic fragments, leaving anchored cationic fragments that convert the neutral poly(ethylene glycol acrylamide) particles into cationic particles. This charge switch leads to particle swelling and a significant increase in overall particle diameter, a visual indication of increased internal mesh size. This allowed the triggered release of entrapped proteins that had been pre-loaded into the particles (Thornton et al., 2008). An enzyme-responsive hydrogel reported by Aimetti and co-workers (Aimetti et al., 2009) used Human Neutrophil elastase (HNE), secreted by neutrophils found at inflammation site, as the triggering enzyme for the hydrogel in the delivery of anti-inflammatory therapeutics. The hydrogel only releases at the site of inflammation due to the presence of neutrophils and performs localized and site-specific delivery avoiding drug-related systemic side-effects. HNE-sensitive linkers were added to poly (ethylene glycol) diacrylate (PEGDA) for the sensitivity of the hydrogel. HNE diffuses into the hydrogel and splits the substrate releasing the therapeutic agent at the site of action. In another study done by Itoh and co-workers (Itoh et al., 2006), enzymatic degradation which is experienced with most drug delivery systems in the body was used as an aid to achieve

controlled delivery of protein drugs. Fluorescein isothiocyanate-labelled albumin (FITC-albumin) was used as the model protein to prove drug loading and release properties of the hollow capsules that were designed. Enzymatic degradation by chitosanase weakens the capsule wall causing it to wrinkle and change shape releasing the therapeutic protein. No change in the capsule was observed in the absence of chitosanase therefore the degradation is specific to the enzyme chitosanase and the capsule is biodegradable, destroyed over time.

2.2.4. Light-Responsive Systems

Amongst the stimuli employed in drug delivery, light has been found to be one of the interesting stimuli due to its remote action as a stimulus allowing spatial control and convenience (Yagai and Kitamura, 2008). Photo responsiveness is exhibited through photochromic photo-switchable molecules such as spyropyran, anthracene and azobenzene which make the system photo-triggerable (Shum et al., 2001). **Figure 2.1** shows azobenzene modified dextran and mechanism of photo-triggering protein release.

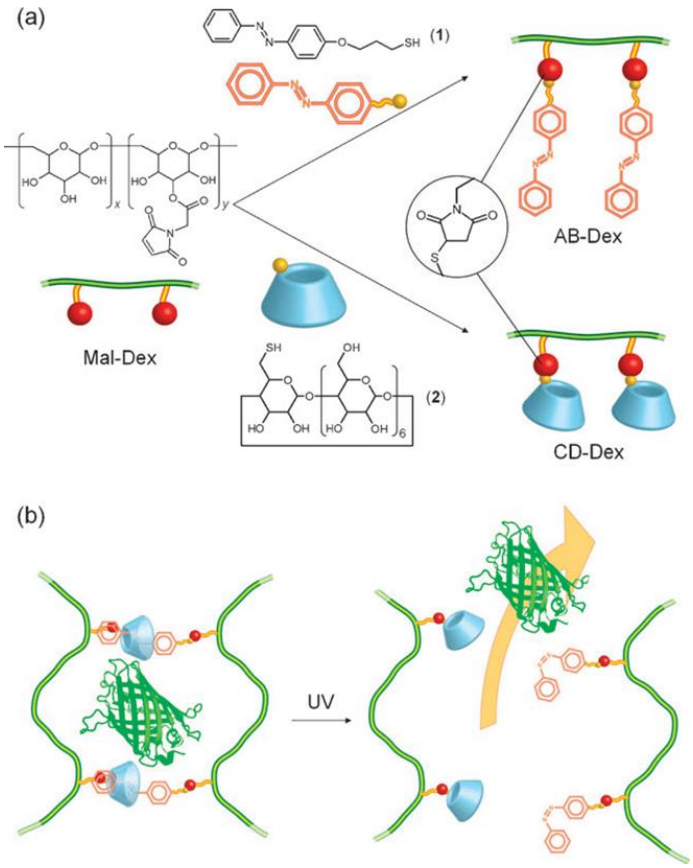

Figure 2.1: (a) Preparation of azobenzene modified dextran (AB–Dex) and cyclodextrin modified dextran (CD-Dex) through the thiol–maleimide reaction. (b) Schematic representation of photo-responsive protein release from the gel composed of trans AB–Dex and CD–Dex. Upon the UV light irradiation azobenzene moieties isomerise from trans to cis configurations, resulting in the dissociation of crosslinking points, and allow the entrapped protein to migrate into the media (Peng et al., 2010). (Reproduced from Peng et al., 2010 with permission of The Royal Society of Chemistry.)

Kang and co-workers (Kang Derwent and Mieler, 2008) reported on light responsive core-shell nanogels formed from gold-silver nanorods (Au-Ag NRs) coated with polymeric shells cross-linked with DNA. Doxorubicin was used as a model drug encapsulated in the gel scaffold. Au-Ag NRs act as photo-thermal convectors by absorbing near infrared photon energy which is then converted to heat and elevates temperature at the target site therefore increasing membrane permeability. This mechanism of action achieves targeted delivery, efficacy and optimal protein levels at target tumour cells (Kumar et al., 1994; Schoenwald, 1997). Light responsive nanosized polyion complex micelles with switchable surface charge designed by Jin et.al (Jin et al., 2014) are nano vehicles suitable for intracellular delivery of proteins. The polyion complex is formed by a light responsive block copolymer, poly (N, N-dimethyl-N-(2-(methacryloyloxy)-ethyl)-N-((2-nitrobenzyl)oxy)-2-oxoithaminium bromide)-block (carboxybetaine methacrylate) (PDMNBMA-b-PCBMA) with anionic bovine serum albumin (BSA) through electrostatic interaction. The surface charge of the polyion complex is changed at the tumor site (acidic pH) from neutral (physiological pH) to positive due to carboxylate group protonation. UV irradiation causes transformation of positively charged PDMNBMA blocks to zwitterionic carboxybetaine which results in polyionic complex micelles disassembling and BSA released promptly. This exogenously controlled light responsive delivery system was designed to overcome the controlled release challenge posed by physiological factors which observed in the use of endogenous stimuli such as pH and temperature (Zhao et al., 2012).

2.2.5. Ultrasound-Responsive Systems

Ultrasound is also an exogenous stimulus used as a trigger for drug release which employs pressure waves with frequency of about 20 kHz and above. The mechanism of ultrasound involves a medium that focuses and reflects and refracts the ultrasonic waves. Ultrasound responsive drug delivery systems that have been designed are microbubbles, nanodroplets, nanobubbles, micelles, liposomes, etc (Chiu et al., 2008; Kim and Lee, 2010). Wang and co-workers (Wang et al., 2009) investigated ultrasound responsive behaviour of polymeric micelles formed from poly(ethylene oxide)-block-poly(2-tetrahydropyranyl methacrylate) (PEO-b-PTHPMA) an amphiphilic diblock copolymer. Upon exposure to high intensity focused ultrasound (HIFU), ultrasonic cavitation occurs at the site of action generating very high local temperature (500K) and pressure (500atm) leading to rapture of polymeric chains therefore release of the encapsulated active agent (Suslick, 1990).

2.2.6. Multi-Responsive Systems

Multi-stimuli responsive drug delivery systems enhance sustained delivery by synergistically acting on the system resulting in a more improved control of release. These can involve a combination of materials that are responsive to two or more stimuli. An example is a multi-stimuli responsive hydrogel designed by Casolaro and co-workers (Casolaro et al., 2014) included pH, temperature and magnetic field as stimuli. Casolaro used α-amino acid residues, including L-valine, structurally similar to poly (*N*-isopropylacrylamide) (pNIP) to form vinyl polyectrolyte hydrogels. The external stimulation of the magnetic field, through the magnetic nanoparticles embedded into the hydrogel, directs the system to the specific target tissue for localized release and induces local hyperthermia stimulating the thermo-responsive part of the system. The mechanism of protein release from the hydrogel is illustrated in **figure 2.2**. At pH 7.4 chain complexation occurs enhancing the stability of the polymer chains. At 37˚C, the hydrogel collapses and the release increased until the collapse is terminated after a few days and the release is decreased. After this, the magnetic field is applied which causes vibration of the hydrogel network accelerating diffusion rate. The magnetic field is suspected to increase hydrogel temperature stimulating the thermo-responsive NIP. The release can be manipulated remotely through external triggers, either by increasing the magnetic field strength and or temperature.

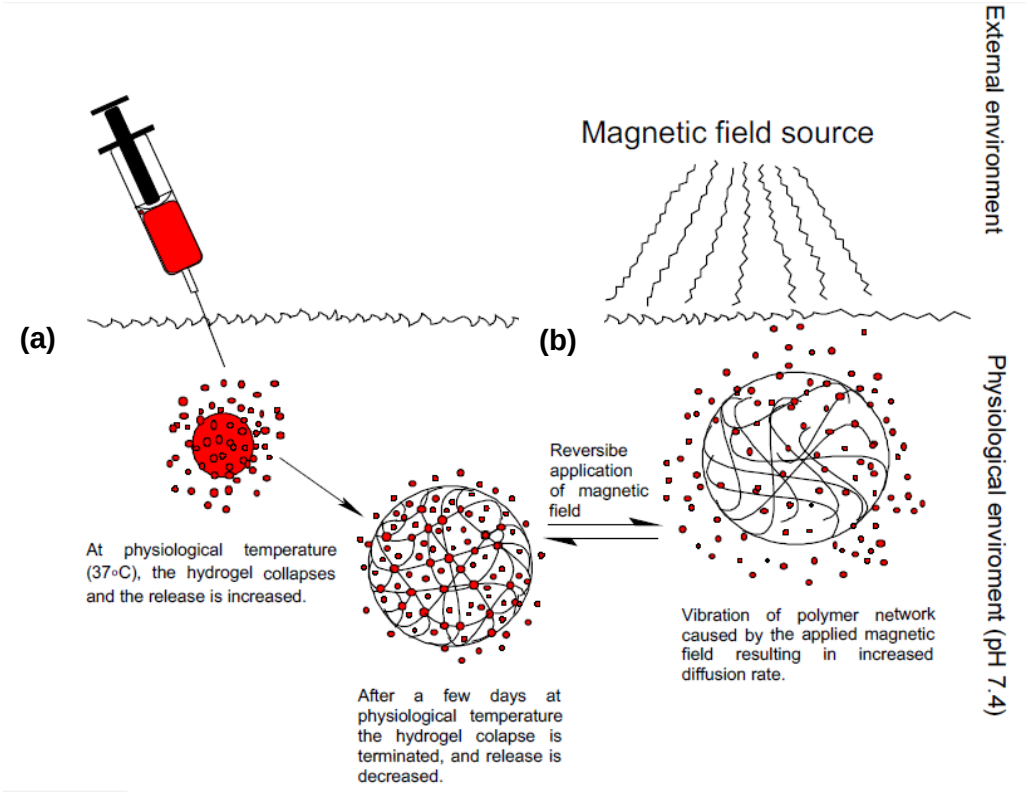

Figure 2.2: Illustration of the mechanism of drug release from a multi-stimuli responsive doxorubicin loaded hydrogel. (a) Physiological temperature (37˚C) causes the hydrogel to collapse and release doxorubicin, with time it regains its original state and (b) shows the application of external magnetic field causing the polymer network to vibrate and release doxorubicin via increased diffusion rate.

Yin and co-workers (Yin et al., 2014) prepared dual-responsive Concanavalin A based microhydrogels sensitive to both pH and glucose for the delivery of insulin. The sensitivity of insulin release from microhydrogels was observed upon small change in pH value, insulin released was rapidly increased with decrease in pH via swelling of the system due to ionization of the amino groups. Increasing the pH leads to hydrogen bonding within the amino groups which forms a complex that restricts the motion in polymer network chains and therefore restricting the release of insulin. Free glucose seizes the specific binding sites of Con A–polymer complex leading to the dissociation of the complex and resulting in a glucose sensitive delivery system. Results observed from characterization of the system show an increase in insulin release with increasing glucose concentration, also a rapid change was observed with every change in glucose concentration. The presence of glucose reduces crosslinking density in microhydrogels and increases their hydrophilicity resulting in swelling. The microhydrogels are biocompatible and they make good systems for self-regulated delivery of insulin (Thornton et al., 2008).

Zakharchenko and colleagues report on thermo-magneto-responsive bilayer self-folding microtubes as carriers of drug loaded microparticles. The bilayer was made from a copolymer poly(N-isopropylacrylamide-co-4-acryloylbenzophenone) (poly(NIPAM-ABP)) which is a combination of thermo-responsive poly(N-isopropylacrylamide) (PNIPAM) and photo-responsive photo-crosslinker, 4-acryloylbenzophenone (ABP) with hydrophobic polycaprolactone (PCL). PCL forms the outer layer of the microtube mixed with magnetic nanoparticles. At low temperature below LCST, the bilayer film folds and encapsulates the drug loaded microparticle and at elevated temperature above LCST, it unfolds and releases the microparticle. The mechanism of thermo-responsiveness of the microtubes is illustrated in **figure 2.3**. Magnetic nanoparticles enable remote control of the microtubes via magnetic field which makes the system multi-stimuli responsive (Zakharchenko et al., 2010).

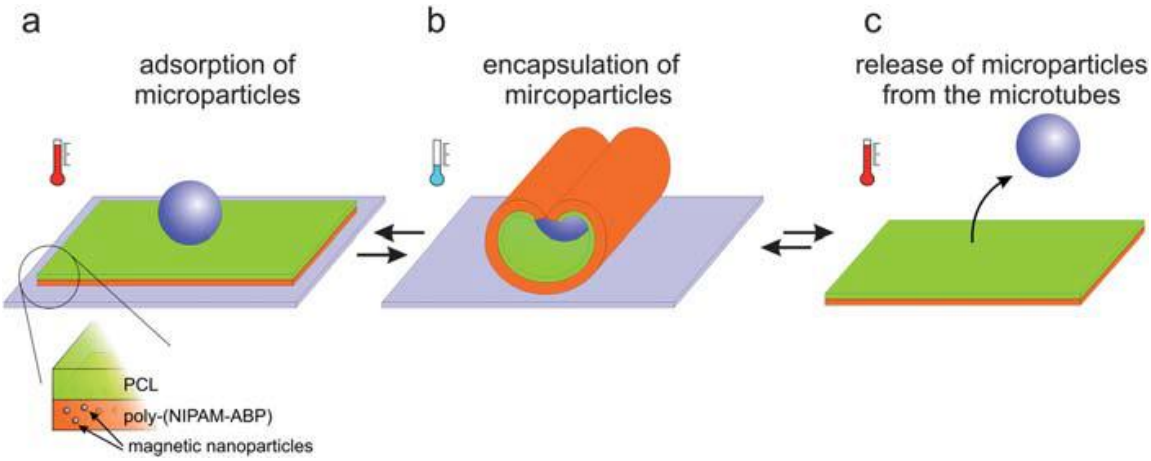

Figure 2.3: Schematic representation of the mechanism of encapsulation and release of microparticles by the bilayer self-folding microtubes. The microtubes are formed from a film of poly(N-isopropylacrylamide-co-4-acryloylbenzophenone) (poly (NIPAM-ABP) and polycaprolactone (PCL) mixed with magnetic nanoparticles. The microparticle (a) adsorbs into the bilayer film; at low temperature (less than LCST), the film (b) folds forming a microtube that encapsulates the microparticle; and upon high temperature (above LCST) (c) it unfolds releasing the microparticle. (Reproduced from Zakharchenko et al. (Zakharchenko et al., 2010) with permission of The Royal Society of Chemistry.)

Another dual responsive delivery system designed by Garbern and co-workers (Garbern et al., 2010) possessed responsiveness to pH and temperature. At higher temperatures, the hydrogel was soluble and formed a stable gel at body temperature. Decreasing pH resulted in to about 5.5 resulted in gel formation. At pH 7.4, a rapid release of the protein from the hydrogel was observed and on the contrary at pH between 5 and 6, the release was slower over 28 days. This system was proved as providing sustained release of large molecules and allowing slow degradation of the polymer. Site specificity was not mentioned in the study done, however tuning of the delivery system gives a possibility of site-specific release and optimal bioavailability. The eye consists of controls such as temperature and pH which pose as

triggering stimuli for drug release; therefore, the responsive delivery approaches mentioned above can be utilized in ocular delivery of therapeutic proteins and peptides.

2.3. THERAPEUTIC PROTEINS AND PEPTIDES FOR OCULAR DELIVERY

Size related challenges faced with the delivery of proteins and peptides through other routes of administration are also experienced in ocular delivery. However, ocular barriers add on to these challenges making it more difficult to achieve optimal bioavailability. Proteins and peptides for the treatment of various ocular disorders are discussed below.

Interferon alpha 2b is a topically administered cytokine recommended for the treatment of conjunctiva-cornea intraepithelial neoplasia due to its good side-effect profile and reduction of recurrence. It is both antineoplastic and antiviral via its mechanism of action that suppresses cell proliferation, augments cytotoxic lymphocyte specificity for target cells and hinders viral replication in infected cells (Ninawe et al., 2010; Thornton et al., 2008). Substance P is a neuropeptide found in corneal nerves responsible for corneal wound healing. The neuropeptide is topically administered with other growth factors to stimulate migration, proliferation and differentiation of corneal epithelial cells during corneal injury (Nakamura et al., 2003).

Corneal injury treatment includes corneal re-epithelialization, which is attained using fibronectin, a glycoprotein existing in plasma as well as extracellular matrices. Fibronectin is also applied topically to treat pertinacious corneal epithelial defects. In the corneal injury, fibronectin collects in the lesion and provides a supplementary matrix for migration and adhesion of epithelial cells, therefore augmenting wound healing and preventing recurrent corneal epithelial defects (Itoh et al., 2006; Yagai and Kitamura, 2008).

Another ocular peptide, cyclosporine A (CsA) derived from fungi, is used in the treatment of dry eye syndrome. It is administered as eye drops and can be used for longer periods without showing adverse effects. It also has a reversible and non-toxic action (Kymionis et al., 2008). CsA blocks T-cell activation resulting in inhibition of inflammatory cytokine production. It also inhibits apoptosis via blockade of the mitochondrial permeability transition pore opening and increased conjunctival goblet cell density (Huang et al., 2008; Peng et al., 2010).

Recently discovered ocular proteins are the vascular endothelial growth factor (VEGF) inhibitors for the treatment of chorio-retinal diseases such as age-related macular degeneration. These are commonly injected intravitreally to regulate angiogenesis, slow

disease progression and eventually reverse the pathogenesis resulting in improved visual acuity and reduced visual loss. Examples include ranibizumab, bevacizumab and pegaptanib. Bevacizumab is preferred for its longer half-life and lower cost compared to ranibizumab (Bakri et al., 2007). Examples of such proteins and peptides are listed in **table 2.3** as well as ocular disorders for which they are indicated.

Table 2.3: A summary of the mechanism of action and delivery of ophthalmic proteins and peptides.

Protein/Peptide	Indication	Mechanism of action	Delivery system	Molecular weight	Structure (Figure 4)	Reference
Substance P	Corneal injury	Stimulates corneal epithelial cell migration and proliferation.	Topical eye drops	~13kDa	[a]	(Kingsley and Marfurt, 1997)
Fibronectin	Persistent corneal epithelial defect	Functions in corneal re-epithelialization by providing a provisional matrix for epithelial cell adhesion and migration.	Topical eye drops	440kDa	[b]	(Bakri et al., 2007; Kingsley and Marfurt, 1997)
Interferon α2a	Herpes simplex, keratitis, Macular edema and AMD	Immunomodulatory agent	Injection (Roferon A®)	19kDa	[c]	(Finger et al., 2008)
Interferon α2b	Ocular surface squamous neoplasia, Conjunctival melanoma	Immunomodulatory agent	Topical drops and subconjunctival injection (Intron A®)	~19kDa	[d]	(Finger et al., 2008; Jarrett and Boulton, 2012; McCulley et al., 1993)
Cyclosporine A	Keratoconjunctivitis sicca and dry eye disease	Immunosuppressive agent that inhibits activation of T lymphocytes.	Eye drops (Restasis®)	~12kDa	[e]	(Gan et al., 2009; Gantyala et al., 2013)
Bevacizumab	Age-related macular degeneration	Vascular endothelial growth factor inhibitor. Regulates angiogenesis.	Intravitreal injection (Avastin®)	149kDa	[f]	(Rauck et al., 2013)
Pegaptinib	Age-related macular degeneration	Selective antagonist of the 165 isoform of vascular endothelial growth factor–A.	Intravitreal injection (Macugen®)	~50kDa	[g]	(Rauck et al., 2013; Shen et al., 2010)

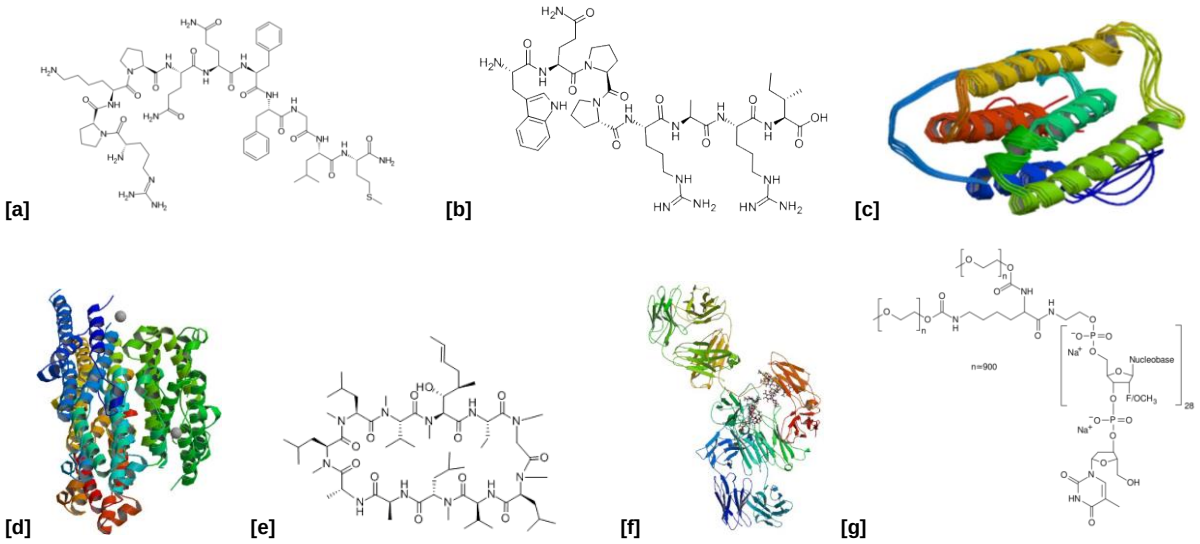

Figure 2.4: Structures of therapeutic proteins and peptides used in the treatment of ocular/ophthalmic disorders as discussed in **table 2.3** above. (a) Substance P; (b) Fibronectin; (c)Interferon α2a; (d) Interferon α2b; (e) Cyclosporine A; (f) Bevacizumab; (g) Pegaptinib

2.4. CURRENT PROGRESS IN RESPONSIVE OCULAR DELIVERY

2.4.1. *In Situ* Forming Ophthalmic/Ocular Delivery System

In situ forming systems (**Table 2.4**) are the most widely investigated stimuli responsive systems for ocular delivery of drugs, especially for topical treatment. These are low viscosity, free flowing liquid formulations that undergo sol-gel phase transition when in contact with the stimulus. The transition occurs in the cul-de-sac in topical administration (Kute et al., 2015). Their flowability prior to administration puts them at an advantage over systems that are inserted in final form before implantation which require highly invasive surgical procedures for placement into the body.

The rationale for the investigation of *in situ* forming ocular/ophthalmic drug delivery systems includes overcoming the following challenges: rapid pre-corneal elimination, normal tear turnover, conjunctival absorption, low bioavailability, frequent administration, high invasion of tissue during implantation, and systemic side-effects due to nasolacrimal drainage of the drug. These lead to insufficient therapeutic levels of the drug and failure to achieve required therapeutic outcome (Hoffman, 2002; Mulvagh et al., 2000; Zhao et al., 2012). A drug dose instilled into the eye is drained at the same time the instillation begins and the dose is eliminated within 5 minutes. This does not allow enough contact time for therapeutic effect hence the designation of *in situ* forming systems (Cao et al., 2007). Also, using high concentrations of the drug attempting to overcome the insufficiency of therapeutic drug levels

leads to toxicity. Therefore, *in situ* forming delivery systems have been found to be a solution to this issue. They prolong residence time allowing optimal absorption of the active agent into the tissue and avoid systemic absorption of the drug (Sieg and Robinson, 1981).

Table 2.4: Examples of the *in situ* forming ocular drug delivery systems illustrated above.

Bioactive	Polymers	Routes of administration	Reference
VEGF inhibitors	PNIPAAm	Intravitreal (injection)	(Kumar et al., 1994)
Fluocinolone acetonide	Polyimide	Intravitreal (implant)	(Zarbin and Rosenfeld, 2010)
Fuconazole	Gellan gum, carragenan	Topical	(Athanasakis et al., 2012)
Bevacizumab	Poly (ethylene glycol)-poly (ε-caprolactone)-poly (ethylene glycol)	Intracameral	(Peng et al., 2014)

Liu and colleagues suggest that ocular therapy would be greatly improved if pre-corneal residence time (drug-tissue contact time) of drugs would be increased. Physiological limitations imposed by protective mechanisms of the eye along with the physiological barriers (tear, cornea, conjunctiva, sclera, choroid, retina and blood retinal barrier) play a role in reducing absorption resulting in short duration of therapeutic effect therefore frequent administration (Kushwaha et al., 2012). The amount of drug that penetrates the cornea and reaches intra-ocular tissue is about 1-6% due to short contact time and drainage (Casolaro et al., 2014; Yin et al., 2014). This makes it difficult to maintain sufficient amounts of the bioactive in the precorneal area with 75% of the bioactive lost through nasolacrimal drainage and systemic absorption (Scott et al., 2002; Zakharchenko et al., 2010). An ideal formulation would be a liquid that will be in contact with the cornea for a longer period of time to improve precorneal residence time and maintain patient compliance (Cohen et al., 1997). *In situ* forming systems have been found to be an alternative that can overcome these limitations while achieving therapeutic effect without affecting vision and patient acceptability compared to ointments and implants (Schoenwald, 1997).

In situ forming systems are useful in achieving controlled delivery and minimum invasion of ocular tissue compared to surgical implantation. Derwent and Mieler (Kang Derwent and Mieler, 2008) report on a thermo-responsive hydrogel to deliver VEGF inhibitors to the posterior segment of the eye for the treatment of AMD. Poly (*N*-isopropylacrylamide) (PNIPAAm) was used as the thermo-responsive polymer combined with PEGDA to enhance mechanical strength and prolong release of the peptide. At room temperature was liquid and

at 37˚C it solidified within a minute. Thermo-responsive characteristic of the hydrogel makes it possible to inject into the vitreous cavity alternative to intraocular delivery of solid implants which requires tissue invasion (Kumar et al., 1994).

Xie et al. designed an injectable PLGA-PEG-PLGA based thermo-responsive hydrogel for intravitreal sustained release of Avastin® (bevacizumab) in the treatment of posterior segment disorders. PLGA-PEG-PLGA aqueous solution is injected intravitreally and forms an *in situ* hydrogel. This study proposes a mechanism of release that entails initial burst release of Avastin® followed by a sustained release with gradual biodegradation of the hydrogel concurrently. In vivo results demonstrated a possibility of an extended Avastin® from the hydrogel in the vitreous humour compared to intravitreal injections (Xie et al., 2015).

2.4.2. Implantable Stimuli Responsive Ocular Delivery Systems

Recently, Du Toit and co-workers (Du Toit et al., 2014) designed an inflammation-responsive delivery system, Intelligent Intraocular implant (I^3), for the treatment of inflammation related vitreoretinal disorders such as uveitis. I^3 was designed to respond to inflammation through recognition of a biochemical process specifically immanent to inflammation. Following this recognition is polymeric erosion in the delivery system via an integral mechanism resulting in the release of the incorporated active agent. Hyaluronic acid was employed for its inflammation responsive properties along with other inflammatory associated polymers. The system is target specific and biodegradable with minimal side-effects compared to previously studied intraocular implants, owing to its specificity of drug release to the presence of inflammation and therefore improving patient outcomes and optimal drug concentrations at the targeted site.

Li et, al. (Li et al., 2008) designed a refillable intraocular implant for treatment of anterior and posterior segment diseases. The device is made up of an electrolysis pump, drug reservoir (silicone rubber) and a flexible transscleral cannula with a one-way valve. Silicone rubber membrane can withstand several punctures and reseal without the drug escaping; hence it is a suitable material for the refillable reservoir. Upon application of voltage or current (~50μA-1.25 mA), electrolysis occurs and consequently the internal pressure increases forcing the valve to open and the drug flows through the cannula into target site; the valve closes upon removal of the stimulus. The amount of drug released is dependent on both the current and duration of exertion. Under normal (5-22mmHg) and abnormal (>22 mmHg in cases such as glaucoma) intraocular pressure (IOP), the device provided satisfactory results. It is estimated that the device can take up to 24 refills at a 3 month frequency which renders a lifetime of 6

years. Superiority over other ocular implants is the extended lifetime without enlarging the device, refilling without a surgical procedure required and permits modification of the drug regimen as per the need (Lo et al., 2008).

Yasin and co-workers (Yasin et al., 2014) report on a multi-reservoir laser-activated implant, On-demand therapeutics (ODTx), that provides controlled delivery of various active agents to the posterior segment of the eye. Though the patent gives little detail on the composition of ODTx, it reveals that the light responsive part of the implant may consist of a titanium tube or a silicone based polymer that is extremely impassable. A certain wavelength of electromagnetic radiation focused on a small part of the impassable layer can tear it and release the active agent. ODTx utilizes already existing non-invasive laser technology that is used in treatment of other ocular conditions. One limitation in this implant is that it is non-biodegradable and may result in long-term complications.

Verisome®, Icon Biosciences Inc. (Sunnyvale, CA, USA), a biodegradable intravitreal injectable *in situ* forming delivery technology that offers long term therapy also reported by Yasin et, al. (Yasin et al., 2014) that is undergoing phase II clinical trials for ranibizumab in the treatment of AMD. It is capable of delivering a wide range of molecules (micro and macro) over weeks to a year. The system is injected intravitreally in liquid form and fuses into a spherule that settles posteriorly in the vitreous chamber. The spherule degrades overtime, concurrently releasing the active agent. In preclinical studies, sustained delivery of the active agent in the vitreous was achieved over 6 months and 12 months in 6.9mg and 13.8mg formulations, respectively (Bakri et al., 2007; Matsuda and Koyasu, 2000).

2.5. FUTURE PROSPECTS

The ocular route holds a great potential for ophthalmologically active therapeutic peptides and proteins intended for treatment of ocular diseases. Proteins and peptides considered for local pharmacological action in the eye include polypeptide antibiotics like cyclosporine, tyrothricin, gramicidin, tyrocidine, bacitracin and polymyxins (Ratnaparkhi et al., 2011). A number of ophthalmic proteins and peptides in use are listed **in table 2.3** and majority is commonly administered topically resulting in low bioavailability and systemic side effects, as reviewed. Although these macromolecules are a challenge to administer, especially ocularly due the complex anatomy of the eye and physiological barriers, stimuli responsive delivery approach is an alternative to overcome these difficulties.

The use of stimuli responsive polymers for localized delivery of ocular drugs exists, however it is not popular, particularly with macromolecular proteins and peptides. According to literature reviewed, *in situ* gel systems are the most commonly found stimuli responsive systems in ocular drug delivery with little done on the delivery of proteins and peptides. Nonetheless, the promising potential of stimuli responsive polymers can improve ocular delivery of proteins and peptides with minimal invasion of ocular tissue. These polymers can be utilized in protein/peptide delivery to both anterior and posterior segments of the eye to increase site specificity, render sustained delivery, enhance bioavailability, and improve patient compliance.

Based on the mechanisms in the delivery of proteins and peptides that have been reviewed, we propose that a number of concepts included in table 2 can be utilized ocularly taking into consideration the stimuli that can be found in the eye and in ophthalmic abnormalities e.g. enzymes (xanthan oxireductase, myeloperoxidase, acid lipase, glutathione-related enzymes, etc), temperature (~37˚C), inflammation (disease), pH (tear fluid, 7.4), ions and also external stimuli such as light, magnetic field and external thermal sources. With this proposition there exists a prospective achievement of minimally invasive delivery with the main focus in intraocular delivery which is commonly carried out through surgical implantation and highly invasive intravitreal injections which may lead to ocular complications such as retinal detachment and cataract formation (Du Toit et al., 2014). Also, patient acceptance is likely with minimal invasive administration alternatively from surgical procedures. In conditions such as age-related macular degeneration, a multi-reservoir stimuli responsive system like the MSN can be used to deliver an anti-vascular endothelial growth factor agent along with an antioxidant and therefore optimizing therapy. It is proposed that antioxidant therapy may be able to minimize disease progress as age- related oxidative changes are part of the causes for AMD (Kingsley and Marfurt, 1997; McCulley et al., 1993; Nelson and Gordon, 1992). In **figure 2.5** we illustrate the probable stimuli and delivery routes for responsive systems to deliver proteins and peptides to both the anterior and posterior segment of the eye.

Responsive delivery of therapeutic proteins and peptides is widely investigated but less work has been done in the ocular route. Therefore, our proposition employs concepts from other routes of administration to point to the future of ocular delivery of peptides and proteins. Nonetheless, we consider challenges that can emerge in the future of this research, such as incompatibilities existing between responsive polymers and the macromolecule of interest and between the stimuli and the ocular tissue. For instance, wavelengths above 900nm are unable to penetrate ocular tissue (Juzenas et al., 2002) and therefore materials that require such wavelengths for activation cannot be employed in ocular delivery. Certain enzyme levels are

decreased significantly in some ocular disorders, catalase in dry eye disease (Malec et al., 2008); systems responsive to such enzymes would be limited.

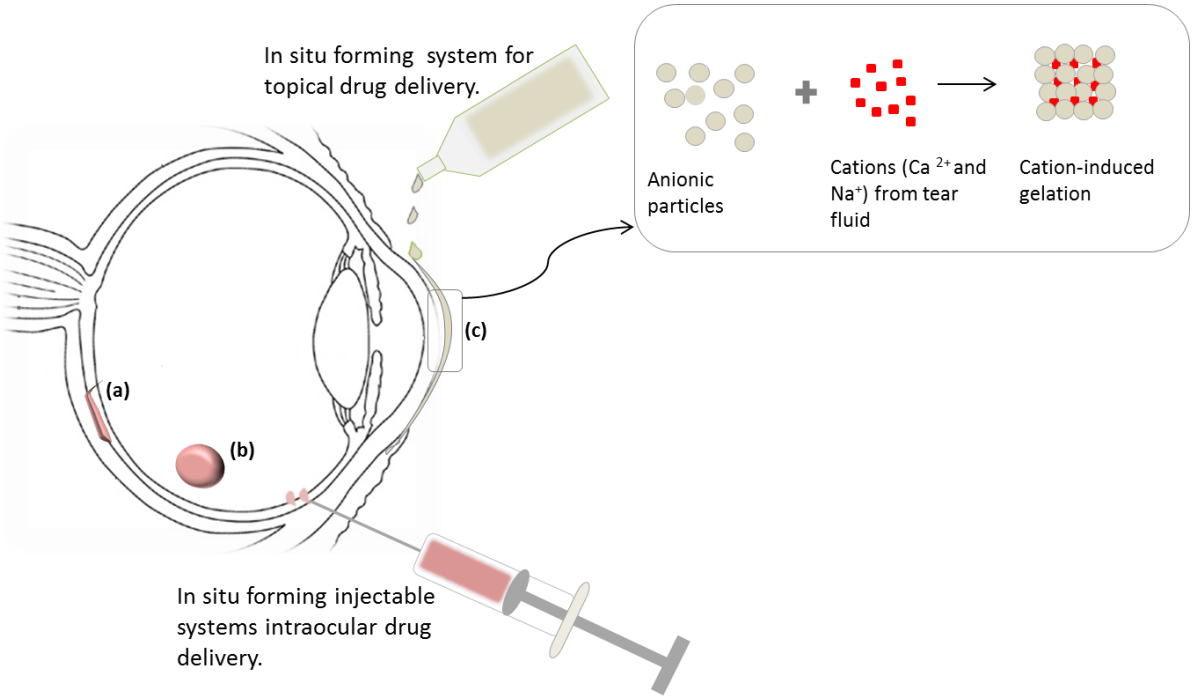

Figure 2.5: Schematic presentation of possible ocular routes for administration of stimuli responsive drug delivery systems. (a) Suprachoroidal implantation, injected as liquid and solidifying in contact with stimuli (e.g. temperature, pH), (b) Intravitreal implant which is also injectable and (c) Topical eye drops that gel when in contact with the eye due to pH and/or temperature.

2.6. CONCLUDING REMARKS

This is a futuristic review as it explores the future of stimuli responsive systems in delivering therapeutic proteins and peptides via the ocular route. Based on the literature reviewed, challenges may be encountered due to size and instability of the proteins and peptides, however, there is ongoing and advancing research in stimuli responsive ocular delivery of these macromolecules to both anterior and posterior segments of the eye and it poses a great potential. Although only a few stimuli have been investigated in this field to date, it can be deduced from this review that the stimuli possible to employ in ocular delivery can be naturally occurring such as temperature and pH or disease specific as inflammation or external remotely controlled such as light and magnetic field. In addition, these responsive systems are a viable solution to the complication of patient compliance due various delivery approaches that are not patient friendly.

2.7. RECENT ADVANCES

Recent approaches have focused on various potential formulations to improve ocular delivery of therapeutic macromolecules. Agrahari et al., developed a novel pentablock copolymer nanoformulation in thermo-responsive hydrogel for prolonged delivery of macromolecules in a controlled manner, avoiding toxic concentrations of the therapeutic in ocular tissue (Agrahari et al., 2016). Cho et al., designed a polymer-based thermo-responsive delivery system for topical administration of therapeutics. This system showed improved bioavailability, increased residence time and duration of action which are ideal properties in the delivery of proteins (Cho et al., 2016). Mandal et al., reports on nanosized polymeric micelles as potential carriers for ocular peptides owing to their stability, high loading capacity, and tissue penetration ability (Mandal et al., 2018). In another study, Yuan and co-workers explored polyvinyl alcohol (PVC) based nanowafers loaded with axitinib, for the treatment of corneal neovascularisation. These nanowafers showed increased residence time, were twice as more effective than topical eyedrops, and released the drug in a controlled manner thus proving effectiveness as topical delivery system for ocular macromolecules (Yuan et al., 2015). Additionally, literature suggests that the stapled peptides strategy could prove beneficial in ocular delivery of peptides to improve binding and enhance drug targeting (Mandal et al., 2019). Non invasive delivery of proteins and peptides is continuously gaining attention in the research of biomedicines, exploring various materials and routes of administration (Bajracharya et al., 2019).

2.8. REFERENCES

Agrahari, V., Hung, W.T., Christenson, L.K., Mitra, A.K., 2016. Composite nanoformulation therapeutics for long-term ocular delivery of macromolecules, Mol. Pharm 13, 2912–2922.

Aimetti, A.A., Tibbitt, M.W., Anseth, K.S., 2009. Human Neutrophil Elastase Responsive Delivery from Poly (ethylene glycol) Hydrogels. Biomacromolecules 10, 1484–1489.

Almeida, H., Amaral, M.H., Lobao, P., Lobo, J.M.S., 2014. *In situ* gelling systems: A strategy to improve the bioavailability of ophthalmic pharmaceutical formulations. Drug Discov. Today 19, 400–412. https://doi.org/10.1016/j.drudis.2013.10.001

Antosova, Z., Mackova, M., Kral, V., Macek, T., 2009. Therapeutic application of peptides and proteins: parenteral forever? Trends Biotechnol. 27, 628–635. https://doi.org/10.1016/j.tibtech.2009.07.009

Athanasakis, K., Fragoulakis, V., Tsiantou, V., Masaoutis, P., Maniadakis, N., Kyriopoulos, J., 2012. Cost-effectiveness analysis of ranibizumab versus verteporfin photodynamic therapy,

pegaptanib sodium, and best supportive care for the treatment of age-related macular degeneration in Greece. Clin. Ther. 34, 446–56. https://doi.org/10.1016/j.clinthera.2012.01.005

Bajracharya, R., Song, J.G., Back, S.Y., Han, H., 2019. Recent Advancements in Non-Invasive Formulations for Protein Drug Delivery. Comput. Structural Biotech. 17, 1290–1308.

Bakri, S.J., Snyder, M.R., Reid, J.M., Pulido, J.S., Ezzat, M.K., Singh, R.J., 2007. Pharmacokinetics of Intravitreal Ranibizumab (Lucentis). Ophthalmology 114, 2179–2182. https://doi.org/10.1016/j.ophtha.2007.09.012

Brown, H., Meltzer, G., Merrill, R., Fisher, M., Ferré, C., Place, V., 1976. Visual effects of pilocarpine in glaucoma comparative study of administration by eyedrops or by ocular therapeutic systems. Arch. Ophthalmol. 94, 1716–1719. https://doi.org/10.1001/archopht.1976.03910040490004

Cao, Y., Zhang, C., Shen, W., Cheng, Z., Yu, L.L., Ping, Q., 2007. Poly(N-isopropylacrylamide)-chitosan as thermosensitive in situ gel-forming system for ocular drug delivery. J. Control. Release 120, 186–94. https://doi.org/10.1016/j.jconrel.2007.05.009

Casolaro, M., Casolaro, I., Bottari, S., Del Bello, B., Maellaro, E., Demadis, K.D., 2014. Long-term doxorubicin release from multiple stimuli-responsive hydrogels based on α-amino-acid residues. Eur. J. Pharm. Biopharm. 88, 424–433. https://doi.org/10.1016/j.ejpb.2014.06.005

Chiu, H.C., Lin, Y.W., Huang, Y.F., Chuang, C.K., Chern, C.S., 2008. Polymer vesicles containing small vesicles within interior aqueous compartments and pH-responsive transmembrane channels. Angew. Chemie - Int. Ed. 47, 1875–1878. https://doi.org/10.1002/anie.200704078

Cho, I.S., Park, C.G., Huh, B.K., Cho, M.O., Khatun, Z., 2016. Thermosensitive hexanoyl glycol chitosan-based ocular delivery system for glaucoma therapy. Acta Biomater 39,124–32.

Cohen, S., Lobel, E., Trevgoda, A., Peled, Y., 1997. A novel in situ-forming ophthalmic drug delivery system from alginates undergoing gelation in the eye. J. Control. Release 44, 201–208.

Du Toit, L.C., Carmichael, T., Govender, T., Kumar, P., Choonara, Y.E., Pillay, V., 2014. In vitro, in vivo, and in silico evaluation of the bioresponsive behavior of an intelligent intraocular

implant. Pharm. Res. 31, 607–34. https://doi.org/10.1007/s11095-013-1184-3

Ducat, E., Deprez, J., Gillet, a., Noël, a., Evrard, B., Peulen, O., Piel, G., 2011. Nuclear delivery of a therapeutic peptide by long circulating pH-sensitive liposomes: Benefits over classical vesicles. Int. J. Pharm. 420, 319–332. https://doi.org/10.1016/j.ijpharm.2011.08.034

Finger, P.T., Sedeek, R.W., Chin, K.J., 2008. Topical Interferon Alfa in the Treatment of Conjunctival Melanoma and Primary Acquired Melanosis Complex. Am. J. Ophthalmol. 145, 124–129. https://doi.org/10.1016/j.ajo.2007.08.027

Gan, L., Gan, Y., Zhu, C., Zhang, X., Zhu, J., 2009. Novel microemulsion in situ electrolyte-triggered gelling system for ophthalmic delivery of lipophilic cyclosporine A: in vitro and in vivo results. Int. J. Pharm. 365, 143–9. https://doi.org/10.1016/j.ijpharm.2008.08.004

Gantyala, S.P., Shekhar, H., Vanathi, M., Sinha, R., Titiyal, Singh, J., 2013. Interferons in Ophthalmology Current Status and Advancing Trends 23, 295–297.

Garbern, J.C., Hoffman, A.S., Stayton, P.S., 2010. Injectable pH- and temperature-responsive poly(N-isopropylacrylamide-co-propylacrylic acid) copolymers for delivery of angiogenic growth factors. Biomacromolecules 11, 1833–1839. https://doi.org/10.1021/bm100318z

Gratieri, T., Gelfuso, G.M., Rocha, E.M., Sarmento, V.H., de Freitas, O., Lopez, R.F.V., 2010. A poloxamer/chitosan in situ forming gel with prolonged retention time for ocular delivery. Eur. J. Pharm. Biopharm. 75, 186–93. https://doi.org/10.1016/j.ejpb.2010.02.011

Hoffman, A.S., 2002. Hydrogels for biomedical applications. Adv. Drug Deliv. Rev. 54, 3–12. https://doi.org/10.1016/S0169-409X(01)00239-3

Horvát, G., Gyarmati, B., Berkó, S., Szabó-Révész, P., Szilágyi, B.Á., Szilágyi, A., Soós, J., Sandri, G., Bonferoni, M.C., Rossi, S., Ferrari, F., Caramella, C., Csányi, E., Budai-Szűcs, M., 2015. Thiolated poly(aspartic acid) as potential in situ gelling, ocular mucoadhesive drug delivery system. Eur. J. Pharm. Sci. 67, 1–11. https://doi.org/10.1016/j.ejps.2014.10.013

Huang, Y.F., Sefah, K., Bamrungsap, S., Chang, H.T., Tan, W., 2008. Selective photothermal therapy for mixed cancer cells using aptamer-conjugated nanorods. Langmuir 24, 11860–11865. https://doi.org/10.1021/la801969c

Huth, U.S., Schubert, R., Peschka-Süss, R., 2006. Investigating the uptake and intracellular fate of pH-sensitive liposomes by flow cytometry and spectral bio-imaging. J. Control. Release

110, 490–504. https://doi.org/10.1016/j.jconrel.2005.10.018

Itoh, Y., Matsusaki, M., Kida, T., Akashi, M., 2006. Enzyme-responsive release of encapsulated proteins from biodegradable hollow capsules. Biomacromolecules 7, 2715–2718. https://doi.org/10.1021/bm060289y

Jarrett, S.G., Boulton, M.E., 2012. Consequences of oxidative stress in age-related macular degeneration. Mol. Aspects Med. 33, 399–417. https://doi.org/10.1016/j.mam.2012.03.009

Jin, Q., Cai, T., Wang, Y., Wang, H., Ji, J., 2014. Light-Responsive Polyion Complex Micelles with Switchable Surface Charge for Efficient Protein Delivery. ACS Macro Lett. 3, 679–683. https://doi.org/10.1021/mz500290s

Juzenas, P., Juzeniene, A, Kaalhus, O., Iani, V., Moan, J., 2002. Noninvasive fluorescence excitation spectroscopy during application of 5-aminolevulinic acid in vivo. Photochem Photobiol Sci 1, 745–748. https://doi.org/10.1039/b203459j

Kang Derwent, J.J., Mieler, W.F., 2008. Thermoresponsive hydrogels as a new ocular drug delivery platform to the posterior segment of the eye. Trans. Am. Ophthalmol. Soc. 106, 204–206.

Kim, M.S., Lee, D.S., 2010. Biodegradable and pH-sensitive polymersome with tuning permeable membrane for drug delivery carrier. Chem. Commun. (Camb). 46, 4481–3. https://doi.org/10.1039/c001500h

Kingsley, R.E., Marfurt, C.F., 1997. Topical substance P and corneal epithelial wound closure in the rabbit. Invest. Ophthalmol. Vis. Sci. 38, 388–95.

Kompella, U.B., Amrite, A.C., Pacha Ravi, R., Durazo, S. a, 2013. Nanomedicines for back of the eye drug delivery, gene delivery, and imaging. Prog. Retin. Eye Res. 36, 172–98. https://doi.org/10.1016/j.preteyeres.2013.04.001

Koyamatsu, Y., Hirano, T., Kakizawa, Y., Okano, F., Takarada, T., Maeda, M., 2014. pH-responsive release of proteins from biocompatible and biodegradable reverse polymer micelles. J. Control. Release 173, 89–95. https://doi.org/10.1016/j.jconrel.2013.10.035

Kumar, S., Haglund, B.O., Himmelstein, K.J., 1994. In Situ -Forming Gels for Ophthalmic Drug Delivery. J. Ocul. Pharmacol. Ther. 10, 47–56. https://doi.org/10.1089/jop.1994.10.47

Kushwaha, S.K., Saxena, P., Rai, A., 2012. Stimuli sensitive hydrogels for ophthalmic drug

delivery: A review. Int. J. Pharm. Investig. 2, 54–60. https://doi.org/10.4103/2230-973X.100036

Kute, P.R., Gondkar, S.B., Saudagar, R.B., 2015. Ophthalmic In-situ Gel: An Overview. World J. Pharm. Pharm. Sci. 4, 549–568.

Kymionis, G.D., Bouzoukis, D.I., Diakonis, V.F., Siganos, C., 2008. Treatment of chronic dry eye: focus on cyclosporine. Clin. Ophthalmol. 2, 829–36. https://doi.org/10.2147/OPTH.S1409

Li, P., Shih, J., Lo, R., Saati, S., Agrawal, R., Humayun, M.S., Tai, Y., Meng, E., 2008. An electrochemical intraocular drug delivery device 143, 41–48. https://doi.org/10.1016/j.sna.2007.06.034

Lo, R., Li, P., Saati, S., Agrawal, R., Humayun, S., Meng, E., 2008. A refillable microfabricated drug delivery device for treatment of ocular diseases. Lab Chip 8, 1027–1030. https://doi.org/10.1039/b804690e

Malec, J., Dot, D., Cejková, J., Br, B., 2008. Decreased expression of antioxidant enzymes in the conjunctival epithelium of dry eye (Sjögren ' s syndrome) and its possible contribution to the development of ocular surface oxidative injuries. Histol. Histopathol. 23, 1477–1483.

Mandal, A., Patel, P., Pal, D., Mitra, A. K., 2019. Multi-Layered Nanomicelles as Self-Assembled Nanocarrier Systems for Ocular Peptide Delivery. AAPS Pharm Sci Tech 20, 1–17.

Mandal, A., Pal, D., Agrahari, V., My Trinh, H., Joseph, M., Mitra, A.K., 2018. Ocular delivery of proteins and peptides: Challenges and novel formulation approaches. Advanced Drug Delivery Reviews 126, 67–95.

Matsuda, S., Koyasu, S., 2000. Mechanisms of action of cyclosporine. Immunopharmacology. https://doi.org/10.1016/S0162-3109(00)00192-2

McCulley, J.P., Horowitz, B., Husseini, Z.M., Horowitz, M., 1993. Topical fibronectin therapy of persistent corneal epithelial defects. Fibronectin Study Group. Trans Am Ophthalmol Soc 91, 367–390.

Miyazaki, S., Suzuki, S., Kawasaki, N., Endo, K., Takahashi, A., 2001. In situ gelling xyloglucan formulations for sustained release ocular delivery of pilocarpine hydrochloride 229, 29–36.

Mulvagh, S.L., DeMaria, A.N., Feinstein, S.B., Burns, P.N., Kaul, S., Miller, J.G., Monaghan, M., Porter, T.R., Shaw, L.J., Villanueva, F.S., 2000. Contrast echocardiography: current and future applications. J. Am. Soc. Echocardiogr. 13, 331-342. https://doi.org/10.1067/mje.2000.105462

Nakamura, M., Kawahara, M., Nakata, K., Nishida, T., 2003. Restoration of corneal epithelial barrier function and wound healing by substance P and IGF-1 in rats with capsaicin-induced neurotrophic keratopathy. Investig. Ophthalmol. Vis. Sci. 44, 2937–2940. https://doi.org/10.1167/iovs.02-0868

Nelson, J.D., Gordon, J.F., 1992. Topical fibronectin in the treatment of keratoconjunctivitis sicca. Chiron Keratoconjunctivitis Sicca Study Group. Am. J. Ophthalmol. 114, 441–447.

Ninawe, P.R., Hatziavramidis, D., Parulekar, S.J., 2010. Delivery of drug macromolecules from thermally responsive gel implants to the posterior eye. Chem. Eng. Sci. 65, 5170–5177. https://doi.org/10.1016/j.ces.2010.06.014

Oak, M., Mandke, R., Singh, J., 2012. Smart polymers for peptide and protein parenteral sustained delivery. Drug Discov. Today Technol. 9, 131–140. https://doi.org/10.1016/j.ddtec.2012.05.001

Peng, K., Tomatsu, I., Kros, A., 2010. Light controlled protein release from a supramolecular hydrogel. Chem. Commun. (Camb). 46, 4094–6. https://doi.org/10.1039/c002565h

Peng, R., Qin, G., Li, X., Lv, H., Qian, Z., Yu, L., 2014. The PEG-PCL-PEG Hydrogel as an Implanted Ophthalmic Delivery System after Glaucoma Filtration Surgery; a Pilot Study. Med. hypothesis, Discov. Innov. Ophthalmol. 3, 3–8.

Pisal, D.S., Kosloski, M.P., Balu-iyer, S. V, 2010. Delivery of Therapeutic Proteins 99, 2557–2575. https://doi.org/10.1002/jps

Qi, H., Chen, W., Huang, C., Li, L., Chen, C., Li, W., Wu, C., 2007. Development of a poloxamer analogs/carbopol-based in situ gelling and mucoadhesive ophthalmic delivery system for puerarin. Int. J. Pharm. 337, 178–87. https://doi.org/10.1016/j.ijpharm.2006.12.038

Ratnaparkhi, M.P., Chaudhari, S.P., Pandya, V.A., 2011. Peptides and Proteins in Pharmaceuticals. Int. J. Curr. Pharm. Res. 3, 1–9.

Rauck, B.M., Friberg, T.R., Medina Mendez, C.A., Park, D., Shah, V., Bilonick, R.A., Wang,

Y., 2013. Biocompatible reverse thermal gel sustains the release of intravitreal bevacizumab in vivo. Investig. Ophthalmol. Vis. Sci. 55, 469–470. https://doi.org/10.1167/iovs.13-13120

Roy, D., Cambre, J.N., Sumerlin, B.S., 2010. Future perspectives and recent advances in stimuli-responsive materials. Prog. Polym. Sci. 35, 278–301. https://doi.org/10.1016/j.progpolymsci.2009.10.008

Ruel-Gariépy, E., Leroux, J.-C., 2004. In situ-forming hydrogels--review of temperature-sensitive systems. Eur. J. Pharm. Biopharm. 58, 409–26. https://doi.org/10.1016/j.ejpb.2004.03.019

Schmucker, C., Loke, Y.K., Ehlken, C., Agostini, H.T., Hansen, L.L., Antes, G., Lelgemann, M., 2011. Intravitreal bevacizumab (Avastin) versus ranibizumab (Lucentis) for the treatment of age-related macular degeneration: a safety review. Br. J. Ophthalmol. 95, 308–17. https://doi.org/10.1136/bjo.2009.178574

Schoenwald, R.D., 1997. Ocular Pharmacokinetics: In Zimmerman, T.J., Textbook of Ocular Pharmacology. p119. https://doi.org/10.1007/978-3-642-69222-2_2

Scott, I.U., Karp, C.L., Nuovo, G.J., 2002. Human papillomavirus 16 and 18 expression in conjunctival intraepithelial neoplasia. Ophthalmology 109, 542–547. https://doi.org/10.1016/S0161-6420(01)00991-5

Sharma, J.P.K., Bansal, S., Banik, A., 2011. Noninvasive routes of proteins and peptides drug delivery. Indian J. Pharm. Sci. 73, 367–75. https://doi.org/10.4103/0250-474X.95608

Shen, J., Deng, Y., Jin, X., Ping, Q., Su, Z., Li, L., 2010. Thiolated nanostructured lipid carriers as a potential ocular drug delivery system for cyclosporine A: Improving in vivo ocular distribution. Int. J. Pharm. 402, 248–53. https://doi.org/10.1016/j.ijpharm.2010.10.008

Shum, P., Kim, J.M., Thompson, D.H., 2001. Phototriggering of liposomal drug delivery systems. Adv. Drug Deliv. Rev. 53, 273-284. https://doi.org/10.1016/S0169-409X(01)00232-0
Sieg, J.W., Robinson, J.R., 1981. Mechanistic studies on transcorneal permeation of fluorometholone. J. Pharm. Sci. 70, 1026–1029.

Srividya, B., Cardoza, R.M., Amin, P.D., 2001. Sustained ophthalmic delivery of ofloxacin from a pH triggered in situ gelling system 73, 205–211.

Suslick, K.S., 1990. Sonochemistry. (cover story). Science (80). 247, 1439.

Thornton, P.D., Mart, R.J., Webb, S.J., Ulijn, R. V., 2008. Enzyme-responsive hydrogel particles for the controlled release of proteins: designing peptide actuators to match payload. Soft Matter 4, 821–827. https://doi.org/10.1039/b714750c

Wang, J., Pelletier, M., Zhang, H., Xia, H., Zhao, Y., 2009. High-frequency ultrasound-responsive block copolymer micelle. Langmuir 25, 13201–13205. https://doi.org/10.1021/la9018794

Wu, C., Qi, H., Chen, W., Huang, C., Su, C., Li, W., Hou, S., 2007. Preparation and evaluation of a Carbopol/HPMC-based in situ gelling ophthalmic system for puerarin. Yakugaku Zasshi 127, 183–191. https://doi.org/10.1248/yakushi.127.183

Xie, B., Jin, L., Luo, Z., Yu, J., Shi, S., Zhang, Z., Shen, M., Chen, H., Li, X., Song, Z., 2015. An injectable thermosensitive polymeric hydrogel for sustained release of Avastin1 to treat posterior segment disease. Int. J. Pharm. 490, 375–383. https://doi.org/10.1016/j.ijpharm.2015.05.071

Yagai, S., Kitamura, A., 2008. Recent advances in photoresponsive supramolecular self-assemblies. Chem. Soc. Rev. 37, 1520–1529. https://doi.org/10.1039/b703092b

Yasin, M.N., Svirskis, D., Seyfoddin, A., Rupenthal, I.D., 2014. Implants for drug delivery to the posterior segment of the eye: A focus on stimuli-responsive and tunable release systems. J. Control. Release 196, 208–221. https://doi.org/10.1016/j.jconrel.2014.09.030

Ye, M., Kim, S., Park, K., 2010. Issues in long-term protein delivery using biodegradable microparticles. J. Control. Release 146, 241–60. https://doi.org/10.1016/j.jconrel.2010.05.011

Yin, R., Wang, K., Du, S., Chen, L., Nie, J., Zhang, W., 2014. Design of genipin-crosslinked microgels from concanavalin A and glucosyloxyethyl acrylated chitosan for glucose-responsive insulin delivery. Carbohydr. Polym. 103, 369–76. https://doi.org/10.1016/j.carbpol.2013.12.067

Yuan, X., Marcano, D.C., Shin, C.S., Hua, X., Isenhart L.C., 2015. Ocular drug delivery nanowafer with enhanced therapeutic efficacy. ACS Nano 9, 1749–58.

Zakharchenko, S., Puretskiy, N., Stoychev, G., Stamm, M., Ionov, L., 2010. Temperature controlled encapsulation and release using partially biodegradable thermo-magneto-sensitive self-rolling tubes. Soft Matter 6, 2633–2636. https://doi.org/10.1039/c0sm00088d

Zarbin, M., Rosenfeld, P.J., 2010. Pathway-based therapies for age-related macular degeneration: an integrated survey of emerging treatment alternatives. Retina 30, 1350–1367. https://doi.org/10.1097/IAE.0b013e3181f57e30

Zhao, H., Sterner, E.S., Coughlin, E.B., Theato, P., 2012. O-Nitrobenzyl alcohol derivatives: Opportunities in polymer and materials science. Macromolecules 45,1723-1736 https://doi.org/10.1021/ma201924h

CHAPTER THREE
PREPARATION AND CHARACTERIZATION OF PHOTO-RESPONSIVE NANOSPHERES FOR CONTROLLED DELIVERY OF MACROMOLECULES

3.1. INTRODUCTION

Therapeutic proteins and peptides have been extensively studied for various therapeutic applications owing to their resemblance to commonly existing physiological molecules. Their large molecular size and provocation of immune response result in low absorption and adverse effects; this poses a challenge in clinical application such as ocular drug targeting as the eye is a small organ with complex tissue barriers restricting the posterior segment. The complexity of ocular anatomy has led to a high demand for prolonged, non-invasive therapies for the treatment of intraocular diseases in order to reduce the frequency of administration and improve patient compliance (Kuno and Fujii, 2011; Yasin et al., 2014). Injectable delivery systems are the best suitable alternative for minimally invasive administration due to their capability of reaching the restricted posterior segment with minimal pain and discomfort experienced compared to highly invasive surgical therapies. Hydrogel based drug delivery has been studied in this field, however, majority of research focused extensively on topical treatments to improve residence time.

Nanocarriers are ideal for sustained delivery of macromolecular therapeutics since they are protective against harsh physiological environment and increase uptake into target tissue by enhancing passage through tissue barriers, and thus overcoming limitations experienced in macromolecular drug delivery (Mahlumba et al., 2016; Weissmueller et al., 2016). Nanocarriers can be designed for localized and tuneable drug release through modification of polymer chemistry to obtain responsive systems through the inclusion of responsive moieties (Singh and Lillard, 2009; Torchilin, 2009). The augmented benefit of particle size and responsiveness is essential for optimization of drug delivery.

As discussed in **Chapter 2**, remotely controlled delivery systems have been largely explored for various pharmaceutical applications due to their riveting capabilities such as adjustment of the rate of response from an external source of stimulus to accomplish minimally invasive drug delivery (Bawa et al., 2009; Fomina et al., 2012; Lee et al., 2015). In order to take advantage of the above-mentioned augmented benefit, in this study, a photo-responsive azo dye, 4, 4'-dihydroxyazobenzene (DHAB) was blended with a biodegradable polymer for the formulation of smart nanospheres. DHAB consists of a chromophore (N=N) that undergoes reversible photo-isomerisation from *trans* to *cis* upon irradiation with UV light of a certain wavelength.

Light was selected as a stimulus for this research because of its remotely controlled effect which makes it non-invasive; it is also independent of chemical environmental changes experienced at different stages of disease progression and increases prospects of targeted delivery (Roy et al., 2010; Wang et al., 2014).

Zein is a natural hydrophobic prolamin polymer extracted from maize, classified under generally recognised as safe (GRAS) materials. Zein was used as the main component of the nanospheres, mainly for its low cost and biocompatibility (Zhang and Han, 2018). It is also biodegradable, non-toxic, and easily forms self-assembled spherical nanosized particles acceptable as drug carriers. However, these nanoparticles tend to aggregate during formulation, hence gelatin was used to coat the surface of nanospheres to reduce aggregation (Sivera et al., 2014). Furthermore, zein has been studied previously as a carrier for various therapeutic agents, including macromolecules (Pascoli et al., 2018; Press et al., 2015). The high content of non-polar amino acids in the structure of zein makes it water insoluble and soluble in aqueous alcohol. These noteworthy properties enable zein based carriers to encapsulate both hydrophobic and hydrophilic bioactives (Luo et al., 2011; Weissmueller et al., 2016). Research further highlights an antioxidative function in zein, resultant from its high aliphatic index, fatty acid content and surface hydrophobicity (Gong et al., 2006).

The aim of this study was to formulate photo-responsive nanospheres for sustained release of a model therapeutic macromolecule. Nanospheres from photosensitized zein, stabilized with gelatin and loaded with a monoclonal antibody, immunoglobulin G (IgG), were successfully formulated. The prepared azoprolamin (AZP) nanospheres were characterised through various techniques to verify their functional properties. Chemical and thermal transitions were studied via Fourier transform infrared (FT-IR) spectroscopy and thermogravimetric analysis (TGA), while structural modifications and physical state was determined through X-ray diffraction (XRD). Morphology of the nanospheres was examined via scanning electron microscopy (SEM) and *in vitro* drug release studies were performed using a sample and separate method.

3.2. MATERIALS AND METHODS

3.2.1. Materials

Zein purified powder from maize; ethanol (EtOH) reagent grade (absolute), gelatin, 4,4' dihydroxyazobenzene (DHAB), Immunoglobulin G from human serum, Hyaluronic acid sodium salt (HA) and genipin were all purchased from Sigma-Aldrich (St. Louis, MO, USA). Sodium chloride was supplied by Merck (Pty Ltd., South Africa).

3.2.2. Preparation of AZP Nanospheres

The AZP blend was prepared by mixing zein with DHAB in a volatile solvent under magnetic stirring overnight and dried under vacuum at 40˚C for approximately 36 hours. Nanospheres were prepared by coacervation method which involves the formation of two liquid phases by partial desolvation of polymer. This is caused by reduction of ethanol concentration of the dissolved polymer through the interaction of ethanol and water which decreases the alcohol concentration resulting in the formation of nanospheres. The solvent is evaporated by magnetic stirring at room temperature, hence the formulation of zein nanospheres is simple and inexpensive (Regier et al., 2012; Sousa, 2010).

The AZP blend was solubilized in 70% aqueous ethanol (0.5mg/ml) under magnetic stirring at a speed of 300rpm, concurrently IgG was dissolved in 150Mm sodium chloride solution (1mg/mL). IgG solution was then added dropwise to the AZP solution with mild stirring for 30 minutes to incorporate the IgG into the nanospheres. Gelatin aqueous solution was then added with continuous stirring at room temperature to remove the ethanol. The ratio of oil to water phase was 1:4. The obtained dispersion was freeze-dried and characterized.

3.2.3. Determination of Particle Size and Surface Morphology of the Nanospheres

Size distribution and polydispersity index (PDI) of the nanospheres were determined using the dynamic laser light scattering technique. Lyophilised nanospheres were dispersed in PBS, transferred into a cuvette, and subjected to laser light through the Zetasizer Nano ZS instrument (Malvern Instruments Ltd., Malvern, UK) for the measurement of particle diameter. Morphology of the nanospheres was studied via scanning electron microscopy (SEM) FEI Quanta 400F (Hillsboro, OR, USA). Dried nanospheres were fixed onto metal stubs using double sided tape and sputter coated with a thin layer of gold under vacuum and observed under the microscope. All measurements were performed in triplicates at 25ºC, with a scattering angle of 90º.

3.2.4. Determination of Chemical interactions of the Nanospheres

To study chemical structures and interactions between components during formulation, infrared spectra were obtained using FT-IR spectrometer (PerkinElmer Spectrum 100). Spectra were recorded in the region from 4000cm^{-1} to 650cm^{-1} wavenumbers at a resolution of 4cm^{-1}. Powder samples of native components and freeze-dried nanospheres were mounted directly onto the attenuated total reflectance (ATR) crystal for analysis and to identify chemical architecture and characteristic functional groups in the formulation.

3.2.5. Evaluation of the Light Response Properties of the Nanospheres

The UV-vis spectra for dried nanospheres were obtained using UV spectrophotometer (Cecil CE 3021, 3000 Series, Cecil Instruments, Cambridge, England) following a method previously explained by Ding et al. (Ding et al., 2016). Briefly, nanospheres were dispersed in phosphate buffer saline (PBS, pH 7.4) in a 10mm standard UV quartz cell and analysed through the UV-vis spectrophotometer. UV irradiated and non-irradiated samples were analysed. Pure PBS was used as a reference solution and samples scanned in the wavelength range of 200nm to 800nm for the confirmation of response to light. Additionally, the change in diameter of the nanosphere as a function of irradiation (UV=365nm) time was tracked by dynamic light scattering. Dried nanospheres were dispersed in PBS (pH 7.4) and exposed to UV light of 365nm through a UV curing box. Samples were extracted at each time point, transferred into a disposable cuvette, and subjected to laser light via the Zetasizer Nano ZS instrument. All measurements were performed in triplicates.

3.2.6. Determination of solid-state Structural Properties of the Nanospheres

The physical state of the nanospheres after the formulation process and blending of zein with DHAB was assessed through X-ray diffraction (XRD) analysis. X-ray patterns of the components were obtained from X-ray diffractometer (MiniFlex 600, Rigaku, Japan), using Nickel-filtered Cu Kα radiation generated at a voltage of 40 kV and a current of 30 mA. Data were collected with a range between 5º and 90º (2θ) at room temperature, at a scanning rate of 5º min^{-1}.

3.2.7. Determination of Thermal decomposition of the Nanospheres

Thermal behaviour of the native components and nanospheres was observed via Thermogravimetric analysis (TGA), heated from 20˚C to 900˚C under nitrogen atmosphere at a flow rate of 20mL/min. The thermal decomposition analysis of the newly formed polymeric blend, nanospheres and all native components was determined using a TGA 400 thermogravimetric analyser (PerkinElmer Inc., MA, USA). Samples (10–20mg) were weighed and placed in a ceramic pan under nitrogen atmosphere. Thermograms were obtained and analysed for thermal decomposition behaviour.

3.2.8. Ultra-Performance Liquid Chromatographic quantification of Immunoglobulin G

A monoclonal antibody, Immunoglobulin G (IgG) was incorporated into the nanospheres as a model protein. Drug loading efficiency was determined by sampling a certain amount of the nanospheres and dissolving it in 70% ethanol with a probe sonicator (Press et al., 2015). Drug loading, encapsulation and efficiency were calculated using **equation 3.2 and equation 3.3**

below. Dried nanospheres were weighed to determine the amount recovered from formulation. The mass of the dried nanospheres was divided by the total mass of the native components to calculate the particle yield (**equation 3.1**) (Zhang and Han, 2018).

$$\text{Particle yield} = \frac{\text{Practical yield}}{\text{Theoretical yield}} \times 100 \quad \text{(Equation 3.1)}$$

$$\text{Drug loading} = \left(\frac{\text{Drug mass in nanospheres}}{\text{Mass of nanospheres}}\right) \times 100 \quad \text{(Equation 3.2)}$$

$$\text{Encapsulation efficiency} = \left(\frac{\text{Drug mass in nanospheres}}{\text{Mass of feed drug}}\right) \times 100 \quad \text{(Equation 3.3)}$$

In vitro drug release was determined using the sample and separate method described by (Souza, 2014). Briefly, dried nanospheres were introduced into a 15ml volume clear cylindrical glass with 5mL of PBS (pH 7.4) and incubated in a shaker bath (Orbital Shaker Incubator, LM-530, Lasec Scientific Equipment. Johannesburg, South Africa) at 20rpm with a constant temperature of 37±0.5˚C. A portion (0.5mL) of the release medium was extracted and replaced with an equal volume of fresh PBS at each time point in order to maintain release conditions for the duration of the study. One sample was exposed to UV light (365nm) irradiation through a UV curing box for 10 minutes prior incubation in the shaker bath. The amount of IgG released was measured through ultra-high performance liquid chromatography (UPLC) using Waters® ACQUITY™LC system (Waters®, Milford, MA, USA) coupled with a photodiode array detector (PDA) and fitted with a Sunfire™ C18 column with a pore size of 3.3µm. Empower® Pro Software (Waters®, Milford, MA, USA) was used for analysis. Cysteine was used as an internal standard for calibration. Acetonitrile: water: trichloroacetic acid was used as a mobile phase with conditions that resulted in detection of IgG at a run time of 2.79 minutes and internal standard at 4.50 minutes. The flow rate for the mobile phase was set at 0.05ml/min and average pressure at 4100psi. Solvents were vacuum filtered and samples pre-filtered with a 0.22µm syringe before injection into the column. A temperature of 37±0.5˚C was maintained in the sample and column. All measurements were undertaken at a wavelength of 280nm in triplicates.

3.3. RESULTS AND DISCUSSION

The aim of this chapter was to synthesize novel photo-responsive nanospheres. The natural biodegradable prolamin, zein, was modified with an azo chromophore to form the photo-responsive AZP. The nanospheres were intended for localized delivery of macromolecules over a prolonged period of time, therefore, the high molecular weight immunoglobulin G was incorporated as a model . AZP nanospheres were successfully obtained and physicochemical

properties as well as drug release behaviour was assessed. Dispersion of AZP nanospheres in a gel matrix for injectability of the system is discussed in the next chapter.

3.3.1. Particle Size and Morphological Examination

The size and morphology of the dried IgG loaded AZP nanospheres was examined using SEM and dynamic light scattering (DLS). The average diameter of the nanospheres shown in **Figure 3.1 a** and **b** was ~145nm for the blank sample, and ~185nm for IgG loaded nanospheres. The nanospheres showed a low PDI of 0.190, indicating uniformity and less aggregation in dispersion (Pauluk et al., 2019). Micrographs from SEM are demonstrated in **figure 3.2** where a spherical shape was confirmed and the size of the nanospheres was <200nm. The average diameter of the nanospheres slightly increased after the incorporation of IgG. This variation in size may be a attributed to the inclusion of a high molecular weight peptide (Hadavi et al., 2018). A few spheres in the macro scale were observed, and this large size may be due to overlapping of the nanospheres resulting from aggregation during solvent evaporation (Ding et al., 2016).

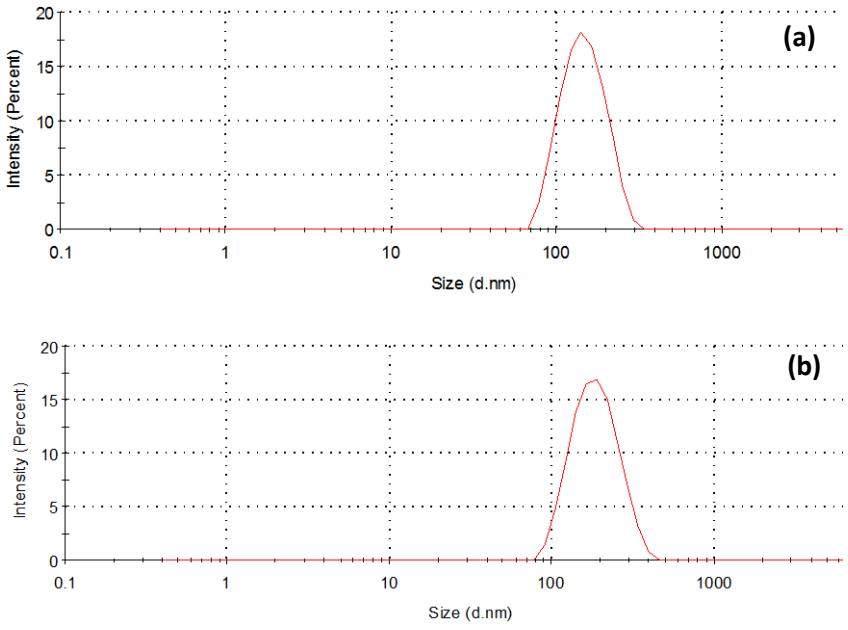

Figure 3.1: Particle size distribution for (a) blank (144.5nm, PDI =0.207) and (b) IgG loaded AZP nanospheres (185.5nm, PDI = 0.190).

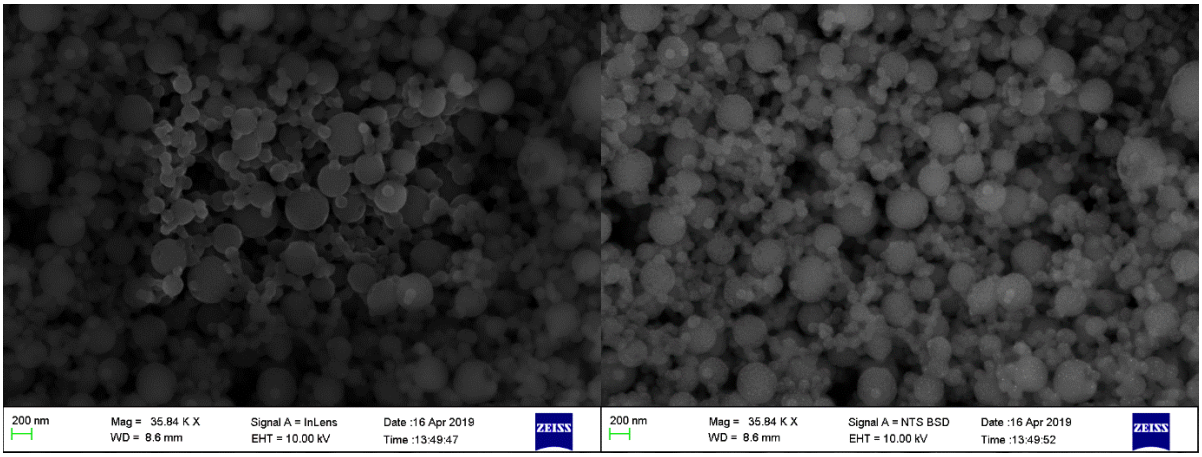

Figure 3.2: Micrographs of freeze-dried IgG loaded AZP nanospheres.

3.3.2. Chemical Transitions and Intermolecular Interactions of the Individual Components and the Nanospheres

FTIR was used to examine the interactions between zein, DHAB, AZP nanospheres and IgG during formulation. Spectra of the lyophilised nanospheres and native components were obtained and are presented in **figure 3.3** and **figure 3.4**. The characteristic bands and peaks are seen at 828cm^{-1} in **figure 3.3**(c), verifying the 4,4' distribution in the aromatic rings where the O-H substituent is at 4th position in both aromatic rings linked by the azo (N=N) group (Babu et al., 2003). The strong absorption at 1231cm^{-1} is assigned to the aromatic C-O stretch, 1508cm^{-1} assigned to the azo group (N=N) responsible for photo-responsiveness of the system, aromatic C-N, C=C and C-H positioned at 1381cm^{-1},1438cm^{-1} and 2925cm^{-1}, respectively. Amide C=O stretching, seen at 1634cm^{-1}, was accounted for by the structure of zein. The interaction between zein and DHAB results in hydrogen bonds formed from amide groups in zein and hydroxyl groups in DHAB, which is also confirmed by the right shift observed in O-H stretching bands from 3287cm^{-1} and 3279cm^{-1}, in zein and DHAB spectra, to 3251cm^{-1} in AZP spectrum due to the amide-hydroxyl interaction (Luo et al., 2011). Based on these results, it was deduced that the AZP blend retained the azo group that is ascribed to the photo-responsive behaviour of the nanospheres, also observed in the spectrum in **figure 3.4** (f).

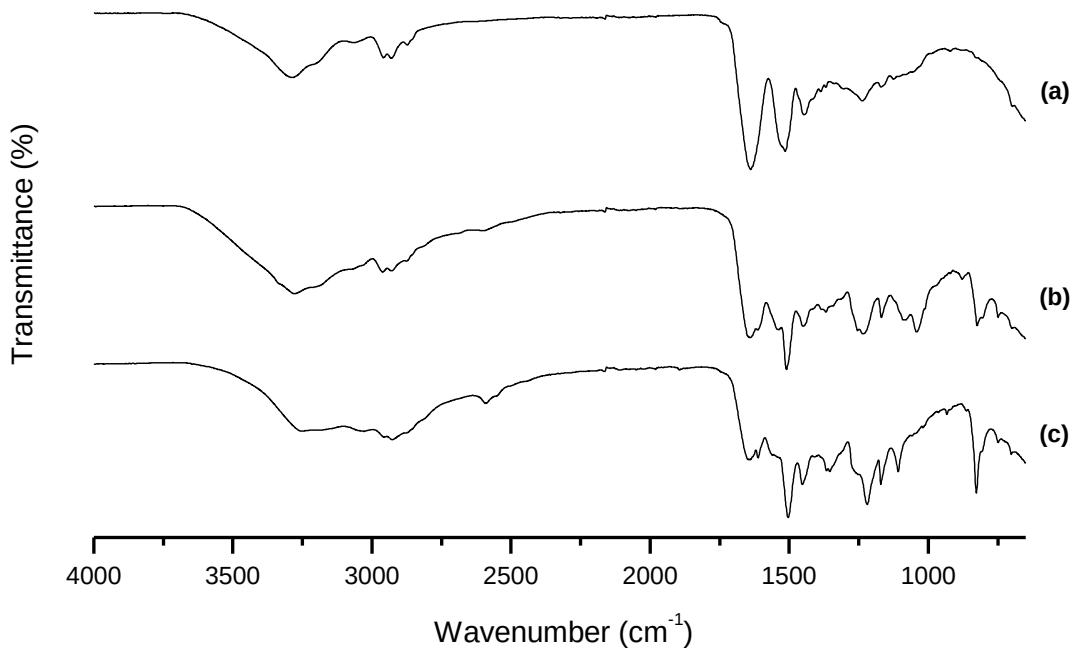

Figure 3.3: FTIR spectra of (a) zein, (b) DHAB and (c) AZP in the range 650cm^{-1}– 4000cm^{-1}.

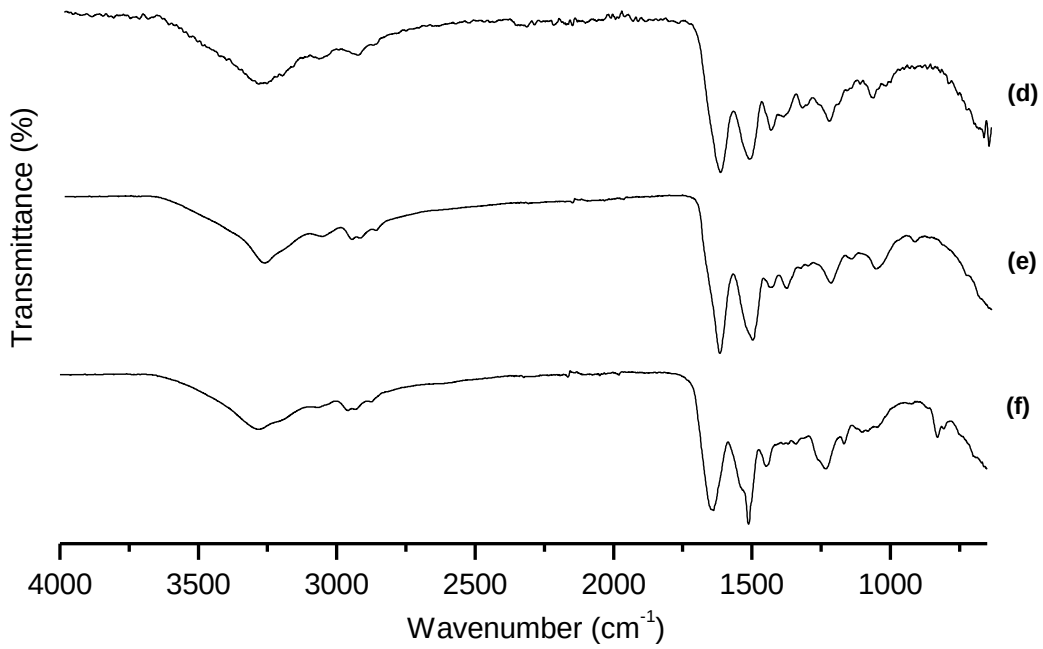

Figure 3.4: FTIR spectra of (d) gelatin, (e) IgG and (f) IgG loaded AZP nanospheres in the range 650cm^{-1}– 4000cm^{-1}.

3.3.3. Photo-response Assessment of the AZP nanospheres using UV-Vis Analysis and Dynamic Light Scattering

To investigate photo-response, UV-Vis spectra of AZP nanosphere aqueous dispersion were obtained before and after UV irradiation and are shown in **figure 3.5**. To incite photo-isomerisation, samples were irradiated with UV light (365nm) to induce conversion from *trans*

to the *cis* structural isomer (Natansohn and Rochon, 2002). Prior to irradiation, a maximum absorption peak was seen at 345nm and a flat and smaller peak at 430nm. After UV irradiation, the peak at 345nm decreased while a slight increase in intensity in the peak at 430nm was observed. Irradiation of the solution with white light resulted in the recovery of the peaks observed before UV irradiation. This decrease in intensity can be described, according to Ding et al. (2016), as the decrease in molar extinction coefficient caused by the reduced concentration of the *trans* isomer in the solution concurrently the *cis* form increases leading to increased intensity at 430nm. This is accounted for by the transformation of the azo group from *trans* to *cis* isomer upon UV irradiation, and recovery (*trans*-to-*cis*) upon exposure to white light (Ding et al., 2016; Rescifina et al., 2016).

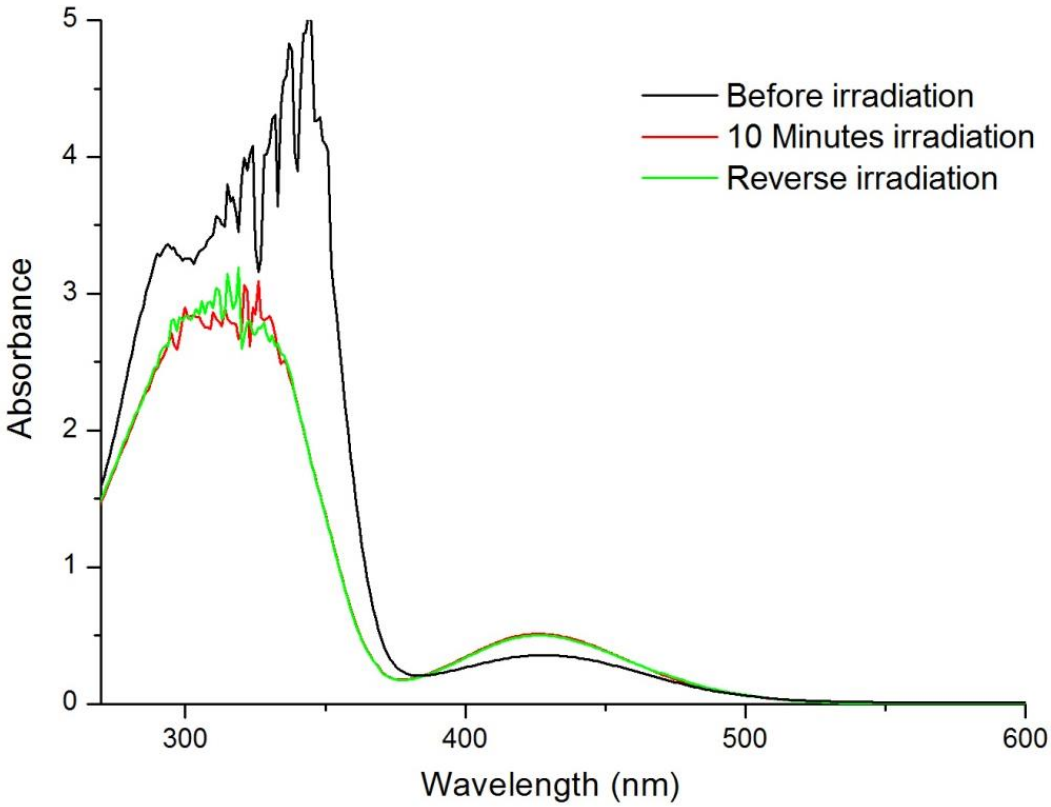

Figure 3.5: UV-vis spectra of IgG loaded AZP nanosphere dispersion post-irradiation at different time points.

Results from dynamic light scattering are presented in **Figure 3.6** where the change in diameter as a function of irradiation is plotted against time. The same sample was used for all time points to avoid inconsistent results. A significant decrease in the diameter of the nanosphere in the first 20 minutes was observed from ~185nm to ~97nm, followed by a constant diameter of 94nm. These results displayed a more compact sphere after UV irradiation and this is ascribed to the photo-isomerisation of the structure from *trans* to *cis* (Pang et al., 2019). The hypothesized mechanism for the above-described process is the UV

(365nm) irradiation of the azo molecule triggering photo-isomerisation from *trans* to *cis*, thus resulting in shrinkage in the size of the nanospheres (Cai et al., 2014).

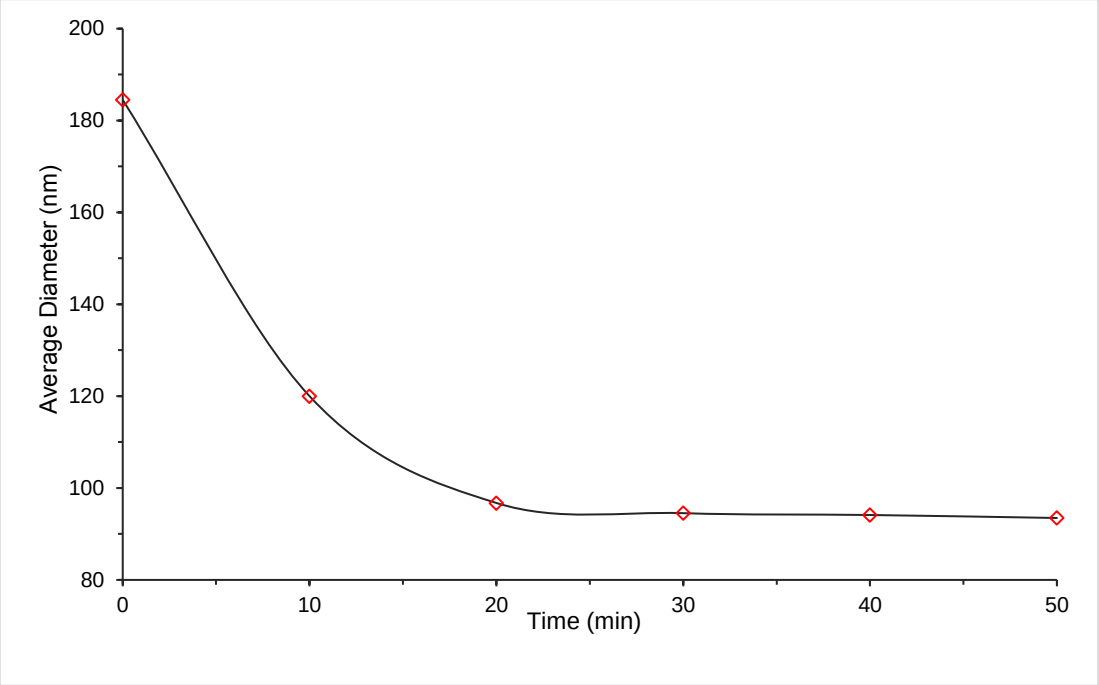

Figure 3.6: Average diameter of IgG loaded AZP nanospheres upon irradiation with UV light (365nm) as a function of time.

3.3.4. Powder X-Ray Diffraction pattern analysis of the Nanospheres and components

The XRD patterns for lyophilised AZP nanospheres, drug and native components are shown in **Figure 3.7**. Intense peaks were observed at 19, 22, 26, 29, 31, 45 and 56 degrees in DHAB and AZP patterns, indicative of the crystalline nature of the azo dye. On the contrary, flatter peaks were seen in zein, gelatin and IgG patterns indicating their amorphous nature. DHAB characteristic peaks, 31, 45 and 56 degrees, were seen in the nanospheres pattern substantiating the unaltered structure of DHAB and suggesting that the photoisomerization property was retained (Yang et al., 2016).

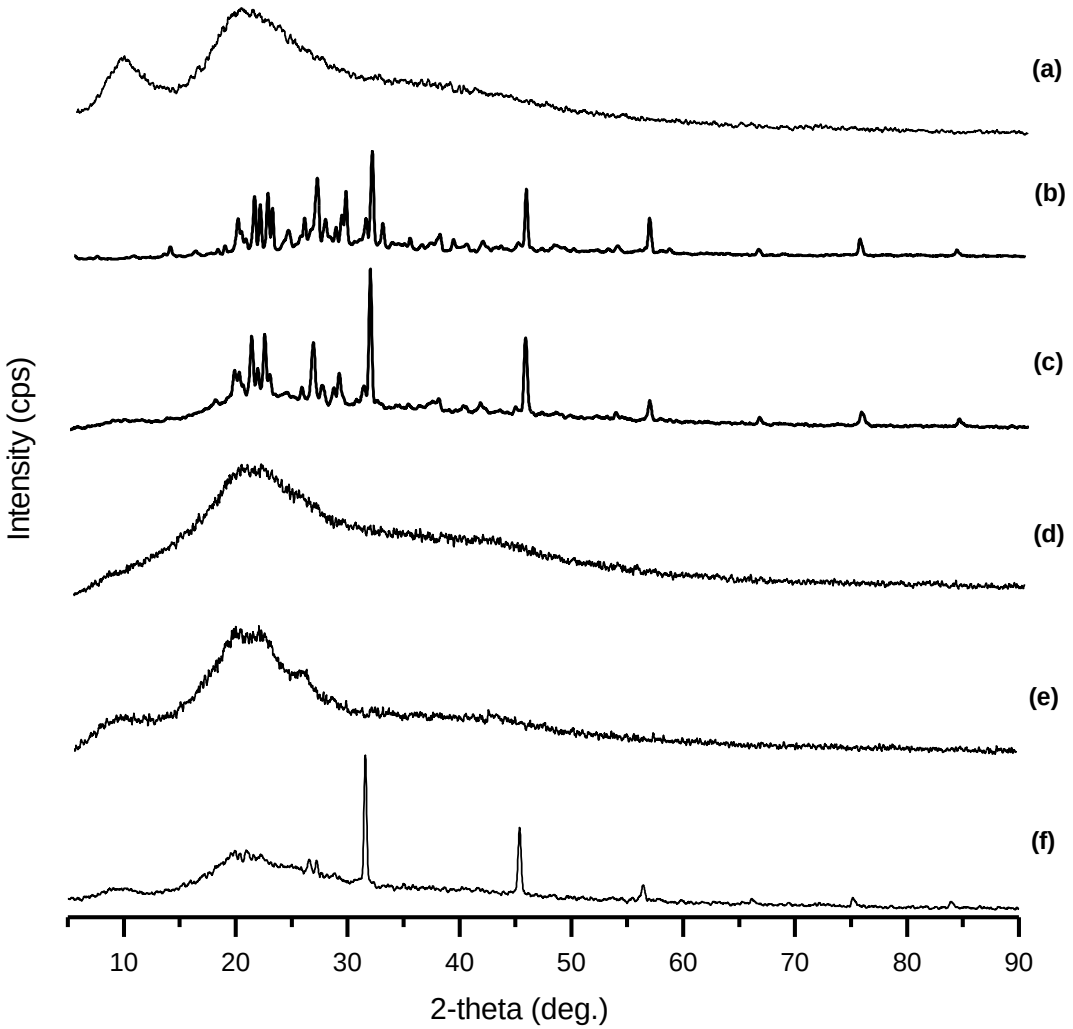

Figure 3.7: X-ray diffractograms of (a) zein, (b) AZP, (c) DHAB, (d) gelatin, (e) IgG and (f) IgG loaded AZP nanospheres.

3.3.5. Determination of Thermal Degradation of the Nanospheres

Thermal stability of the lyophilised AZP nanospheres, AZP and bulk components was investigated using thermogravimetric analysis under nitrogen flow and thermograms are presented in **figure 3.8** and **figure 3.9**. DHAB onset of degradation was observed at ~150ºC while other components had a lower onset of degradation temperature between 60ºC and 110ºC, indicating loss of water from the samples (Hadavi et al., 2018). Zein shows thermal resistance in the initial phase but undergoes more weight loss at the end. Furthermore, DHAB had the highest stable thermal residue of 35% while zein had the lowest (13%) and the nanospheres followed a similar degradation pattern to that of AZP with the total thermal stable residue of 26%. This indicates that the presence of the crystalline DHAB increases the total stable residue and therefore enhances thermal resistance of both the blend and nanospheres.

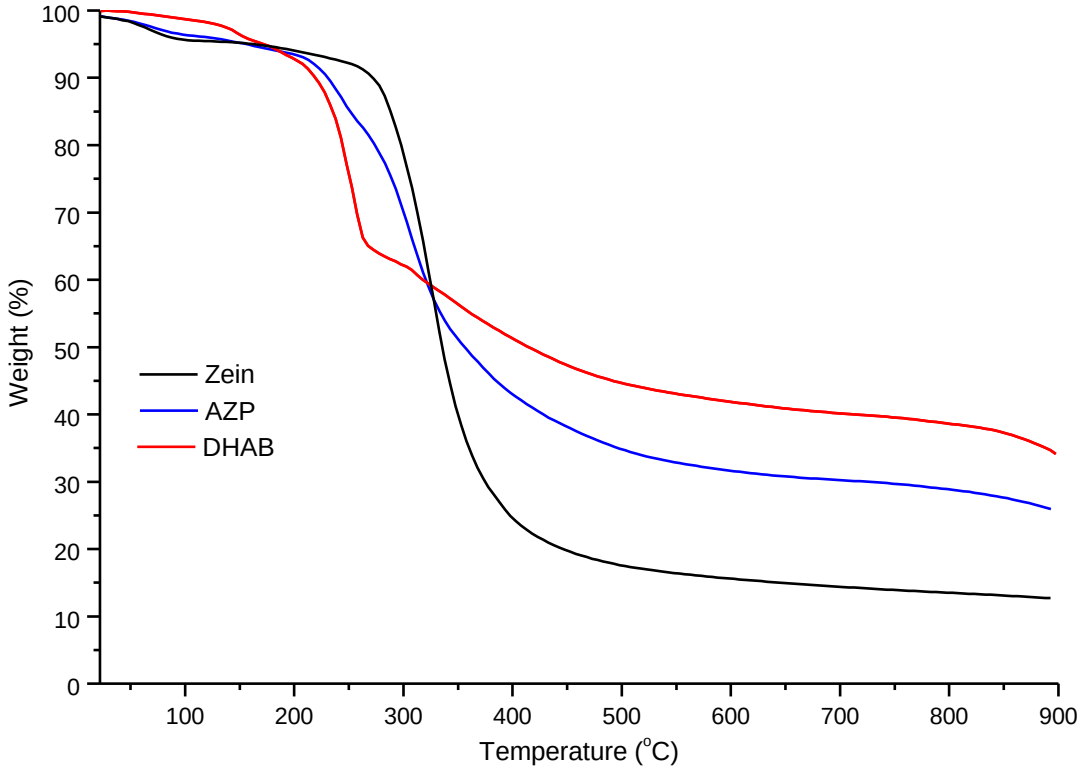

Figure 3.8: TGA thermograms of zein, AZP and DHAB.

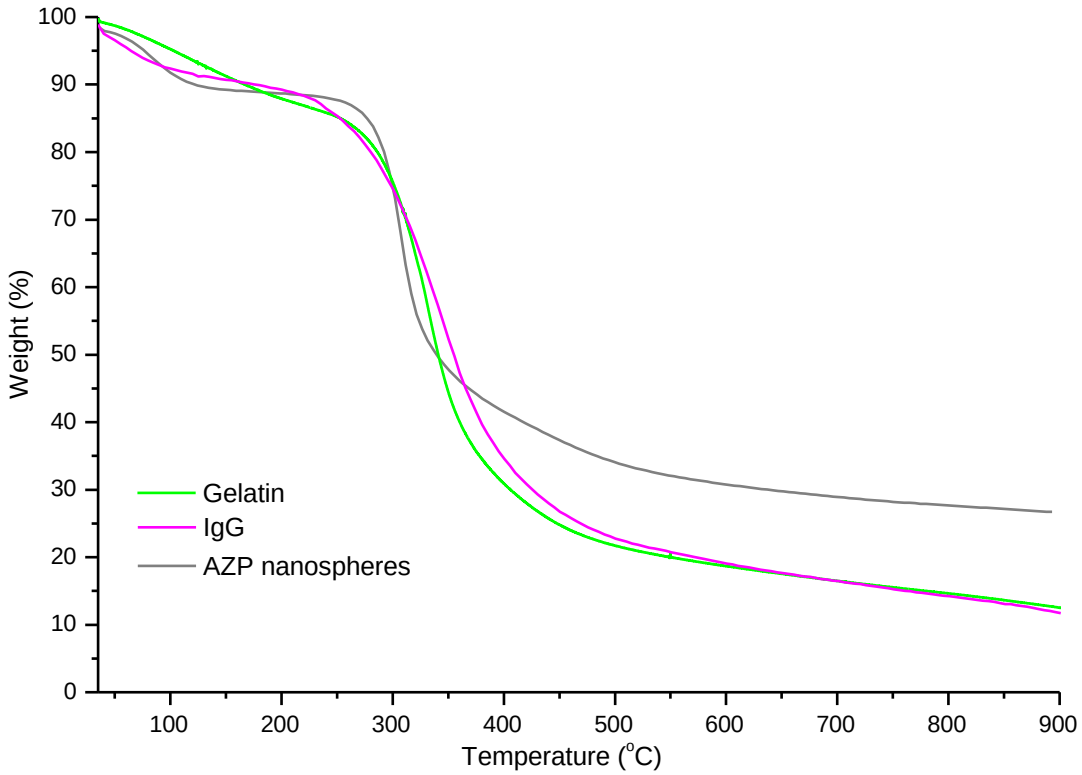

Figure 3.9: TGA thermograms of gelatin, IgG and IgG loaded AZP nanospheres.

3.3.6. *In Vitro* Drug Release and Encapsulation efficiency of the Nanospheres

A monoclonal antibody, IgG, was incorporated into AZP nanospheres as a model drug. For the quantification of IgG, a method was optimised by running the internal standard, cysteine,

and IgG through chromatography (UPLC). Separation peaks obtained are presented in **figure 3.10**, where the retention time for IgG is 2.79 and signal to noise ratio (SNR=2H/h) of 5. The surface area of the chromatogram was used to determine the concentration of IgG.

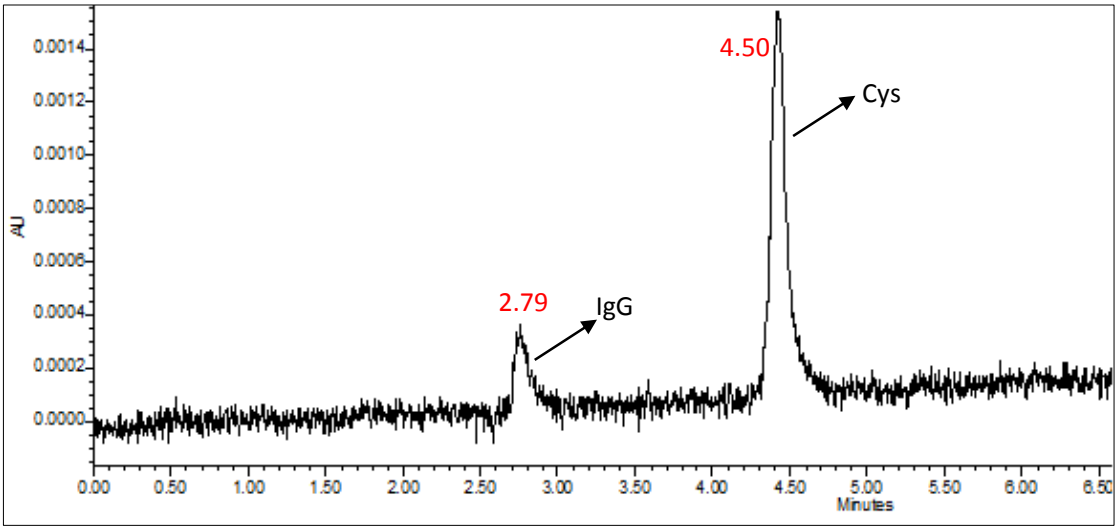

Figure 3.10: Chromatogram showing the separation peaks for IgG and Cysteine.

The ratios of the area under the curve of IgG and that of cysteine were plotted against concentration (mg.mL^{-1}).The calibration curve displayed in **figure 3.11** was generated to quantify IgG from both non-irradiated and irradiated AZP nanospheres using the method described in section **3.2.8**. The drug loading capacity of the nanospheres, calculated using **equation 1** and **equation 2**, was 83%.

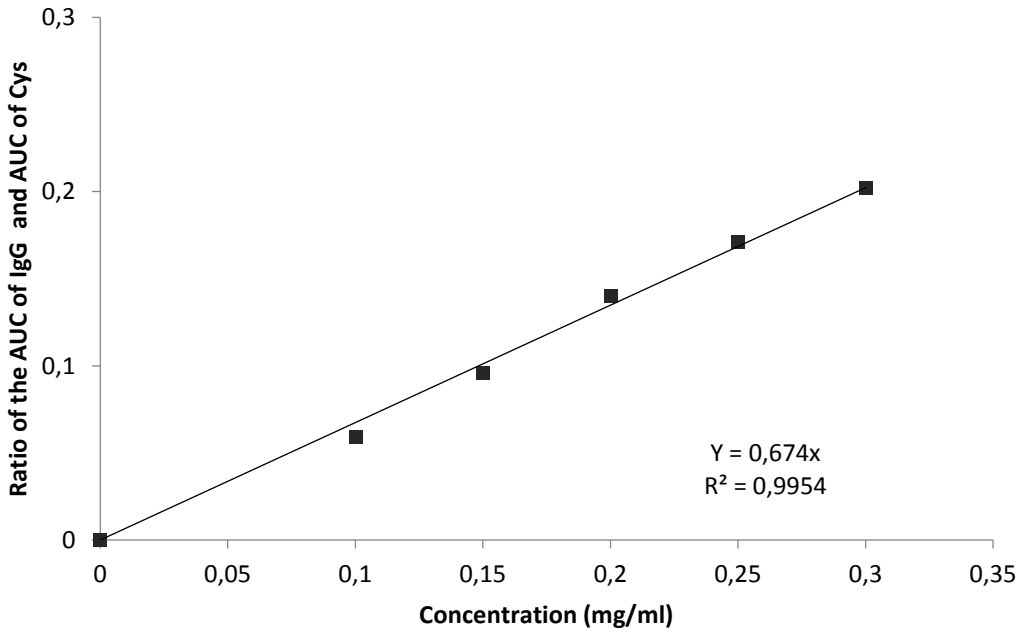

Figure 3.11: Calibration curve for quantification of IgG in PBS (pH=7.4)

In **figure 3.12**, *in vitro* release of IgG from non-irradiated and UV irradiated AZP nanospheres is shown. In the first 24 hours, 25% of IgG was released from non-irradiated nanospheres and 15% from the UV irradiated nanospheres; this initial burst release of IgG is explained as the release of free drug that is not interacted with the polymer (Hadavi et al., 2018). The rest of the drug was gradually released over 4 weeks up to 60% and 84% at day 32 from non-irradiated and irradiated nanospheres, respectively. The total drug released from the UV irradiated nanospheres at day 32 was 24% less than that of non-irradiated nanospheres; this may be due to the irradiation which results in a compact nanosphere and reduction of free volume, thus decreasing rate of diffusion and prolonging the release of IgG. $p \leq 0.05$ was obtained confirming the significant effect of UV irradiation on the nanospheres.

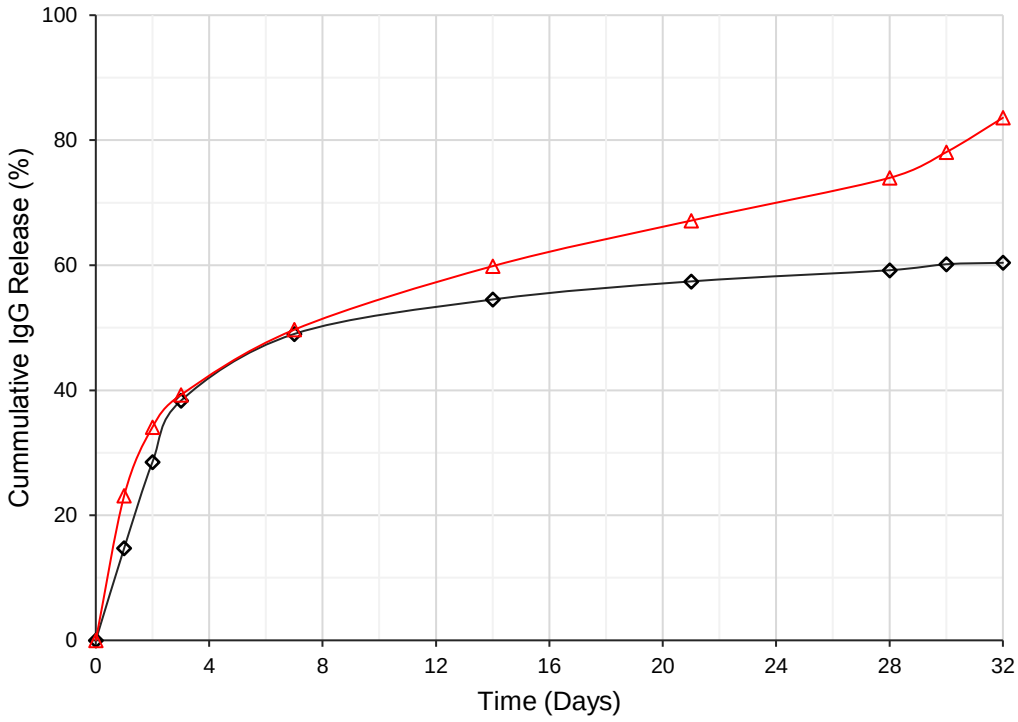

Figure 3.12: Cumulative IgG release from non-iiradiated nanospheres (red line) and UV irradiated AZP nanospheres (black line) over 32 days (p=0.003).

The proposed mechanism, previously described by Cai et al. (2014), of the reversible photo-induced IgG release is illustrated in **figure 3.13**, wherein, the AZP loaded nanosphere is subjected to UV light of wavelength 365nm for a set amount of time and the *trans*-azo groups change into the *cis* form, resulting in reduced diameter of the nanosphere. The rate of diffusion decreases to allow slow release of IgG and in the reverse process where the nanospheres are irradiated with white light, azo groups reverse to *trans* form and the size of the sphere and rate of diffusion are increased (Cai et al., 2014).

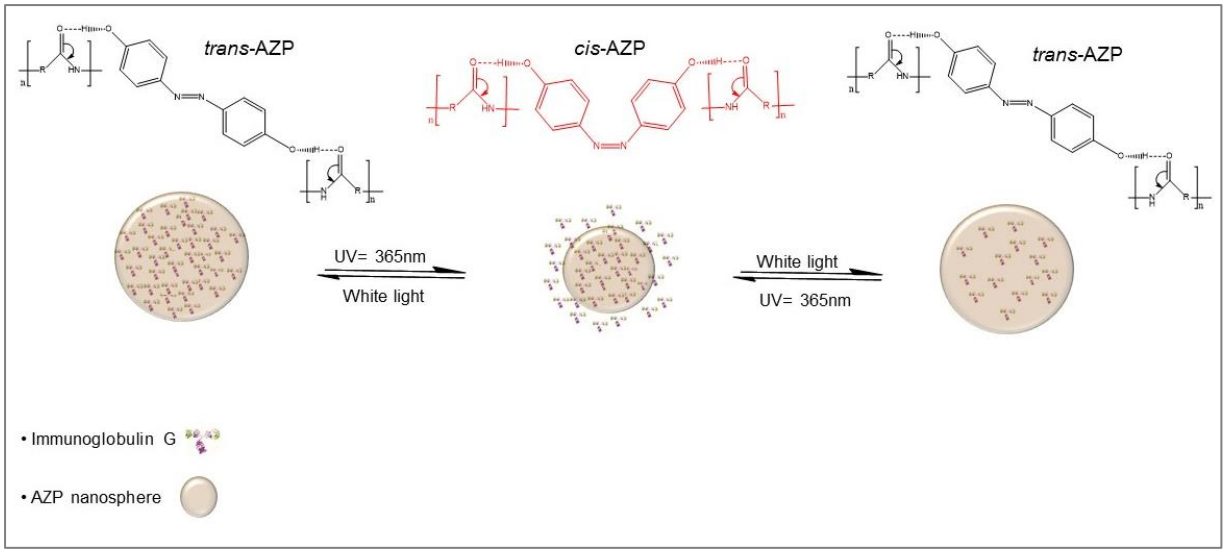

Figure 3.13: Schematic representation of the transformation from *trans*-to-*cis*-to-*trans* and change in the size of AZP nanospheres upon UV irradiation and white light.

3.4. CONCLUDING REMARKS

An injectable photo-responsive polymeric nanosystem (HA-NSP), incorporating IgG, was successfully prepared. Nanospheres with average particle diameter of <200nm and high encapsulation efficiency (83%) were formulated using the coacervation method and dispersed in HA gel. Photo-responsiveness of the system was observed through irradiation at 360nm, UV analysis and size variation upon irradiation. IgG release from the nanospheres was monitored over 32 days and the profile shows up to 60% of drug was released from UV irradiated nanospheres, in a sustained manner. This novel photo-responsive HA-NSP nanosystem can be used as a less invasive alternative in the delivery of macromolecules to reduce the frequency of administration, achieve targeted therapy and increase patient tolerance.

3.5. REFERENCES

Babu, R.R., Kumaresan, S., Vijayan, N., Gunasekaran, M., 2003. and its characterization 256, 387–392. https://doi.org/10.1016/S0022-0248(03)01369-1

Bawa, P., Pillay, V., Choonara, Y.E., Toit, L.C., 2009. Stimuli-responsive polymers and their applications in drug delivery. Soft Matter 4, 1–15. https://doi.org/10.1088/1748-6041/4/2/022001

Cai, Y., Lu, J., Zhou, F., Zhou, X., Zhou, N., Zhang, Z., Zhu, X., 2014. Cyclic amphiphilic random copolymers bearing azobenzene side chains: Facile synthesis and topological effects on self-assembly and photoisomerization. Macromol. Rapid Commun. 35, 901–907. https://doi.org/10.1002/marc.201300913

Ding, L., Li, J., Jiang, R., Song, W., 2016. Photoresponsive Polymeric Reversible nanoparticles via Self-Assembly of Reactive ABA Triblock Copolymers and Their Transformation to. Materials (Basel). 9, 1–13. https://doi.org/10.3390/ma9120980

Fomina, N., Sankaranarayanan, J., Almutairi, A., 2012. Photochemical mechanisms of light-triggered release from nanocarriers. Adv. Drug Deliv. Rev. 64, 1005–1020. https://doi.org/10.1016/j.addr.2012.02.006

Gong, S., Wang, H., Sun, Q., Xue, S.T., Wang, J.Y., 2006. Mechanical properties and in vitro biocompatibility of porous zein scaffolds. Biomaterials 27, 3793–3799. https://doi.org/10.1016/j.biomaterials.2006.02.019

Hadavi, M., Hasannia, S., Faghihi, S., Mashayekhi, F., Homazadeh, H., Mostofi, S.B., 2018. Zein nanoparticle as a novel BMP6 derived peptide carrier for enhanced osteogenic differentiation of. Artif. Cells, Nanomedicine, Biotechnol. 46, 559–567. https://doi.org/10.1080/21691401.2018.1431649

Kuno, N., Fujii, S., 2011. Recent Advances in Ocular Drug Delivery Systems. Polymers (Basel). 3, 193–221. https://doi.org/10.3390/polym3010193

Lee, B.K., Yun, Y.H., Park, K., 2015. Smart nanoparticles for drug delivery: Boundaries and opportunities. Chem. Eng. Sci. 125, 158–164. https://doi.org/10.1016/j.ces.2014.06.042

Luo, Y., Zhang, B., Whent, M., Yu, L.L., Wang, Q., 2011. Preparation and characterization of zein/chitosan complex for encapsulation of ??-tocopherol, and its in vitro controlled release study. Colloids Surfaces B Biointerfaces 85, 145–152.

https://doi.org/10.1016/j.colsurfb.2011.02.020

Mahlumba, P., Choonara, Y.E., Kumar, P., Du Toit, L.C., Pillay, V., 2016. Stimuli-responsive polymeric systems for controlled protein and peptide delivery: Future implications for ocular delivery. Molecules 21, 1–21. https://doi.org/10.3390/molecules21081002

Natansohn, A., Rochon, P., 2002. Photoinduced motions in azo-containing polymers. Chem. Rev. 102, 4139–4175. https://doi.org/10.1021/cr970155y

Pang, J., Gao, Z., Tan, H., Mao, X., Xu, J., Kong, J., 2019. Fabrication , Investigation , and Application of Light-Responsive 7, 1–10. https://doi.org/10.3389/fchem.2019.00620

Pascoli, M., Lima, R. De, Fraceto, L.F., 2018. Zein Nanoparticles and Strategies to Improve Colloidal Stability : A mini review. Front. Chem. 6, 1–5. https://doi.org/10.3389/fchem.2018.00006

Pauluk, D., Padilha, A.K., Khalil, N.M., Mainardes, R.M., 2019. Food Hydrocolloids Chitosan-coated zein nanoparticles for oral delivery of resveratrol : Formation , characterization , stability , mucoadhesive properties and antioxidant activity. Food Hydrocoll. 94, 411–417. https://doi.org/10.1016/j.foodhyd.2019.03.042

Press, D., Hashem, F.M., Al-Sawahli, M.M., Nasr, M., Ahmed, O.A.A., 2015. Optimized zein nanospheres for improved oral bioavailability of atorvastatin. Int. J. Nanomedicine 10, 4059–4069. https://doi.org/10.2147/IJN.S83906

Regier, M.C., Taylor, J.D., Borcyk, T., Yang, Y., Pannier, A.K., 2012. Fabrication and characterization of DNA-loaded zein nanospheres. J. Nanobiotechnology 10, 1–13.

Rescifina, A., Abbadessa, A., Rapisardi, R., Andrea, A., 2016. Synthesis and characterization of copolycarbonates having azobenzene units in the main chain as an active group for optical logic gate devices. Polym. Chem. 7, 6318–6329. https://doi.org/10.1039/C6PY01326K

Roy, D., Cambre, J.N., Sumerlin, B.S., 2010. Future perspectives and recent advances in stimuli-responsive materials. Prog. Polym. Sci. 35, 278–301. https://doi.org/10.1016/j.progpolymsci.2009.10.008

Singh, R., Lillard, J.J.W., 2009. Nanoparticle-based targeted drug delivery. Exp. Mol. Pathol. 86, 215–223. https://doi.org/10.1016/j.yexmp.2008.12.004

Sivera, M., Kvitek, L., Soukupova, J., Panacek, A., Prucek, R., Vecerova, R., Zboril, R., 2014.

Silver Nanoparticles Modified by Gelatin with Extraordinary pH Stability and Long-Term Antibacterial Activity. PLoS One 9, 103675. https://doi.org/10.1371/journal.pone.0103675

Sousa, F.F.O., Luzardo-Alvarez, A., Perez-Estevez, A., Seone-Prado, R., Blanco-Mendez, J., 2010. Development of a novel AMX-loaded PLGA / zein microsphere for root canal disinfection. Biomed. Mater. 5, 1–10. https://doi.org/10.1088/1748-6041/5/5/055008

Souza, S.D., 2014. A Review of In Vitro Drug Release Test Methods for Nano-Sized Dosage Forms. Adv. Pharm. 2014, 1–12.

Torchilin, V., 2009. Multifunctional and stimuli-sensitive pharmaceutical nanocarriers. Eur. J. Pharm. Biopharm. 71, 431–44. https://doi.org/10.1016/j.ejpb.2008.09.026

Wang, B., Chen, K., Yang, R., Yang, F., Liu, J., 2014. Stimulus-responsive polymeric micelles for the light-triggered release of drugs. Carbohydr. Polym. 103, 510–9. https://doi.org/10.1016/j.carbpol.2013.12.062

Weissmueller, N.T., Lu, H.D., Hurley, A., Prud, R.K., 2016. Nanocarriers from GRAS Zein Proteins to Encapsulate Hydrophobic Actives. Biomaterials 17, 3828–3837. https://doi.org/10.1021/acs.biomac.6b01440

Yang, S.B., Rabbani, M.M., Ji, B.C., Han, D., 2016. Optimum Conditions for the Fabrication of Zein / Ag Composite Nanoparticles from Ethanol / H 2 O Co-Solvents Using Electrospinning. Nanomaterials 6, 1–11. https://doi.org/10.3390/nano6120230

Yasin, M.N., Svirskis, D., Seyfoddin, A., Rupenthal, I.D., 2014. Implants for drug delivery to the posterior segment of the eye: A focus on stimuli-responsive and tunable release systems. J. Control. Release 196, 208–221. https://doi.org/10.1016/j.jconrel.2014.09.030

Zhang, S., Han, Y., 2018. Preparation , characterisation and antioxidant activities of rutin-loaded zein-sodium caseinate nanoparticles. PLoS One 13, 1–13. https://doi.org/10.1371/journal.pone.0194951

CHAPTER FOUR
DEVELOPMENT AND CHARACTERISATION OF INJECTABLE NANOSPHERES LADEN IN HYALURONIC ACID GEL NANOSYSTEM

4.1. INTRODUCTION

Hydrogels have gained popularity in biomedical applications for their unique properties and in research for minimally invasive drug delivery approaches (Guvendiren et al., 2012). Hydrogels are semi-solid, cross-linked water-swollen polymers suitable for numerous therapeutic applications owing to their versatility, elasticity and ability to encapsulate drugs and polymeric nanoparticles within their mesh (Fathi et al., 2015; Liu et al., 2019).

Hyaluronic acid (HA) is a naturally occurring polysaccharide with desirable physical and mechanical properties suitable for drug delivery (Dubbini et al., 2015; Widjaja et al., 2013). It is bio-adhesive, biocompatible and easy to formulate into a simple viscoelastic shear-thinning hydrogel that is able to deliver drug loaded nanoparticles with minimal tissue invasion (Egbu et al., 2017; Wang and Han, 2017). Crosslinking HA gels improves viscosity and mechanical properties for homogenous dispersion of nanoparticles and to avoid sedimentation (Khunmanee et al., 2017). Genipin, originating from fruits of Gardenia jasminoides, has been widely studied for crosslinking of natural polymers for biomedical applications due its low cytotoxicity over other crosslinkers (Roether et al., 2019). In this study, HA modified with genipin was used as a hydrogel matrix; genipin was added according to optimised recommendations from previous investigations (Nejad et al., 2018).

Directly incorporating drugs into hydrogels results in a shorter drug release time, as a consequence of fast diffusion caused by high water content in the hydrogel (Drapala et al., 2014). As described in **Chapter 3**, nanocarriers improve passage through tissue and control drug release into target tissue, however, administration of drug loaded solid implantable delivery systems requires invasive surgical procedures and injection is not applicable due to aggregation and sedimentation which leads to high residue in the syringe after injection and insufficient therapeutic levels at the target site. Injectable hydrogels can overcome these drawbacks as they possess the advantage of minimal invasive administration and reach for asymmetrical target sites (Lee, 2018). Drug loaded solid nanoparticles can be dispersed in an injectable hydrogel for homogeneity, ease of administration, and optimal therapeutic concentrations at target tissue to improve patient adherence. In addition, hydrogel-nanoparticle combinations provide diverse synergistic properties superior to their individual composites (Thoniyot et al., 2015; Zhao et al., 2015).

Photo-responsive IgG loaded AZP nanospheres were dispersed in HA gel using a method, previously described by Thoniyot et al., to form the injectable HA-NSP nanosystem (Thoniyot et al., 2015). The prepared HA-NSP and its components were characterized through various techniques, to verify the formation of a novel nanosystem. Injectability, mechanical properties and rheology of the HA-NSP were studied through texture analysis (TA) and rheometer, and finally, *in vitro* cytotoxicity evaluation was determined using human retinal pigment epithelium (HRPE) cell lines via Annexin V and dead cell assay. This assay is easy, fast, and convenient; it requires minimal sample preparation and provides quantitative data for both live and dead cells via annexin v and a dead cell marker. Investigation of the possible cytotoxicity of delivery systems using *in vitro* cell models is more practical because of reproducibility, low cost, and simplicity, whereas, carrying out these experiments *in vivo* is complicated and invasive. In addition, numerous experimental parameters can be explored *in vitro* (Shafaie et al., 2016).

4.2. MATERIALS AND METHODS

4.2.1. Materials

Hyaluronic acid sodium salt from streptococcus and Genipin were purchased from Sigma-Aldrich (St. Louis, MO, USA). Cryopreserved HRPE cells, Retinal pigment epithelial basal medium, supplements (FBS, L-glutamine, GA-1000), and growth factor (FGF-B) were all purchased from Lonza Walkersville Inc. (Walkersville, MD, USA), and AZP nanospheres were synthesized from the laboratory.

4.2.2. Preparation of Hyaluronic acid gel and Incorporation of AZP nanospheres

The nanosphere-in-hydrogel system (HA-NSP) was formulated by dispersing nanospheres in an aqueous solution and a gelling agent was added, followed by a crosslinker (Thoniyot et al., 2015). Genipin was used as the crosslinker and hyaluronic acid (HA) as a gelling agent, and various concentrations were explored to find the composition best suited for the purpose of the nanosystem. Freeze-dried IgG loaded AZP nanospheres were dispersed in distilled water, HA was added into the dispersion stirring until completely dissolved, and finally, genipin was added to the gel to obtain the nanosphere-in-gel system.

4.2.3. Determination of Chemical Interactions of the Photo-responsive Nanosystem

The chemical structures and interactions between HA gel and nanospheres were studied using FT-IR spectrometer (PerkinElmer Spectrum 100) with infrared spectra recorded in the region from 4000cm^{-1} to 650cm^{-1} wavenumbers at a resolution of 4cm^{-1}. Gels were prepared by freeze-drying and dried samples were mounted directly onto the attenuated total

reflectance (ATR) crystal for analysis to identify chemical architecture and characteristic functional groups in the formulation.

4.2.4. Determination of the Thermal Transitions of the Photo-responsive Nanosystem

Thermal properties of the nanosystem and its components were explored using differential scanning calorimetry (DSC) (Mettler Toledo, Schwerzernback, Switzerland). Freeze-dried samples were weighed (3-10mg) into aluminium pans and analysed under nitrogen atmosphere (Afrox, Germiston, Gauteng, South Africa) with 200mL/min flow rate acting as the purge gas to decrease oxidation. An empty aluminium pan was used as a reference, and samples were then heated from 25ºC to 300ºC at the rate of 10ºC/min.

4.2.5. Determination of Thermal Decomposition of the Nanosystem

Analysis of thermal decomposition of the freeze-dried HA and HA-NSP gels was observed via thermogravimetric analysis (TGA) heated from 20˚C to 900˚C under nitrogen atmosphere, flow rate 20mL/min. This was carried out using a TGA 400 thermogravimetric analyser (PerkinElmer Inc., MA, USA). Samples weighing 10-20mg were placed in a ceramic pan under nitrogen atmosphere. Thermograms were obtained and analysed for thermal decomposition properties of the gels.

4.2.6. Determination of Injectability of the Photo-responsive Nanosystem

To investigate the consistency and injectability of the hydrogel, the texture analyser (Stable Micro Systems TA-XT2, Surrey, UK) was employed. For the injectability test, all measurements (HA-NSP, and HA) were carried out in triplicate at room temperature. All tests were performed in compression mode using 27G and 31G needles. For the test, a needle was fitted into a 1mL syringe and placed in a holder vertically with the needle downward. A cylinder probe (P/50R) was aligned to the plunger plate for displacement of the volume, mimicking the manual syringe injection. The compression speed was set at 1mm/s for a distance of 20mm. During the test, the probe compresses the syringe plunger, forcing the contents of the syringe out and the maximum force used is recorded (Cilurzo et al., 2011; Zhang et al., 2018). All measurements were performed in triplicates.

4.2.7. Determination of Rheological Properties of the Photo-responsive Nanosystem

Rheology was used to study the shear viscosity of a pure HA gel and the genipin crosslinked HA gel, as well as the rheological behaviour of the HA-NSP nanosystem. Measurements were carried out on a rotational rheometer (Thermo Fisher Scientific HAAKE^{TM} MARS^{TM}, Waltham, MA, USA) equipped with RheoWin software for data analysis. Samples were loaded onto the

rheometer; a frequency sweep from 0.1 to 10Hz and a strain sweep from 0.1 to 100Pa were performed on the samples to determine storage (G') and loss (G") moduli for rheological investigation. All measurements were performed in triplicates.

4.2.8. *In Vitro* Cytotoxicity Testing of the Photo-responsive Nanosystem using H-RPE Cell Lines

Retinal pigment epithelium (RPE) is a multifunctional, nonproliferating cell monolayer located between the vascular choroid and the retina, forming the outer layer of the blood-retinal barrier. These cells function as a nutrient supplier, structural maintenance, functional integrity of the retina as well as regulating of drug transport into the inner parts of the eye (Hellinen et al., 2019). RPE dysfunction is associated with the development of various retinal pathologies such as macular degeneration which may result in irreversible blindness in elderly people (Fronk and Vargis, 2016). H-RPE cell lines were used for cytocompatibility testing on the HA-NSP nanosystem.

4.2.8.1. Cell culturing using H-RPE Cell Lines

H-RPE cell lines were grown in culture flasks containing a growth medium (RtEGM) which comprises of the retinal pigment epithelial basal medium supplemented with GA-1000, L-glutamine, and FGF-B as a growth factor. This method was obtained from the supplier. Briefly, the serum free growth medium and plating medium (RtEGM with 2% FBS) were prepared in a sterile environment. The appropriate amount of plating medium was added to the culture flask and the flask was equilibrated in a humidified incubator (NuAire In-VitroCell™ ES NU-5710, Plymouth, MN, USA) under the atmosphere of 5% CO_2 at 37°C for a period of 30 minutes. The cryovial containing cryopreserved cells was thawed in a water bath at 37°C and cells were resuspended in the cryovial, followed by dispensing into the equilibrated culture flask using a micropipette and thereafter, maintained in the incubator for the duration of cell growth. The medium was changed to serum free growth medium at 24 hours after seeding and every second day thereafter. When cells reached 80-90% confluence, the medium was aspirated and discarded, and cells washed with HEPES-BSS followed by addition of Trypsin/EDTA (2mL) and allowing cell detachment for 3-6 minutes. Trypsin neutralizing solution (4mL) was then added, and the suspension was centrifuged at 1500rpm for 5 minutes. The supernatant was discarded, resultant pellet resuspended in fresh plating medium and poured into sterile culture flasks. For cryopreservation, cells were frozen in a cryoprotective mixture containing 5%v/v DMSO under liquid nitrogen atmosphere.

4.2.8.2. Cell counting utilizing Trypan blue solution Assay and a Haemocytometer

After detaching and resuspending the cells as described in **section 4.2.8.1**, the total number of viable cells was counted. Briefly, Trypan blue solution (20µL) was added to the suspended cells (20µL). The haemocytometer chamber was filled with the trypan blue solution and cell suspension mixture, and light microscopy (Olympus CKS microscope, Olympus, Japan) was used to examine the chamber for cell counting. Trypan blue solution only stains dead cells, therefore, to determine the number of live cells in suspension, unstained cells were counted.

4.2.8.3. *In vitro* cytotoxicity evaluation of the Photo-responsive Nanosystem utilizing Annexin V and Dead cell assay

Cytotoxicity effect of the HA-NSP and individual components in HRPE cell lines was assessed using the Annexin v & Dead cell assay (Millipore Corp., Billerica, USA) according to the manufacturer's protocol. Briefly, HRPE cells were seeded into 12-well plates at a density of $1x10^4$ cells/cm^2. Cells were maintained in the incubator under humidified atmospheric conditions of 5% CO_2 at 37°C for 24 hours before treatment. The culture was then removed from the incubator into a laminar flow unit. Various treatments tested were, IgG loaded nanospheres, IgG, zein, HA gel, HA-NSP and Triton X as the positive control. All treatments were prepared in solution and suspension under sterile conditions before adding them to the cell culture. Cells were incubated for a further 24 hours and 48 hours at 37°C. Thereafter, cells were detached and centrifuged according to the method mentioned in section **4.2.8.1**. Resultant pellets were resuspended in fresh medium to create single suspensions. A 100µL of cell suspension was added to each tube, followed by 100µL Annexin v & Dead cell reagent. Cell samples were vortexed and left in the dark for 20 minutes at room temperature to allow for staining before analysis. Samples were analysed through the Muse™ Cell Analyzer (Millipore Corp., Billerica, USA) and all measurements were performed in triplicate. The relative cell viability was calculated using **equation 4.1**.

$$\text{Relative cell viability } (\%) = \frac{\text{Sample}}{\text{Control}} \text{ x}100 \qquad \text{(Equation 4.1)}$$

4.3. RESULTS AND DISCUSSION

Homogenous dispersion of IgG loaded photo-responsive AZP nanospheres in HA gel was successful and the injectable HA-NSP was obtained. Genipin was used to enhance the viscosity of the HA hydrogel in order to avoid sedimentation of the dispersed nanospheres. Genipin reacts with primary amino groups of proteins and amino acids to produce blue pigments (Wang et al., 2011). This pigment was observed in the HA gels modified with genipin. The colour variation is shown in **Figure 4.1** where **a** and **c** are pure HA gels with a clear colour,

b, the HA-GP gel showing a light blue colour, and **d**, HA-NSP nanosystem displaying the dispersion of nanospheres in the hydrogel. The darker pigment in HA-NSP may be attributed to the presence of amino groups in the composition of AZP nanospheres as well as their brown colour. A non-UV method was used to study cell cytotoxicity to avoid interference from the UV sensitive component of the formulation. Additionally, H-RPE primary cell lines can only attain cell division over limited passaging before reaching replicative failure, therefore experiments in this study were carried out in earlier passages to avoid compromising results (Klimanskaya, 2006; Kuznetsova et al., 2016).

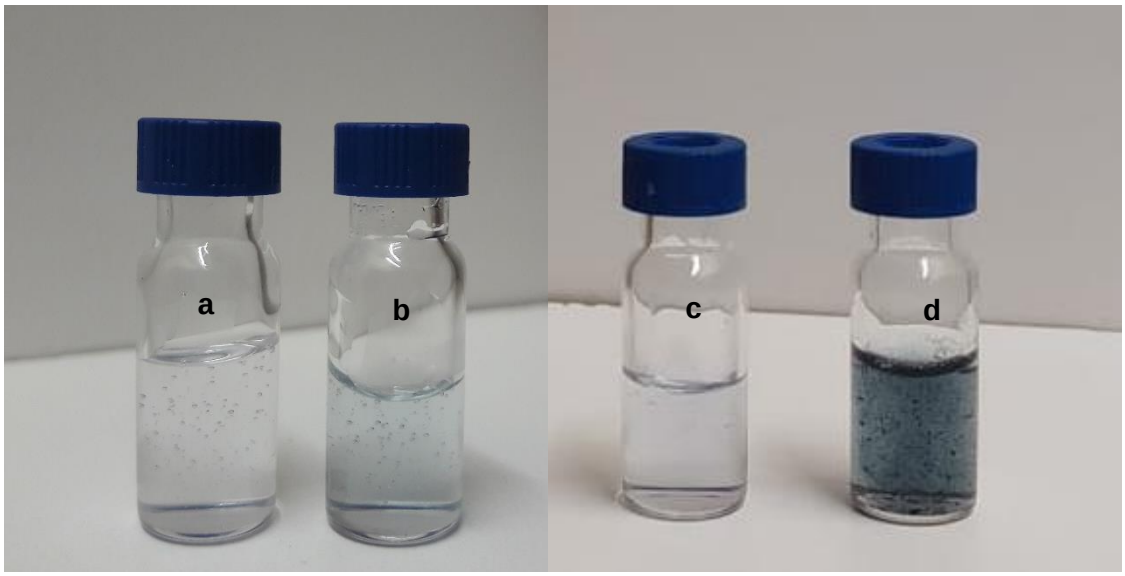

Figure 4.1: Images of the formulations (a) pure HA gel, (b) HA-GP gel, (c) pure HA gel, and (d) HA-NSP nanosystem.

4.3.1. Evaluation of Chemical Transitions and Intermolecular Interactions of the components and Photo-responsive Nanosystem

FTIR was used to assess the interaction between HA gel and AZP nanospheres in HA-NSP. Gels were freeze-dried before scanning via attenuated total reflectance. The following characteristic peaks were observed in the spectra; stretching vibrations at 3327cm^{-1} and 3295cm^{-1}, protein amide I at (C=O) at 1635cm^{-1} and 1643cm^{-1}, C-O stretching at 1058cm^{-1} and 1074cm^{-1} for HA gel and AZP nanospheres, respectively (Gilarska et al., 2018). The presence of genipin in HA-GP was clearly observed. There were no significant differences in the spectra of HA-GP gel and HA-NSP, however, a slight shift in the peaks was detected in HA-NSP spectrum from 3289cm^{-1}, 1643cm^{-1} and 1058cm^{-1} to 3271cm^{-1}, 1627cm^{-1} and 1050cm^{-1}. This is an indication of weak hydrogen bonding between the gel and nanospheres (Chen et al., 2019).

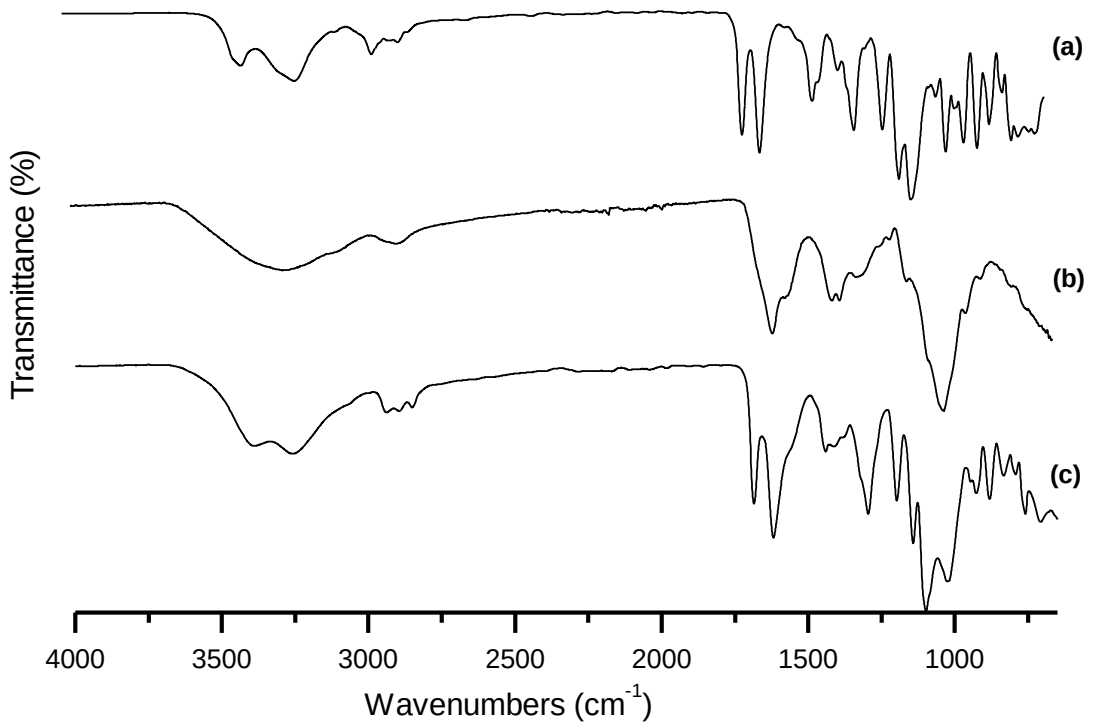

Figure 4.2: FTIR spectra of (a) genipin, (b) pristine HA and (c) genipin crosslinked HA hydrogel.

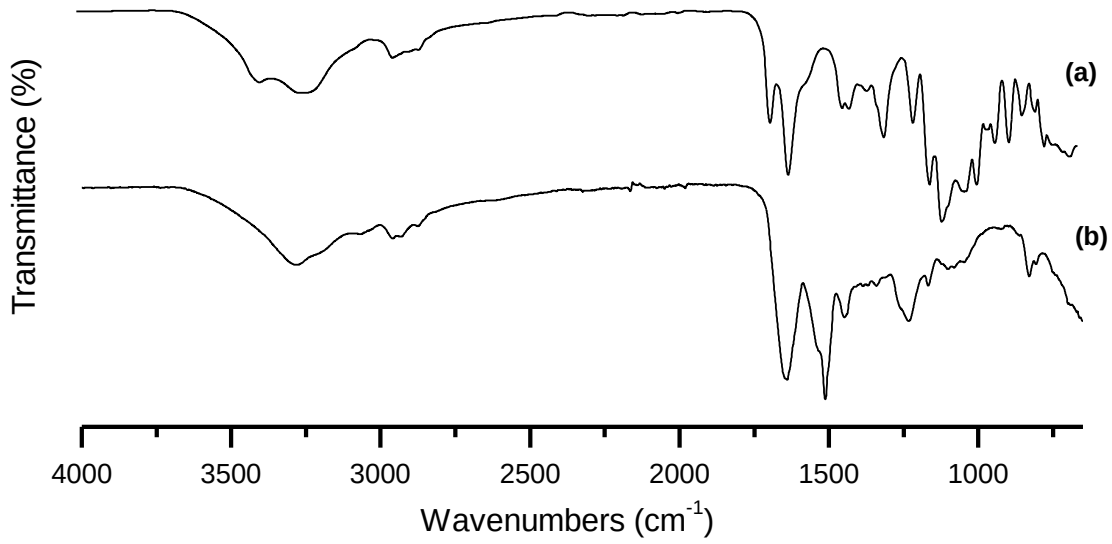

Figure 4.3: FTIR spectra of (a) IgG loaded AZP nanospheres and (b) HA-NSP.

4.3.2. Thermal and Thermodynamic Analysis of the Photo-responsive Nanosystem

Thermal behaviour of the nanospheres, HA gel and HA-NSP was analysed using differential scanning calorimetry. Samples were freeze-dried and analysed in the temperature range 25ºC-300ºC; results are presented in **figure 4.4**. Thermogram for pristine HA (**figure 4.4a**) showed a broad endothermic melting point at 117ºC and a sharp exothermic crystallization

point at 238ºC. HA gel (**figure 4.4b**) showed a sharp endothermic peak at 117ºC corresponding to its melting point and a broader exothermic peak at 238ºC suggesting that the gel is more prone to degradation compared to the native HA (Sithole et al., 2018). AZP nanospheres thermogram (**figure 4.4c**) exhibited a broad exothermic peak at 276ºC. A distinct sharp endothermic melting point at 117ºC was observed in the thermogram for HA-NSP (**figure 4.4d**) and a broad exothermic peak at 239ºC confirming that the nanosystem's thermal behaviour is more endothermic, therefore, the dispersed AZP nanospheres can be released from the gel without substantial energy involved in the process.

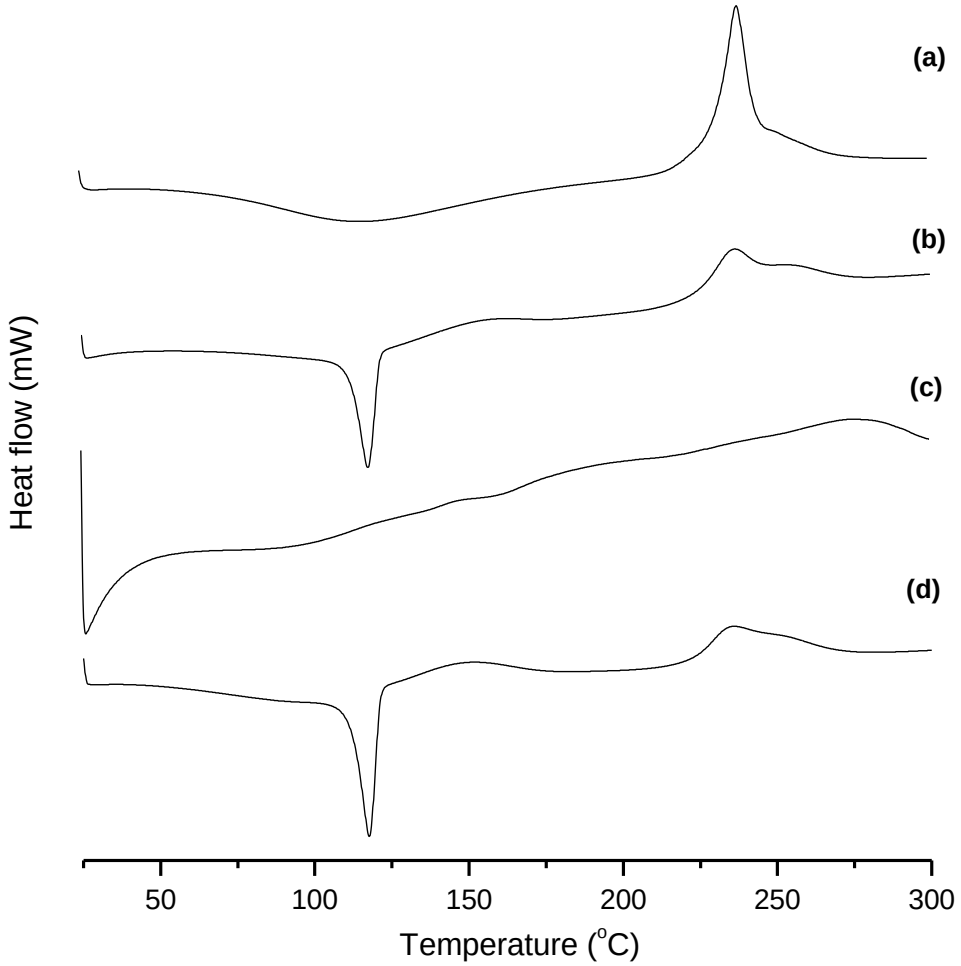

Figure 4.4: DSC thermograms of (a) Pristine HA, (b) HA gel, (c) NSP and (d) HA-NSP, measured from 25ºC to 300ºC.

4.3.3. Thermogravimetric Analysis of the Photo-responsive Nanosystem

Thermogravimetric analysis provides data about degradation of materials and identification of new formed compounds. TGA thermograms displayed in **figure 4.5** show the degradation pattern and stability of HA-NSP and its components, AZP nanospheres and HA gel. Gels were freeze-dried before carrying out measurements. HA-NSP underwent a two-step degradation process at 120ºC and 237ºC, whereas the components showed single degradation points with HA at 235ºC and AZP nanospheres at 280ºC. AZP nanospheres had the lowest residue (11%)

and HA-NSP had the highest residues (21%), confirming its thermal stability, thus suggesting that the combination of HA gel and AZP nanospheres is more stable than the individual components.

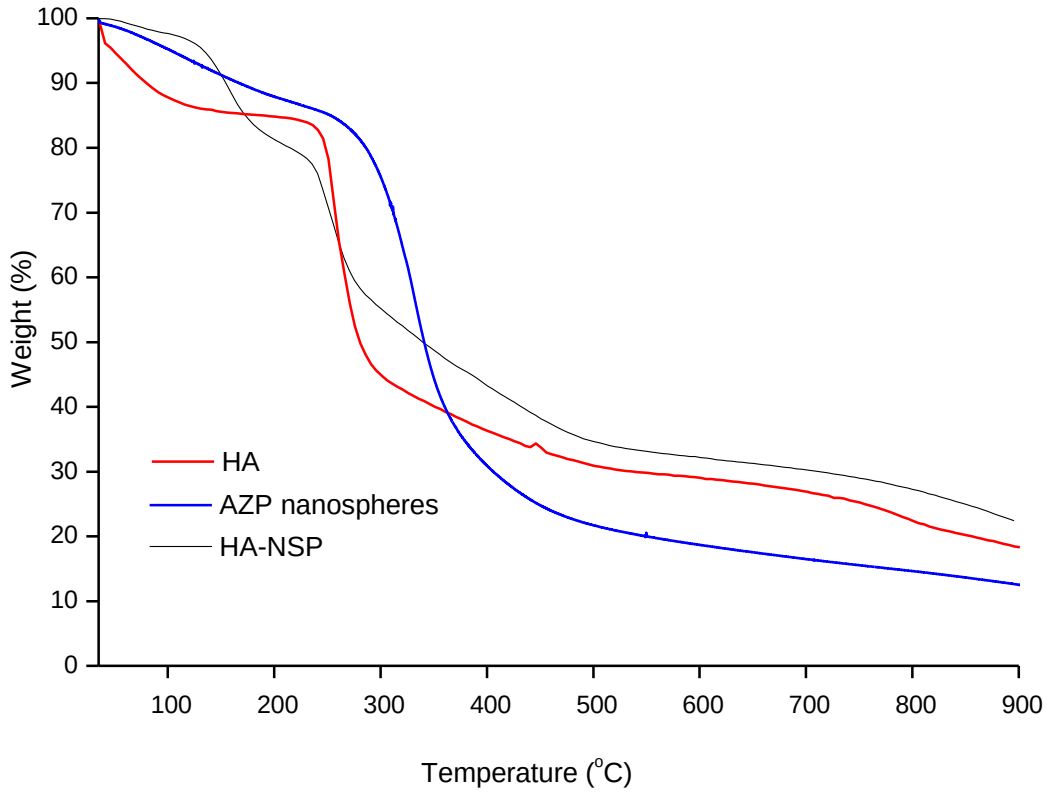

Figure 4.5: TGA thermograms of HA, AZP nanospheres and HA-NSP.

4.3.4. Determination of Injectability of the Photo-responsive Nanosystem

Injectability of the HA gel and HA-NSP was measured as the force required to inject the hydrogel through a 1mL syringe fitted with 27G and 31G needles. HA-NSP is a composition of chromophore-equipped nanospheres dispersed in HA gel. The force required for injection works on 3 parts, (i) the resistance of the syringe plunger, (ii) the kinetic energy to the contents of the syringe, and (iii) forcing the liquid through the needle (Allahham et al., 2004). This process is affected by the viscosity of the sample and the size of the needle used. **Figure 4.6** presents the maximum force it takes to inject the samples. The HA gel required 9N and 14N whereas the HA-NSP took 10N and 18N to inject through 27G and 31G needles, respectively. **Figure 4.7** displays graphs obtained from the injectability tests conducted on HA gel and HA-NSP (**a, b)** through a 27G needle and (**c, d)** a 31G needle. Two parameters that affected the force of injection are, the decrease in the size of the needle and the dispersion of nanospheres in the gel which resulted in increased maximum force required for injection. These results remain within two thirds of the recommended value of the maximum force for a manual injection which is 30N, therefore, the HA-NSP is suitable for injection through various routes

of administration. Furthermore, for ease of administration and minimal discomfort, 10N is the recommended maximum force and this qualifies the 27G needle as the best suited selection for this formulation (Wang et al., 2018).

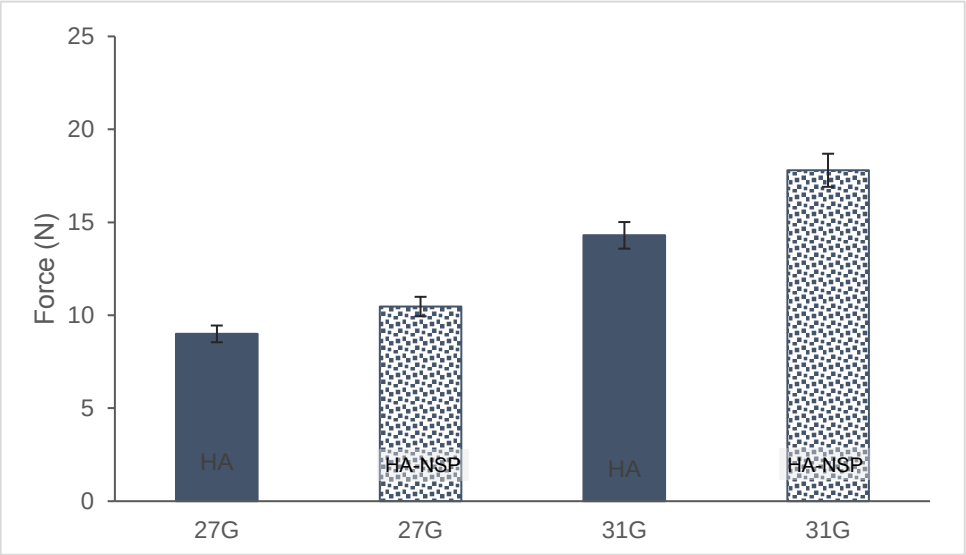

Figure 4.6: Maximum injection force for 1% HA gel and HA-NSP using two needle sizes, 27G and 31G.

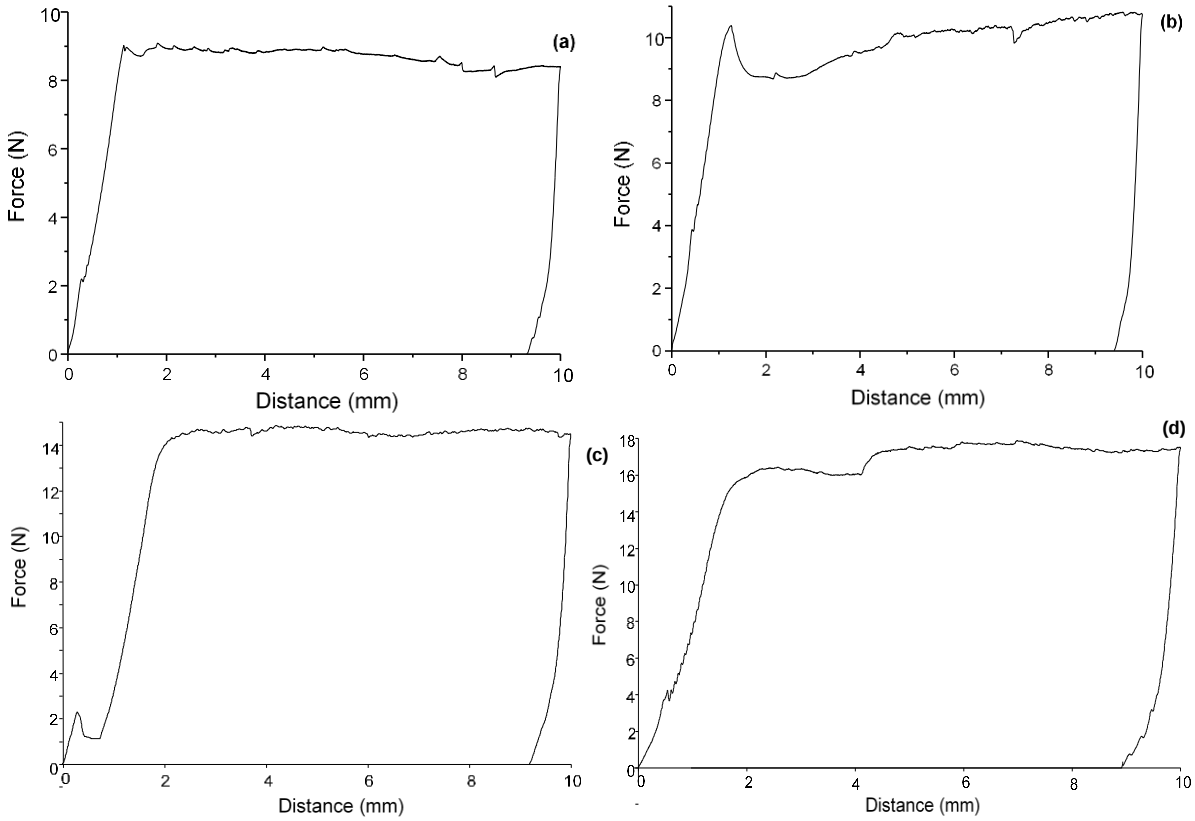

Figure 4.7: Injectability test for (a) 1%w/v HA gel through 27G, (b) HA-NSP through 27G, (c) 1%w/v HA gel through 31G, (d) HA-NSP through 31G needles.

4.3.5. Rheological behaviour of the Photo-responsive Nanosystem

Shear viscosity measurements of the pure HA and HA-GP gels were performed to study the mechanical variation caused by addition of genipin. In **figure 4.8**, a slightly higher shear viscosity is observed in the HA-GP gel over the pure HA gel with a p-value 0.0006 substantiating the significant difference between these two hydrogels. These results confirm that adding genipin to pure HA increases viscosity of the gel. HA lacks the primary amino groups that genipin is known to react with, however, it is postulated that its highly reactive hydroxy groups are capable of forming glycosidic bonds with genipin which are stable in water (Roether et al., 2019; Selyanin et al., 2015).

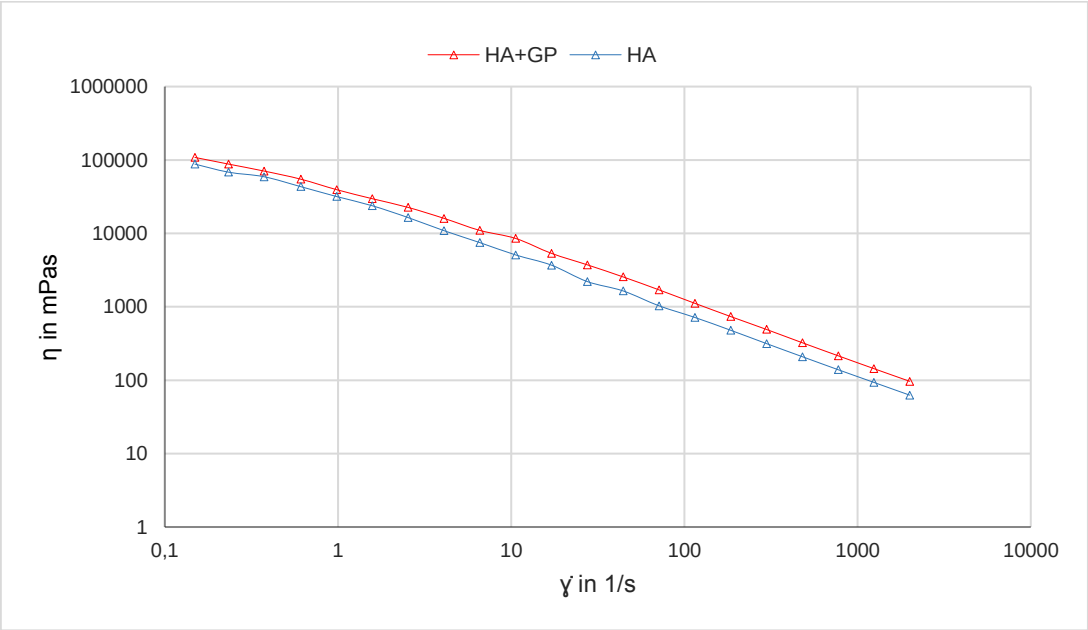

Figure 4.8: Shear viscosity measurements of pure HA gel and genipin crosslinked HA hydrogel (*p*=0.0006).

Rheological behaviour of HA-NSP was determined through the mechanical properties which are, viscosity, elastic (G') and viscous (G") modulus. These are important parameters in the determination of hydrogel injectability (Chen et al., 2017). Viscosity is a measurement of material's resistance to deformation upon stress application and a response to shear stress variations taking place during injection of hydrogel formulations. Elastic and viscous moduli measure the elasticity or rigidity of a hydrogel and provide information about the viscoelastic response upon shear, in this case, during injection (Kechai et al., 2015).

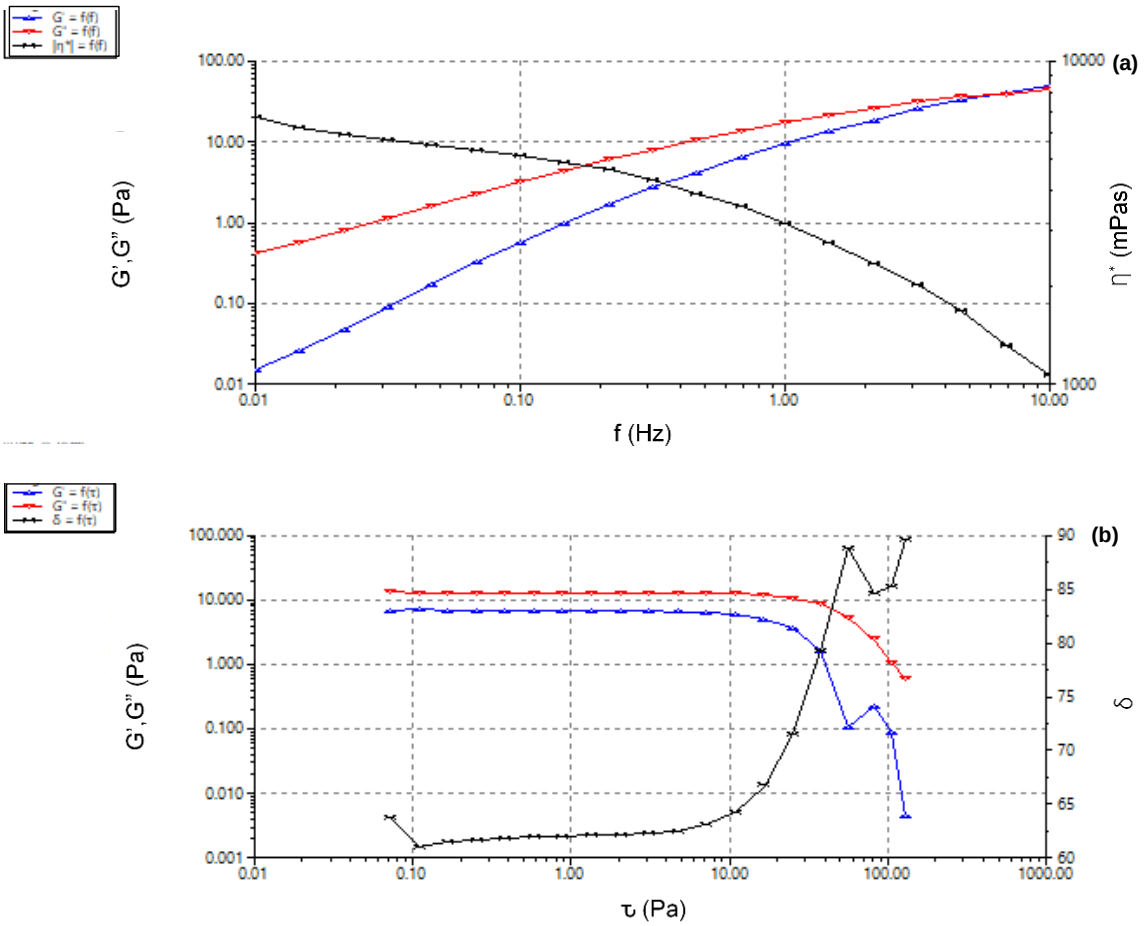

Figure 4.9: Rheology of HA-NSP (a) frequency sweep, (b)stress sweep.

A frequency sweep from 0.1Hz to 10Hz at 1% strain, strain sweep of up to 100Pa, and yield stress tests were conducted at 25ºC as this is the temperature of the environment in which an injection would be performed. Viscoelastic behaviour was observed in **figure 4.9a** wherein, the loss modulus was dominant below the crossover frequency 8Hz (G'=G"=75±0.5Pa) and storage modulus was dominant above this frequency. Complex viscosity decreased with the increase in frequency, indicating shear thinning behaviour of the HA-NSP nanosystem (Soiberman et al., 2018). The crossover point is the transition from viscous gel character where G">G' to elastic behaviour, G'>G". Material yielding was observed from the strain sweep in **figure 4.9b** indicated by a drop in storage and loss moduli after 47.22Pa strain. This yield strain is the point at which material starts to flow and this is essential for ease of injection of the formulation. Viscosity decreased with increasing shear stress confirming shear thinning behaviour of HA-NSP and further indicating homogenous dispersion of the nanospheres in the gel. Shear thinning gels experience a high shear rate exerted by the walls during injection, which results in reasonable force of injection as a consequence of the decreased viscosity. (Rad et al., 2019; Xu et al., 2013).

4.3.6. Cell cytotoxicity studies

HRPE cells treated with injectable photo-responsive nanosystem (HA-NSP), NSPs, zein, HA gel and IgG solution were analysed using annexin v & dead cell assay. Results are presented in **figure 4.10** as relative cell viability from the treated cultures of HRPE cells for up to a period of 48 hours and microscopic images are displayed in **figure 4.11**. The relative viability of HRPE cells remained over 80% ($p \leq 0.05$) in all treated cultures. There was no significant change in viability from cells treated with both zein and IgG compared with untreated control cells, which confirmed the cytocompatibility of these components. Literature has attributed the cytocompatibility of zein to its degradation products that are beneficial to cell proliferation (Farris et al., 2017). HA gel decreased cell viability by 20% over 48 hours, whereas IgG loaded nanospheres and the HA-NSP decreased cell viability by 8% and 11%, respectively. Where relative cell viability is ≥70%, the material is considered non-cytotoxic (ISO, 2009), therefore, these results show that the HA-NSP nanosystem is non-cytotoxic to HRPE cell lines.

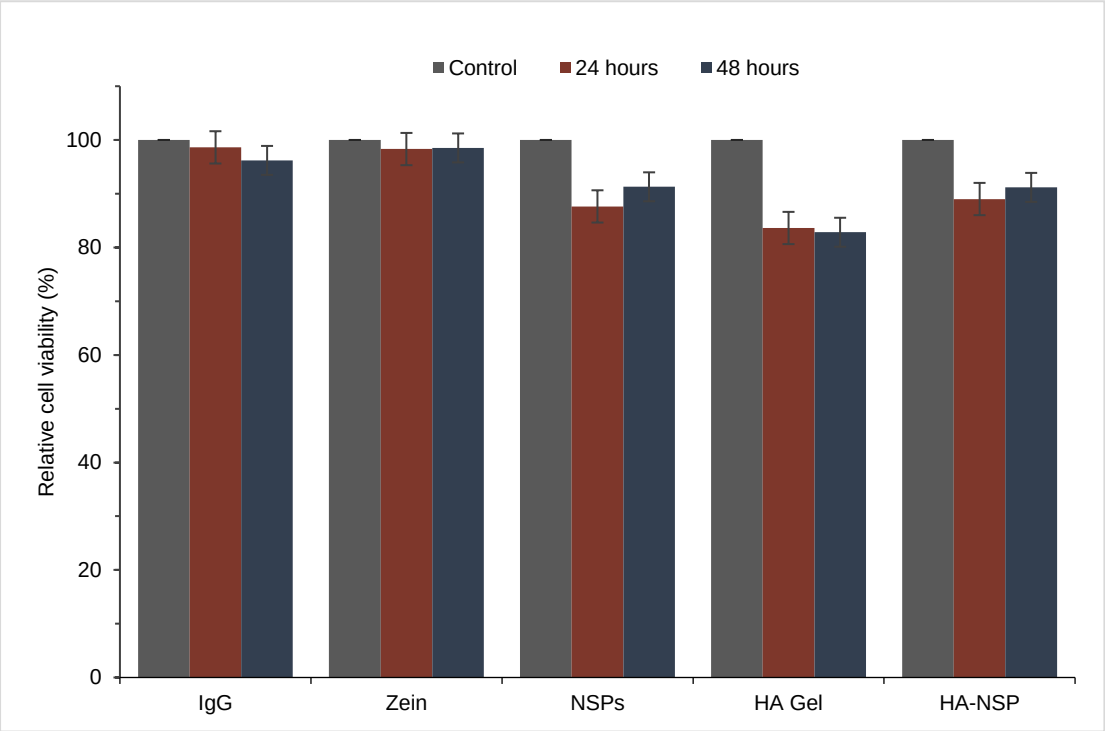

Figure 4.10: Cytotoxicity testing of native components, IgG and HA-NSP on HRPE cells cultured for up to 48 hours.

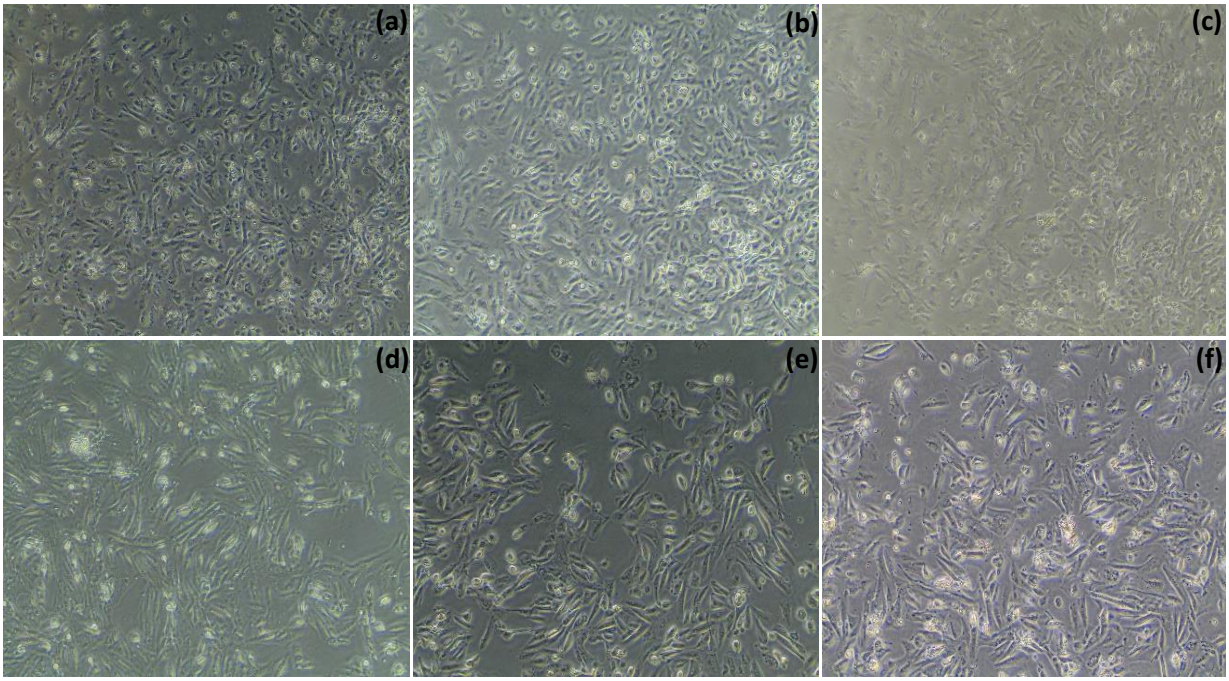

Figure 4.11: Images showing the various treatments after 48 hours of incubation, (a) untreated cells, (b) IgG, (c) zein, (d) NSP, (e) HA gel and (d) HA-NSP.

Furthermore, Annexin v and dead cell assay provides results distinguishing mechanism of toxicity by two cell death pathways, namely, apoptosis (programmed cell death) and necrosis which is a passive cell death process usually caused by external injury to the cell (Méry et al., 2017). Annexin v binds to the externalised phosphatidylserine (PS) from asymmetrical cell membrane in apoptotic cells and the dead cell marker 7-AAD binds to necrotic cells (Schwab et al., 2003). Apoptosis eventually results in necrosis (Cummings et al., 2013). Late apoptosis is detected when the cell is positive for both PS and 7-AAD. Apoptosis profiles obtained from the study are displayed in **figure 4.12**. Treated HRPE cell death after 48 hours is presented in **figure 4.13** as the percentage apoptosis and necrosis. These results show that the dominant pathway for cell death was apoptosis for all treatments. HA gel showed the highest percentage of necrotic cells (7%) and this may be attributed to the presence of genipin (Wang et al., 2011), however, this percentage was 0,25% for HA-NSP confirming that cytocompatibility was improved in the composition of HA gel and AZP nanospheres which is the HA-NSP nanosystem.

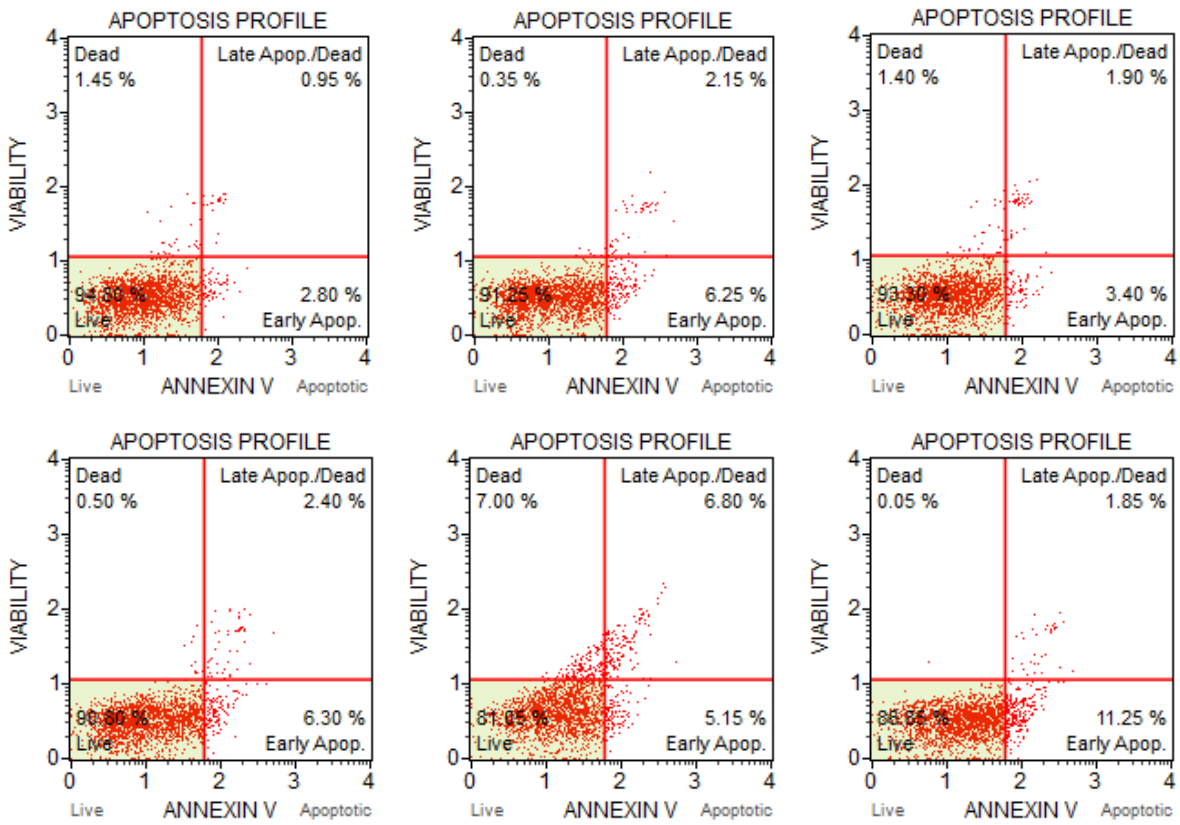

Figure 4.12: Apoptosis profiles for (a) untreated cells, (b) IgG, (c) zein, (d) NSP, (e) HA gel and (f) HA-NSP.

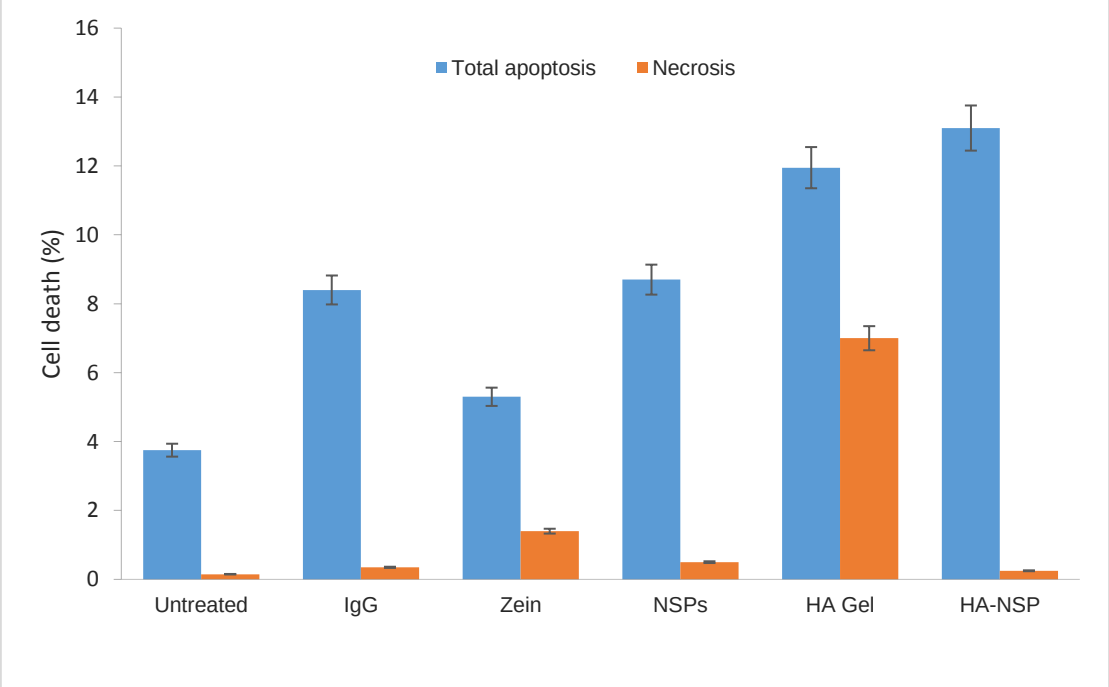

Figure 4.13: HRPE cell death presented as percentage apoptosis and necrosis (p=0.004).

4.4. CONCLUDING REMARKS

A novel injectable photo-responsive nanosystem, HA-NSP, was developed as a carrier for macromolecular protein/peptide drugs. HA-NSP consists of photo-responsive IgG loaded AZP nanospheres homogenously dispersed in HA gel. The higher shear viscosity of HA-GP gel compared to pure HA gel and HA-NSP shear-thinning properties were confirmed by rheological measurements. Injectability was monitored from two different needle sizes, and results showed a smaller force required to inject the gels with an increased in needle size, which is indicative of the ease of injection. *In vitro* cell cytotoxicity study carried out using HRPE primary cell lines showed a relative cell viability ≥80% from both nanospheres and HA-NSP, thus confirming non-toxicity and potential safety for use *in vivo*. This study confirmed that the developed HA-NSP nanosystem is non-cytotoxic, injectable, and able to accomplish prolonged protein/peptide release in a controlled fashion.

4.5. REFERENCES

Allahham, A., Mainwaring, D., Stewart, P., Marriott, J., 2004. Development and application of a micro-capillary rheometer for in-vitro evaluation of parenteral injectability. J. Pharm. Pharmacol. 56, 709–716. https://doi.org/10.1211/0022357023457

Chen, M.H., Wang, L.L., Chung, J.J., Kim, Y., Atluri, P., Burdick, J.A., 2017. Methods To Assess Shear-Thinning Hydrogels for Application As Injectable Biomaterials. ACS Biomater. Sci. Eng. 3, 3146–3160. https://doi.org/10.1021/acsbiomaterials.7b00734

Chen, S., Han, Y., Wang, Y., Yang, X., Sun, C., Mao, L., Gao, Y., 2019. Zein-hyaluronic acid binary complex as a delivery vehicle of quercetagetin: Fabrication, structural characterization, physicochemical stability and in vitro release property. Food Chem. 276, 322–332. https://doi.org/10.1016/j.foodchem.2018.10.034

Cilurzo, F., Selmin, F., Minghetti, P., Adami, M., Bertoni, E., Lauria, S., Montanari, L., 2011. Injectability evaluation: An open issue. AAPS PharmSciTech 12, 604–609. https://doi.org/10.1208/s12249-011-9625-y

Cummings, B.S., Wills, L.P., Schnellmann, R.G., 2004. Measurement of Cell Death in Mammalian Cells. Curr. Protoc. Pharmacol. 25, 1–30. https://doi.org/10.1002/0471141755.ph1208s25.Measurement

Drapala, P.W., Jiang, B., Chiu, Y.C., Mieler, W.F., Brey, E.M., Kang-Mieler, J.J., Pérez-Luna, V.H., 2014. The effect of glutathione as chain transfer agent in PNIPAAm-based thermo-responsive hydrogels for controlled release of proteins. Pharm. Res. 31, 742–753.

https://doi.org/10.1007/s11095-013-1195-0

Dubbini, A., Censi, R., Butini, M.E., Giovanna, M., Agas, D., Vermonden, T., Martino, P. Di, Agas, D., Vermonden, T., Martino, P. Di, 2015. Injectable hyaluronic acid/PEG-p (HPMAm-lac)-based hydrogels dually cross-linked by thermal gelling and Michael addition. Eur. Polym. J. 72, 423–437. https://doi.org/10.1016/j.eurpolymj.2015.07.036

Egbu, R., Brocchini, S., Khaw, P.T., Awwad, S., 2017. Antibody loaded collapsible hyaluronic acid hydrogels for intraocular delivery. Eur. J. Pharm. Biopharm. 124, 95–103. https://doi.org/10.1016/j.ejpb.2017.12.019

Farris, E., Brown, D.M., Ramer-tait, A.E., Pannier, A.K., 2017. Chitosan-zein nano-in-microparticles capable of mediating in vivo transgene expression following oral delivery. J. Control. Release 249, 150–161. https://doi.org/10.1016/j.jconrel.2017.01.035

Fathi, M., Barar, J., Aghanejad, A., Omidi, Y., 2015. Hydrogels for ocular drug delivery and tissue engineering. Tabriz Univ. Med. Sci. 5, 159–164. https://doi.org/10.15171/bi.2015.31

Fronk, A.H., Vargis, E., 2016. Methods for culturing retinal pigment epithelial cells : a review of current protocols and future recommendations. J. Tissue Eng. 7, 1-23. https://doi.org/10.1177/2041731416650838

Gilarska, A., Lewandowska-łańcucka, J., Horak, W., Nowakowska, M., 2018. Collagen/chitosan/hyaluronic acid – based injectable hydrogels for tissue engineering applications – design, physicochemical and biological characterization. Colloids Surfaces B Biointerfaces 170, 152–162. https://doi.org/10.1016/j.colsurfb.2018.06.004

Guvendiren, M., Lu, H.D., Burdick, J.A., 2012. Shear-thinning hydrogels for biomedical applications. Soft Matter 8, 260-272. https://doi.org/10.1039/c1sm06513k

Hellinen, L., Pirskanen, L., Tengvall-unadike, U., Urtti, A., 2019. Retinal Pigment Epithelial Cell Line with Fast Differentiation and Improved Barrier Properties. Pharmaceutics 11, 1–12.

ISO, 2009. Biological evaluation of medical devices — Part 5: Tests for in vitro cytotoxicity. ISO 10993-5.

Kechai, N. El, Bochot, A., Huang, N., Nguyen, Y., Ferrary, E., Agnely, F., 2015. Effect of liposomes on rheological and syringeability properties of hyaluronic acid hydrogelsintended for local injection of drugs. Int. J. Pharm. 487, 187–196.

https://doi.org/10.1016/j.ijpharm.2015.04.019

Khunmanee, S., Jeong, Y., Park, H., 2017. Crosslinking method of hyaluronic-based hydrogel for biomedical applications. J. Tissue Eng. 8, 1–16. https://doi.org/10.1177/2041731417726464

Klimanskaya, I., 2006. [11] Retinal Pigment Epithelium. Methods Enzymol. 418, 169–194. https://doi.org/10.1016/S0076-6879(06)18011-8

Kuznetsova, A. V, Aleksandrova, M.A., Kurinov, A.M., Chentsova, E. V, Pavel, V., 2016. Plasticity of adult human retinal pigment epithelial cells. Int. J. Clin. Exp. Med. 9, 20892–20906.

Lee, J.H., 2018. Injectable hydrogels delivering therapeutic agents for disease treatment and tissue engineering. Biomater. Res. 22, 1–14. https://doi.org/10.1186/s40824-018-0138-6

Liu, W., Borrell, M.A., Venerus, D.C., Mieler, W.F., Kang-mieler, J.J., 2019. Characterization of Biodegradable Microsphere-Hydrogel Ocular Drug Delivery System for Controlled and Extended Release of Ranibizumab. Transl. Vis. Sci. Technol. 8, 1–13.

Méry, B., Guy, J., Vallard, A., Espenel, S., Ardail, D., Rodriguez-lafrasse, C., Rancoule, C., Magné, N., Ipnl, N.D.L., Lyon-sud, F.F.D.M., Lyon, C.B., 2017. In Vitro Cell Death Determination for Drug Discovery : A Landscape Review of Real Issues. J. Cell Death 10, 1–8. https://doi.org/10.1177/1179670717691251

Nejad, Z.M., Torabinejad, B., Davachi, S.M., Zamanian, A., Garakani, S.S., Najafi, F., Nezafati, N., 2018. Synthesis, physicochemical, rheological and in-vitro characterization of double-crosslinked hyaluronic acid hydrogels containing Dexamethasone and PLGA/Dexamethasone nanoparticles as hybrid systems for specific medical applications. Int. J. Biol. Macromol. 126, 193–208. https://doi.org/10.1016/j.ijbiomac.2018.12.181

Rad, E.R., Thomas, S., Vahabi, H., 2019. Injectable poloxamer / graphene oxide hydrogels with well - controlled mechanical and rheological properties. Polym. Adv. Technol. 30, 1–11. https://doi.org/10.1002/pat.4654

Roether, J., Oelschlaeger, C., Willenbacher, N., 2019. Hyaluronic acid cryogels with non-cytotoxic crosslinker genipin. Mater. Lett. X 4, 100027. https://doi.org/10.1016/j.mlblux.2019.100027

Schwab, C.E., Tuschl, H., Schwab, C.E., Tuschl, H., 2003. Human & Experimental Toxicology In vitro studies on the toxicity of isoniazid in different cell lines. Hum. Exp. Toxicol. 22, 607–615. https://doi.org/10.1191/0960327103ht401oa

Selyanin, M.A., Boykov, P.Y., Khabarov, V.N., Polyak, F., 2015. Molecular and Supramolecular Structure of Hyaluronic Acid. Hyaluronic Acid 97–119. https://doi.org/10.1002/9781118695920.ch4

Shafaie, S., Hutter, V., Cook, M.T., Brown, M.B., Chau, D.Y.S., 2016. In Vitro Cell Models for Ophthalmic Drug Development Applications 5, 94–108. https://doi.org/10.1089/biores.2016.0008

Sithole, M.N., Choonara, Y.E., du Toit, L.C., Kumar, P., Marimuthu, T., Kondiah, P.P.D., Pillay, V., 2018. Development of a Novel Polymeric Nanocomposite Complex for Drugs with Low Bioavailability. AAPS PharmSciTech 19, 303–314. https://doi.org/10.1208/s12249-017-0796

Soiberman, U., Kambhampati, S.P., Wu, T., Mishra, M.K., Oh, Y., Sharma, R., Wang, J., Elah, A., Towerki, A., Yiu, S., Stark, W.J., Kannan, R.M., Hopkins, J., Eye, K., Hospital, S., Arabia, S., 2018. Subconjunctival injectable dendrimer-dexamethasone gel for the treatment of corneal inflammation. Biomaterials 125, 38–53. https://doi.org/10.1016/j.biomaterials.2017.02.016.Subconjunctival

Thoniyot, P., Tan, M.J., Karim, A.A., Young, D.J., 2015. Nanoparticle – Hydrogel Composites: Concept , Design , and Applications of these Promising , Multi-Functional Materials. Adv. Sci. 2, 1–13. https://doi.org/10.1002/advs.201400010

Wang, C., Lau, T.T., Loh, W.L., Su, K., Wang, D., 2011. Cytocompatibility study of a natural biomaterial crosslinker — Genipin with therapeutic model cells. J. Biomed. Mater. Res. B Appl. Biomater. 97, 58–65. https://doi.org/10.1002/jbm.b.31786

Wang, K., Han, Z., 2017. Injectable hydrogels for ophthalmic applications. J. Control. Release 268, 212–224.

Wang, Q., Sun, C., Xu, B., Tu, J., Shen, Y., 2018. Synthesis , physicochemical properties and ocular pharmacokinetics of thermosensitive in situ hydrogels for ganciclovir in cytomegalovirus retinitis treatment. Drug Deliv. 25, 59–69. https://doi.org/10.1080/10717544.2017.1413448

Widjaja, L.K., Bora, M., Ng, P., Huat, P., Lipik, V., Wong, T.T.L., Venkatraman, S.S., 2014. Hyaluronic acid-based nanocomposite hydrogels for ocular drug delivery applications. J.

Biomed. Mater. Res. 102, 3056–3065. https://doi.org/10.1002/jbm.a.34976

Xu, X., Weng, Y., Xu, L., Chen, H., 2013. Sustained release of avastin ® from polysaccharides cross-linked hydrogels for ocular drug delivery 60, 272–276. https://doi.org/10.1016/j.ijbiomac.2013.05.034

Zhang, Q., Fassihi, M.A., Fassihi, R., 2018. Delivery Considerations of Highly Viscous Polymeric Fluids Mimicking Concentrated Biopharmaceuticals: Assessment of Injectability via Measurement of Total Work Done “WT.” AAPS PharmSciTech 19, 1520–1528. https://doi.org/10.1208/s12249-018-0963-x

Zhao, F., Yao, D., Guo, R., Deng, L., Dong, A., Zhang, J., 2015. Composites of Polymer Hydrogels and Nanoparticulate Systems for Biomedical and Pharmaceutical Applications. Nanomaterials 5, 2054–2130. https://doi.org/10.3390/nano5042054

CHAPTER FIVE
CONCLUSIONS AND FUTURE RECOMMENDATIONS

5.1. CONCLUSIONS

The aim of this study was to develop a novel stimuli responsive delivery system for minimally invasive delivery of macromolecules over a prolonged period of time, in order to provide convenience to the patients and therefore improve compliance. Novel stimuli responsive delivery approaches have become the alternative to highly invasive surgical therapies owing to their post-administration manipulation of release behaviour which occurs without tissue invasion. The focus of these approaches has been on gelling polymers as carriers of therapeutic agents.

In this research, a novel injectable nanosystem (HA-NSP) comprising of photo-responsive nanospheres dispersed in a hydrogel was designed, formulated, and characterized for the purpose of prolonged delivery of macromolecular therapeutics such as monoclonal antibodies for age-related macular degeneration treatment. Zein, photo-responsive chromophore (DHAB) and hyaluronic acid (HA) were selected as the suitable components for the preparation of the injectable HA-NSP using Immunoglobulin G (IgG) as the model drug. Photo-responsive AZP nanospheres from zein and DHAB blend, with a particle diameter of <200nm and 83% encapsulation efficiency, were successfully prepared via coacervation method and dried by lyophilisation. The photo-responsive property of the HA-NSP nanosystem is afforded by the AZP nanospheres which undergo photo-isomerization under UV light (365nm) and their size decreased; this change in size was observed via dynamic light scattering.

Injectability of the HA-NSP nanosystem was confirmed by texture analysis in which a maximum injection force of 10N through the 27G needle was observed, indicative of ease of injection. These findings were supported by data from rheology, displaying shear-thinning behaviour of the HA-NSP nanosystem which is attributed to the presence of HA. Data obtained from *in vitro* drug release study was substantial to confirm prolonged release of the macromolecular IgG in a sustained manner, up to 60% over 32 days.

The injectable HA-NSP was evaluated *in vitro* for cytotoxicity effect on primary human retinal pigment epithelium (HRPE). All treatments exhibited cell death via apoptosis pathway more than necrosis. The nanosystem displayed positive cytocompatibility results suggesting biocompatibility. Though cell cytotoxicity findings suggest potential compatibility of the HA-

NSP nanosystem *in vivo*, the actual *in vivo* animal study would provide detailed data of how the delivery system behaves in an actual physiological environment.

5.2. FUTURE RECOMMENDATIONS

The overall results from the study of the novel injectable photo-responsive HA-NSP nanosystem suggest suitability of the delivery system to achieve minimally invasive site-specific delivery of any macromolecular therapeutic, such as anti-VEGF agents for treatment of chorio-retinal diseases in the posterior segment of the eye. The end goal of this research is commercialisation of the HA-NSP nanosystem. However, further investigations are necessary and are recommended to explore the system's behaviour *in vivo* and its potential capabilities arising from native components used, such as zein.

Previous research suggests that degradation products from zein are advantageous for cell proliferation (Farris et al., 2017), and a cell proliferation study would provide more data to confirm this property. Studies also suggest that zein possesses anti-oxidant properties due to its high aliphatic index and fatty acid content (Gong et al., 2006), and further characterisations are needed to substantiate the suitability of this delivery system for diseases such as age-related macular degeneration (AMD) which is characterised by oxidative stress (Yamashiro et al., 2012).

Ex-vivo tissue penetration and cell attachment studies are necessary to further explore the properties of the formulated nanospheres and HA-NSP nanosystem to predict their potential behaviour in the physiological environment before *in vivo* animal studies. The cell cytotoxicity investigation conducted provided positive results for prediction of the potential effect of HA-NSP on tissue (Shafaie et al., 2016), however, *in vivo* animal studies are recommended to study the actual effect on animal tissue, to compare the nanosystem with existing commercial products, and to explore different routes of administration in order to support the current findings. IgG was used a model therapeutic antibody; however, the plan is to study anti-VEGF agents *in vivo* as the preferred first line therapy for ocular angiogenesis (Urbancic et al., 2020). This will provide evidence to corroborate the hypotheses of the functionality of this delivery system and readiness for further investigations leading to commercialisation.

Injectability of the HA-NSP nanosystem was studied using various needle sizes. Measurements using a range of needle lengths would also be beneficial as some delivery routes require longer length needles in order to reach site of delivery with minimal tissue invasion. Examples include, the restricted space of the delicate eye tissue with irregular target

sites in the posterior segment (Wang and Han, 2017). Needle sizes used in intraocular injections vary from 27G to 33G with 30G being the commonly used size. Intravitreal injection procedures require a needle size 27G or smaller with variations of length and a maximum limit of 18mm (Oztas et al., 2016).

The universal applicability of the HA-NSP nanosystem for prolonged release of macromolecules can be confirmed by incorporating various macromolecules and comparing *in vitro* drug release patterns. Finally, a release study extending over a longer period can be explored to see how far the HA-NSP nanosystem can prolong the delivery of macromolecules.

5.3. REFERENCES

Farris, E., Brown, D.M., Ramer-tait, A.E., Pannier, A.K., 2017. Chitosan-zein nano-in-microparticles capable of mediating in vivo transgene expression following oral delivery. J. Control. Release 249, 150–161. https://doi.org/10.1016/j.jconrel.2017.01.035

Gong, S., Wang, H., Sun, Q., Xue, S.T., Wang, J.Y., 2006. Mechanical properties and in vitro biocompatibility of porous zein scaffolds. Biomaterials 27, 3793–3799. https://doi.org/10.1016/j.biomaterials.2006.02.019

Oztas, Z., Akkin, C., Afrashi, F., Nalcaci, S., 2016. The short-needle intravitreal injection technique. Int. J. Ophthalmol 9(6), 929-930. https://doi.org/10.18240/ijo.2016.06.24

Shafaie, S., Hutter, V., Cook, M.T., Brown, M.B., Chau, D.Y.S., 2016. In Vitro Cell Models for Ophthalmic Drug Development Applications 5, 94–108. https://doi.org/10.1089/biores.2016.0008

Urbancic, M., Klobucar, P., Zupan, M., Urbancic, K., Lavric, A., 2020. Anti-VEGF treatment of diabetic macular oedema: Two-year visual outcomes in routine clinical practice. J. Ophthalmol 2020, 1-8. https://doi.org/10.1155/2020/6979758

Wang, K., Han, Z., 2017. Injectable hydrogels for ophthalmic applications. J. Control. Release 268, 212–224.

Yamashiro, K., Tomita, K., Tsujikawa, A., Nakata, I., Akagi-Kurashige, Y., Miyake, M., Ooto, S., Tamura, H., Yoshimura, N., 2012. Factors associated with the response of age-related macular degeneration to intravitreal ranibizumab treatment. Am. J. Ophthalmol. 154, 125–36. https://doi.org/10.1016/j.ajo.2012.01.010

molecules

MDPI

Review

Stimuli-Responsive Polymeric Systems for Controlled Protein and Peptide Delivery: Future Implications for Ocular Delivery

Pakama Mahlumba, Yahya E. Choonara, Pradeep Kumar, Lisa C. du Toit and Viness Pillay *

Wits Advanced Drug Delivery Platform Research Unit, Department of Pharmacy and Pharmacology, School of Therapeutic Science, Faculty of Health Sciences, University of the Witwatersrand, Johannesburg, 7 York Road, Parktown 2193, South Africa; pakama.mahlumba@students.wits.ac.za (P.M.); yahya.choonara@wits.ac.za (Y.E.C.); pradeep.kumar@wits.ac.za (P.K.); lisa.dutoit@wits.ac.za (L.C.T.)

* Correspondence: viness.pillay@wits.ac.za; Tel.: +27-11-717-2274

Academic Editor: Chih-Chang Chu

Received: 7 June 2016; Accepted: 27 July 2016; Published: 30 July 2016

Abstract: Therapeutic proteins and peptides have become notable in the drug delivery arena for their compatibility with the human body as well as their high potency. However, their biocompatibility and high potency does not negate the existence of challenges resulting from physicochemical properties of proteins and peptides, including large size, short half-life, capability to provoke immune responses and susceptibility to degradation. Various delivery routes and delivery systems have been utilized to improve bioavailability, patient acceptability and reduce biodegradation. The ocular route remains of great interest, particularly for responsive delivery of macromolecules due to the anatomy and physiology of the eye that makes it a sensitive and complex environment. Research in this field is slowly gaining attention as this could be the breakthrough in ocular drug delivery of macromolecules. This work reviews stimuli-responsive polymeric delivery systems, their use in the delivery of therapeutic proteins and peptides as well as examples of proteins and peptides used in the treatment of ocular disorders. Stimuli reviewed include pH, temperature, enzymes, light, ultrasound and magnetic field. In addition, it discusses the current progress in responsive ocular drug delivery. Furthermore, it explores future prospects in the use of stimuli-responsive polymers for ocular delivery of proteins and peptides. Stimuli-responsive polymers offer great potential in improving the delivery of ocular therapeutics, therefore there is a need to consider them in order to guarantee a local, sustained and ideal delivery of ocular proteins and peptides, evading tissue invasion and systemic side-effects.

Keywords: bioavailability; in situ; ocular barriers; ocular delivery; pre-corneal elimination; protein and peptide delivery; stimuli responsive polymer

1. Introduction

Therapeutic proteins and peptides are advantageous over small molecule drugs in that they mimic similar molecules found in the human body; they are biocompatible and highly potent. However, limitations (both drug related and patient related) do exist, caused by their high molecular weight, poor transfer across biological membranes, provocation of immune responses, short half-lives and instability of the molecules [1,2]. The controlled release of therapeutic proteins is regarded as a way to increase the efficacy while reducing side effects, and therefore improving the patient's quality of life [3].

The most commonly used route of administration for proteins and peptides is the parenteral route, i.e., injection/intravenous infusion providing direct administration into the bloodstream. Though this route can overcome some of the limitations, it is costly, painful and results in low patient

APPENDIX B

International Journal of
Molecular Sciences

MDPI

Article

Fabrication and Characterisation of a Photo-Responsive, Injectable Nanosystem for Sustained Delivery of Macromolecules

Pakama Mahlumba [1], Pradeep Kumar [1], Lisa C. du Toit [1], Madan S. Poka [2], Philemon Ubanako [1] and Yahya E. Choonara [1,*]

[1] Wits Advanced Drug Delivery Platform Research Unit, Department of Pharmacy and Pharmacology, School of Therapeutic Science, Faculty of Health Sciences, University of the Witwatersrand, Johannesburg, 7 York Road, Parktown 2193, South Africa; pakama.mahlumba@students.wits.ac.za (P.M.); pradeep.kumar@wits.ac.za (P.K.); lisa.dutoit1@wits.ac.za (L.C.d.T.); philemon.ubanako@wits.ac.za (P.U.)
[2] Division of Pharmaceutical Sciences, School of Pharmacy, Sefako Makgatho Health Sciences University, Pretoria 0208, South Africa; madan.poka@smu.ac.za
* Correspondence: yahya.choonara@wits.ac.za; Tel.: +27-11-717-2052

Abstract: The demand for biodegradable sustained release carriers with minimally invasive and less frequent administration properties for therapeutic proteins and peptides has increased over the years. The purpose of achieving sustained minimally invasive and site-specific delivery of macromolecules led to the investigation of a photo-responsive delivery system. This research explored a biodegradable prolamin, zein, modified with an azo dye (DHAB) to synthesize photo-responsive azoprolamin (AZP) nanospheres loaded with Immunoglobulin G (IgG). AZP nanospheres were incorporated in a hyaluronic acid (HA) hydrogel to develop a novel injectable photo-responsive nanosystem (HA-NSP) as a potential approach for the treatment of chorio-retinal diseases such as age-related macular degeneration (AMD) and diabetic retinopathy. AZP nanospheres were prepared via coacervation technique, dispersed in HA hydrogel and characterised via infrared spectroscopy (FTIR), X-ray diffraction (XRD) and thermogravimetric analysis (TGA). Size and morphology were studied via scanning electron microscopy (SEM) and dynamic light scattering (DLS), UV spectroscopy for photo-responsiveness. Rheological properties and injectability were investigated, as well as cytotoxicity effect on HRPE cell lines. Particle size obtained was <200 nm and photo-responsiveness to UV = 365 nm by decreasing particle diameter to 94 nm was confirmed by DLS. Encapsulation efficiency of the optimised nanospheres was 85% and IgG was released over 32 days up to 60%. Injectability of HA-NSP was confirmed with maximum force 10 N required and shear-thinning behaviour observed in rheology studies. In vitro cell cytotoxicity effect of both NSPs and HA-NSP showed non-cytotoxicity with relative cell viability of ≥80%. A biocompatible, biodegradable injectable photo-responsive nanosystem for sustained release of macromolecular IgG was successfully developed.

Keywords: zein; macromolecules; photo-responsive; nanospheres; sustained release; biodegradable; injectable; hydrogel

Citation: Mahlumba, P.; Kumar, P.; Lisa C. du Toit; Poka, M.S.; Ubanako, P.; Choonara, Y.E. Fabrication and Characterisation of a Photo-Responsive, Injectable Nanosystem for Sustained Delivery of Macromolecules. *Int. J. Mol. Sci.* **2021**, *22*, 3359. https://doi.org/10.3390/ijms22073359

Academic Editor: Purusotam Basnet

Received: 24 February 2021
Accepted: 23 March 2021
Published: 25 March 2021

APPENDIX C

PREPARATION AND CHARACTERISATION OF PHOTO-RESPONSIVE NANOSPHERES FOR INTRAOCULAR DELIVERY

Pakama Mahlumba, Pradeep Kumar, Lisa C. Du Toit, Yahya E. Choonara and Viness Pillay*

Wits Advanced Drug Delivery Platform Research Unit, Department of Pharmacy and Pharmacology, School of Therapeutic Sciences, Faculty of Health Sciences, University of the Witwatersrand, Johannesburg, 7 York Road, Parktown, 2193, South Africa.

*Viness.pillay@wits.ac.za

Purpose: A photo-reactive polymeric complex was prepared using a prolamine-based polymer and an azo dye for the formulation of photo-responsive nanospheres that are potentially capable of drug encapsulation and stimuli responsive intraocular delivery of bioactive agents for treatment of disorders in the posterior segment of the eye (vitreoretinal disorders). This study investigated the physicochemical properties of the nanospheres.

Methods: Nanospheres were prepared using single emulsion method. Dynamic light scattering technique was used to assess particle size. Particles were further subjected to imaging through the scanning electron microscope to assess shape. The presence of a photo-responsive functional group was investigated using Fourier transform infrared spectroscopy for evaluation of appropriate bond formation and additionally, ultraviolet spectroscopy was employed to measure the photo switch wavelength to confirm the presence of the photo-reactive azo bond.

Results: The size of the spheres was observed in the nano range (1-100nm) and scanning electron microscope images displayed the spherical shape of the particles. Obtained FTIR data showed a broad band at 3267cm-1 characteristic of a phenolic hydroxyl functional group, N=N stretch observed at 1515cm-1 confirming the photo-responsive functional group. UV measurements demonstrated a photo switch wavelength within the 340-366nm range which further substantiates the presence of the photo-reactive moiety in the nanospheres.

Conclusions: The nanospheres possess a photo-responsive property and can therefore be employed in remotely controlled stimuli responsive delivery of bioactive agents.

APPENDIX D

STRICTLY CONFIDENTIAL

ANIMAL ETHICS SCREENING COMMITTEE (AESC)

CLEARANCE CERTIFICATE NO. 2017/11/74/D

APPLICANT: Ms P Malumba

SCHOOL: Pharmacy and Pharmacology
DEPARTMENT:
LOCATION:

PROJECT TITLE: In vivo assessment of antiVeGF delivery from a Geocolloid system in a rabbit eye model

Number and Species

65X (experimental study) and 8X (Pilot study) 4-6 week old male and female New Zealand white rabbits

Approval was given for the use of animals for the project described above at an AESC meeting held on 2017/11/28. This approval remains valid until 22 January 2020.
Unreported changes to the application may invalidate the clearance given by the AESC
An annual progress report must be provided

The use of these animals is subject to AESC guidelines for the use and care of animals, is limited to the procedures described in the application form and is subject to any additional conditions listed below:

Signed: _____ (Chairperson, AESC) Date: 9/2/2018

I am satisfied that the persons listed in this application are competent to perform the procedures therein, in terms of Section 23 (1) (c) of the Veterinary and Para-Veterinary Professions Act (19 of 1982)

Signed: _____ (Registered Veterinarian) Date: 8 February 2018

cc: Supervisor: Professor V Pillay
Director: CAS

Works 2000/lain0015/AESCCert.wps